AN ABSTRACT OF THE THESIS OF

JACK HENRY SHREFFLER for the degree DOCTOR OF PHILOSOPHY
(Name) (Degree)

in OCEANOGRAPHY presented on January 13, 1975
(Major Department) (Date)

Title: A NUMERICAL MODEL OF HEAT TRANSFER TO THE ATMOSPHERE FROM AN ARCTIC LEAD

Abstract approved: Redacted for privacy
Dr. Clayton A. Paulson

A two-dimensional, eddy diffusivity model is developed to predict sensible and latent heat fluxes from an Arctic lead, a narrow break of open water in the pack ice. Numerical solutions are obtained for a set including the continuity equation and conservation equations for heat, momentum, stress, water vapor and condensate. Unlike previous models, lower boundary conditions require that heat and vapor must be transferred essentially by molecular means through a thin, surface sublayer. The boundary conditions are shown to be consistent with laboratory and geophysical observations.

Numerical experimentation illustrates the dependence of heat flux predictions on the basic model assumptions. In general, the formulation of the lower boundary condition tends to moderate the changes in flux predictions as model parameters are varied over ranges deemed reasonable from available observational data.

A situation is investigated where the air-water temperature difference, $\Delta\theta$, is 25°C and the friction velocity, u_*, is 16 cm/sec. The predicted sensible heat flux at a 20 meter fetch is about 28 mw/cm^2, using model parameters estimated to be most appropriate. Neglecting buoyancy effects, the predicted sensible flux scales with $\Delta\theta u_*$. The predicted temperature profile is in fair agreement with one observed by Badgley (1966) under these conditions. The predicted latent heat flux for this case is about 30% of the sensible flux, although the latent flux may exceed the sensible flux if $\Delta\theta$ is less than 10°C. A prediction of the sensible heat flux in the absence of wind, the minimum flux possible over a lead, is approximated by $0.224(\Delta\theta) + 0.00515(\Delta\theta)^2$ mw/cm^2.

A Numerical Model of Heat Transfer to the Atmosphere from an Arctic Lead

by

Jack Henry Shreffler

A THESIS

submitted to

Oregon State University

in partial fulfillment of
the requirements for the
degree of

Doctor of Philosophy

June 1975

APPROVED:

Redacted for privacy

Associate Professor of Oceanography
in charge of major

Redacted for privacy

Dean of School of Oceanography

Redacted for privacy

Dean of Graduate School

Date thesis is presented January 13, 1975

Typed by Clover Redfern for Jack Henry Shreffler

ACKNOWLEDGMENT

I wish to thank Dr. Clayton A. Paulson, my thesis advisor, for giving me the opportunity to pursue this research project and my committee members and fellow students who have helped me gain the necessary insights.

My understanding of numerical methods and the use of digital computers was greatly enhanced while at the National Center for Atmospheric Research in 1972 on a Summer Fellowship in Scientific Computing. Mrs. Jeanne Adams, of the NCAR Computing Facility, was particularly helpful. NCAR is sponsored by the National Science Foundation.

Availability of the PDP-15 computer, free of cost, in the School of Oceanography has allowed great latitude in numerical experimentation and vastly improved the quality of the research. I estimate that equivalent computer time on the CDC 3300 would have cost in excess of twenty thousand dollars. I wish to thank Bob Dietrich and Godfrey Watson for their efforts to keep the PDP-15 operational.

This research was supported by a subcontract from the University of Washington under NSF Grant OPP71-04031.

Deeply appreciated and always to be remembered is the aid of Carol, the Ms. of my heart and mate for my life.

TABLE OF CONTENTS

LIST OF FIGURES

LIST OF TABLES

A NUMERICAL MODEL OF HEAT TRANSFER TO THE ATMOSPHERE FROM AN ARCTIC LEAD

1. INTRODUCTION

As its ultimate objective, this study is aimed at providing a means for theoretical prediction of turbulent heat flux from an Arctic lead, a narrow break of open water in the pack ice. Under winter conditions the surface of a lead may easily be 30°C hotter than the overlying air. Even though only a small percentage of the Arctic is composed of leads, the upward heat flux must play a major role in the heat budget of the Arctic region (Badgley, 1966).

Figure 1.1 depicts a typical lead situation. As an idealization one may consider a neutrally buoyant atmosphere encountering an abrupt increase in surface temperature and vapor pressure; the lead may be considered of infinite extent in the crosswind direction. A numerical model treating this situation would have as its primary objectives the prediction of profiles of the turbulent fluxes of sensible and latent heat at various fetches, under different wind speeds and air-lead temperature differences. Also of interest would be the alteration of stress and velocity profiles, which, although induced by the heat flux, will secondarily influence the magnitude of the flux. The related geophysical problem promotes assumptions of small roughness lengths (over ice, snow and water) which change little or not at all.

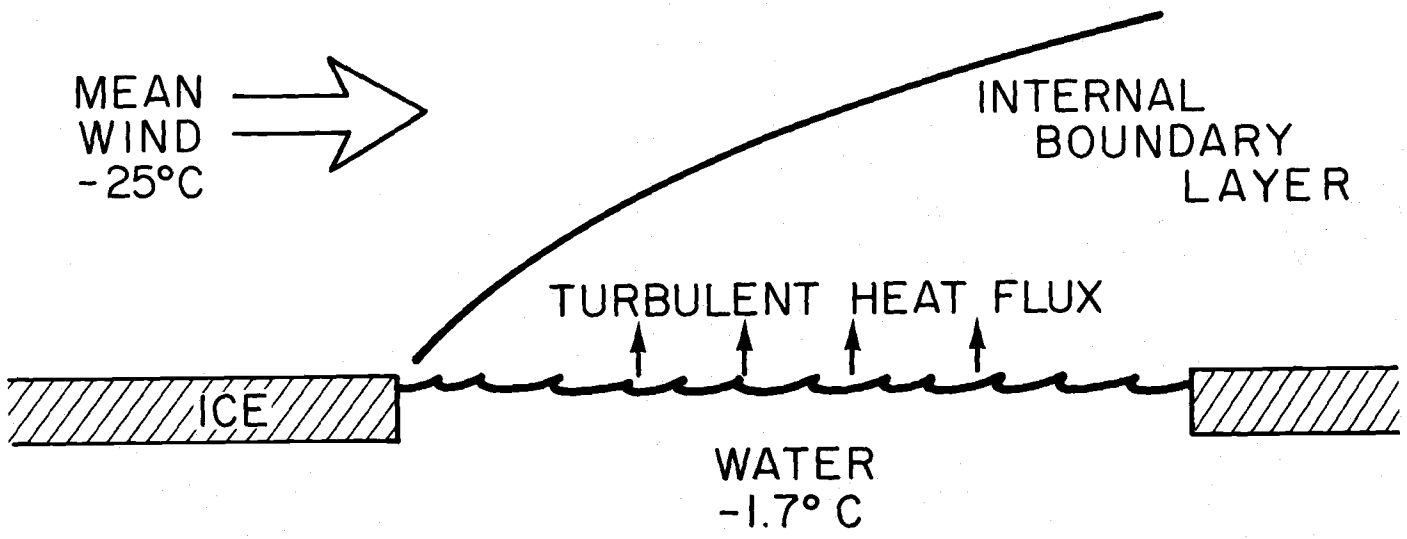

Figure 1.1. An idealized Arctic lead.

Although some of the results may be non-dimensionalized, the lead should be thought of as several tens of meters in width. If a numerical model can be shown to be an accurate heat flux predictor, and surveys delineate typical lead conditions as well as the distribution of open water and thin ice in the Arctic Basin, then the impact of leads on the total heat exchange between the ocean and atmosphere may be judged.

The radiative flux is not treated in this study and may be a significant contributor to the total heat transfer. Badgley (1966) estimates that the net upward long wave radiation may be 25% of the sensible heat flux under winter conditions. The establishment of a constant heat flux layer applies strictly to turbulent plus radiative transfer, and the latter may show significant variation in the lower one meter (Priestly, 1959). Coantic and Seguin (1971) make theoretical estimates of the radiative heat flux divergence in the surface layer over water. Results for the lowest surface temperature, 5°C, and the lowest friction velocity, 8 cm/sec, indicate that the variation of sensible heat flux may approach 10 percent of its surface value in the lower two meters due to the radiative flux divergence. However, this result is computed with a relatively small air-water temperature difference of 5°C. The typical lead situation would have a larger temperature difference, higher wind speed and lower surface temperature (lower vapor pressure), and hence the percentage

variation of the sensible heat flux may be significantly less. On the other hand, Coantic and Seguin base their calculations on absorption of infrared solely by water vapor. Over the lead, the existence of condensed water droplets would further complicate the radiative transfer.

Investigations of the situation where air flow encounters an abrupt change in surface characteristics have concentrated principally on those involving roughness change under neutral conditions. However, some attempts have been made to predict heat flux following a step increase in surface temperature. Assuming logarithmic profiles for both temperature and horizontal velocity, Elliott (1958) predicts the height of the internal boundary layer (IBL), the region where air is subject to heating by the new surface temperature. Using conservation of heat, the surface flux may then be calculated. The approach is dubious because of the need to assume the profiles a priori and the assumption that there is a flux discontinuity at the top of the IBL. Miyake (1965) uses dimensional arguments to arrive at expressions for the surface heat flux and height of the IBL. However, no appeal is made to conservation of heat, and the model fails in this respect. A review of Russian work is presented by Panchev and Donev (1971). Few details are given, but the main predictions are the height of the IBL and vertical temperature profiles. Results are dimensional and reflect fetches of up to three kilometers, not particularly useful for small scale leads. P. A. Taylor (1970) presents an eddy diffusivity

model which is perhaps the most adequate of those found in the literature. However, objections may be raised concerning the lower boundary conditions and the heavy reliance on relationships which hold only under conditions of horizontal homogeneity. Also some of the results indicate instability in the solution; for instance, the shear stress at the top of the IBL becomes infinite after a relatively short fetch, equivalent to 20 meters assuming a roughness length of 0.02 centimeters.

Evaluation of a numerical model is hampered by a paucity of data. In addition to the theoretical development, Miyake (1965) presents observations of wind velocity and temperature profiles from experiments carried out over artificial ponds of 20 meters diameter at Barrow, Alaska. Similar data of higher quality is presented by Badgley (1966). Bau On Young et al. (1973) present wind tunnel data which has some applicability in evaluating the model. A discussion of the data and comparison with the author's model will be presented in this dissertation.

This study concentrates on a two-dimensional eddy diffusivity model which has been developed to treat the lead situation. Since it is difficult to conceive of a model which does not employ an eddy diffusivity assumption to some degree, an explanation of the assumption in this model is necessary. The model is aimed primarily at producing heat flux predictions and uses the eddy diffusivity assumption in a fundamental way: the heat flux is computed indirectly from a

predicted temperature gradient by assuming the form and magnitude of an eddy transfer coefficient for heat. This type of simple model has not yet been adequately explored, particularly with respect to the lower boundary conditions. The current model is unique in that the lower boundary condition on temperature enforces an equality between molecular and turbulent heat fluxes at the top of the surface molecular sublayer, and this crucial assumption recognizes that heat must always be transferred at the surface solely by molecular means. The existence of a molecular sublayer is a reasonable assumption mentioned by many authors; Sverdrup (1937) adequately states the case concerning water vapor transfer from the ocean. However, the molecular sublayer has apparently never been directly incorporated into this type of numerical model. Use of such a lower boundary condition necessitates the solution of two-point boundary value problems; a computational technique is developed which allows considerable flexibility in imposing boundary conditions in two-dimensional models and solves profiles with high accuracy near the surface, where finite difference schemes may have difficulty representing rapidly changing vertical derivatives.

Criticism of an eddy diffusivity model may center on the assumption of a particular form of the eddy transfer coefficient for heat, which, while well known under horizontally homogeneous conditions, would probably not hold in the lead situation. Therefore, an

investigation is made into the possible utilization of the second moment equations in a model. Such a model would, for instance, carry a conservative equation for heat flux, so computations of that primary quantity would be direct.

Employed in this study is a philosophy which asserts that it is both a virtue and an art to keep a numerical model simple when first considering some physical process. Every model contains assumptions, such as assigned constant values, which are the subject of sometimes heated debate. Only in very simple models is it possible to make a systematic determination of the effects of the assumptions on the results. Models may easily become so complex that only a few runs are possible within allotted computer time, and it can only be hoped that the assumptions are appropriate. Only by a thorough understanding of a simple model will it be known in which directions to expand, if indeed any added complexity is necessary. It is the purpose of this study to produce the best possible two-dimensional eddy diffusivity model to provide heat flux predictions from an Arctic lead. To this end, a broad spectrum of basic assumptions are tested, and heuristic discussions of relevant equations are undertaken to provide insight into the behavior of the model.

In Chapter 2 the model equations and boundary conditions for sensible heat transfer are set forth. In Chapter 3 solutions based on the assumption of heat as a passive contaminant are investigated. The

effect of heat flux on stress and wind velocity are included in a full simulation discussed in Chapter 4. The latent heat flux is dealt with separately in Chapter 5. Chapter 6 is devoted to a detailed discussion of the computational method employed in the eddy diffusivity model. The possibility of using a set of first and second moment equations in an Arctic lead model, thereby improving on the eddy diffusivity model, is evaluated in Chapter 7. The numerical model is designed for simulation of a forced convection situation; Chapter 8 deals with the special case of windless convection. A summary of the study is found in Chapter 9.

2. THE MODEL: EQUATIONS AND BOUNDARY CONDITIONS

2.1 Notation

The definitions of the most commonly used symbols are given below. Fluctuating turbulent quantities are in lower case, and the covariance between them is designated by an overbar. Dimensional computations and results are in cgs units.

x	downwind coordinate
z	vertical ordinate
U	mean horizontal velocity
W	mean vertical velocity
k	von Karman's constant (0.4)
u_*	friction velocity ($\sqrt{\tau}$)
K, K_m	eddy coefficient for momentum ($\tau / \frac{\partial U}{\partial z}$)
K_h	eddy coefficient for heat
K_e	eddy coefficient for water vapor
α_h	the ratio K_h / K_m
α_e	the ratio K_e / K_m
g	acceleration of gravity (980 cm/sec)
z_0	roughness length
z_H	roughness parameter for temperature
z_E	roughness parameter for water vapor

D	thickness of the molecular sublayer
Ri	gradient Richardson number
H	heat flux ($\overline{\theta w}$)
L	Monin-Obukhov length ($-u_*^3 T_0 / gk\,\overline{\theta w}$)
ν	viscosity
κ	molecular diffusivity for heat
ψ	molecular diffusivity for vapor
τ	stress ($-\overline{uw}$)
ϵ	dissipation of stress
q	specific humidity
q_B	specific humidity at surface
q_D	specific humidity at top of the molecular sublayer
q_0	specific humidity at roughness length
q_A	ambient specific humidity
θ	potential temperature
θ_D	potential temperature at top of the molecular sublayer
θ_B	potential temperature at surface
θ_0	potential temperature at roughness length
θ_A	ambient potential temperature
ϕ_m	non-dimensional wind shear
ϕ_h	non-dimensional temperature gradient

2.2 The Equations

The basic set consists of conservation equations for heat, momentum, and stress, and the equation of continuity. Throughout this dissertation, "heat" will refer to sensible heat if no other designation is given.

$$U \frac{\partial \theta}{\partial x} + W \frac{\partial \theta}{\partial z} = \frac{\partial}{\partial z} \left(K_h \frac{\partial \theta}{\partial z} \right) \tag{2-1}$$

$$U \frac{\partial U}{\partial x} + W \frac{\partial U}{\partial z} = \frac{\partial}{\partial z} \left(K \frac{\partial U}{\partial z} \right) \tag{2-2}$$

$$U \frac{\partial \tau}{\partial x} + W \frac{\partial \tau}{\partial z} = \frac{\partial}{\partial z} \left(K \frac{\partial \tau}{\partial z} \right) + \overline{w^2} \frac{\partial U}{\partial z} - \frac{g}{T_0} \overline{\theta u} - \epsilon \tag{2-3}$$

$$\frac{\partial U}{\partial x} + \frac{\partial W}{\partial z} = 0 \tag{2-4}$$

Two additional equations, those for water vapor and condensed water droplets, will be considered in Chapter 5 where latent heat flux is investigated.

The stress Equation (2-3) is a reduced form of the moment equation for $-\overline{uw}$, where an eddy diffusion term has replaced the third moment and pressure transport terms, and other terms have been eliminated when deemed small by dimensional analysis. Mellor (1973) discusses the reduction of the Navier-Stokes equations to second moment equations applicable to the atmospheric surface layer.

Tennekes and Lumley (1972) discuss how insignificant terms may be identified and eliminated from the equations. The form of the stress dissipation term, assumptions on the terms of (2-3) necessary to produce a closed set of equations, and results of the full-set simulation will be discussed in Chapter 4. Solutions of the heat equation (2-1) are of prime importance to satisfy the objective of the study and will be considered in detail in Chapter 3.

2.3 Boundary Conditions

It is assumed that a neutrally stratified flow in a constant stress layer encounters an abrupt change in surface temperature. In the lead situation, changes in surface roughness will probably be small; in the model it is assumed that the roughness remains constant. The upwind boundary conditions, applied at $x = 0$, are

$$\begin{aligned} \theta &= \theta_A \\ U &= (u'_*/k)\ln(z/z_0) \\ W &= 0 \\ \tau &= (u'_*)^2 \end{aligned} \qquad (2\text{-}5)$$

where primes indicate quantities at $x < 0$. After the step change in surface temperature is encountered, the following conditions are applied at the upper boundary

$$\frac{\partial \theta}{\partial z} = 0 \qquad \text{and} \qquad \theta = \theta_A$$

$$\frac{\partial U}{\partial z} = \frac{u'_*}{kz} \qquad \text{and} \qquad U = (u'_*/k)\ln(z/z_0) \tag{2-6}$$

$$\frac{\partial \tau}{\partial z} = 0 \qquad \text{and} \qquad \tau = (u'_*)^2$$

W is determined by continuity. Only one of the dual conditions on each quantity in (2-6) may be satisfied exactly, but the solution may be continued in the vertical until the other is very nearly satisfied. A reliable procedure was to force $\frac{\partial \theta}{\partial z} = 0$ and increase the range of vertical integration until $|\theta-\theta_A|/|\theta_B-\theta_A| < 0.0007$.

The lower boundary condition on temperature is of critical importance. The usual approach (Elliott, 1958; Taylor, 1970) is to assign the surface temperature at the roughness length; this appears to be an error brought about by adapting a roughness-change model to treat the temperature-change problem and failing to recognize the inherent difference between the manners in which heat and momentum are transferred at a rough surface. Very near the surface, momentum transfer may be achieved primarily by pressure fluctuations acting on roughness elements. Although it is merely an asymptotic approximation, the mean wind velocity may indeed become zero above the surface. No mean velocity gradient is necessary at the surface since momentum transfer may have virtually no molecular component. However, for a heat flux to exist, there must be a mean temperature

gradient at the surface; heat is transferred solely by molecular means at the surface. The existence of a thin surface sublayer, through which heat is transferred primarily by molecular means, is not in doubt; only the thickness of such a layer is open to debate. In reality, there will also be a transition layer with a blending of molecular and turbulent transfer. The model, however, is two-layered with no transition layer; consequently, the thickness of the molecular sublayer, D, is an effective thickness which might be determined from a temperature profile in the turbulent layer. One estimate of D may be obtained from laboratory data for flow over a flat plate; in such a case it has been found that momentum is transferred through a surface layer of thickness $11\nu/u_*$ by purely molecular means, assuming an abrupt transition from viscous to turbulent flow (Tennekes and Lumley, 1972, p. 160). It will be a basic assumption in this study that the thickness of the molecular layer for heat will also be $11\nu/u_*$, even on slightly rough surfaces such as water. If similarity between molecular transfer of heat and momentum over a flat plate is accepted, the sublayer thickness for heat should be increased by a factor of the Prandtl number (ν/κ) to the -1/3 power (Schlichting, 1960, p. 323). The Prandtl number for air is about 0.72, so the molecular layer for heat might be taken 11 percent thicker than that for momentum. Likewise, considering the Schmidt number (ν/ψ), the molecular layer for vapor might be taken 18 percent thicker. It will be demonstrated

in Section 3.2 that such adjustments in D would change the predicted fluxes by less than five percent. The difficulty in empirically determining D is that temperature gradients, unlike velocity gradients, are not usually large in the near-surface turbulent layer. In Chapter 3 other values of D will be discussed as well as the type of data needed to refine the estimate. The assumption of a molecular sublayer of thickness D implies a maximum possible heat flux for a given temperature step and friction velocity, regardless of the transfer properties in the turbulent layer. Specification of the temperature at the top of the molecular sublayer is tantamount to specification of the surface heat flux. In order to support a moderate heat flux, the temperature change across the molecular sublayer may easily be 40 percent of the total change from the surface to the ambient. This temperature change must not be ignored since the equations of the model describe turbulent flow and hence react to the temperature at the lower edge of the turbulent layer; the lower edge of the turbulent layer is the top of the molecular sublayer, not the surface.

The proper lower boundary condition on temperature is a statement of equality between the molecular and turbulent heat fluxes at the top of the molecular sublayer. The condition is imposed at the greater of z_0 or D, since the equations are applicable to the turbulent layer. Figure 2.1 illustrates typical temperature profiles

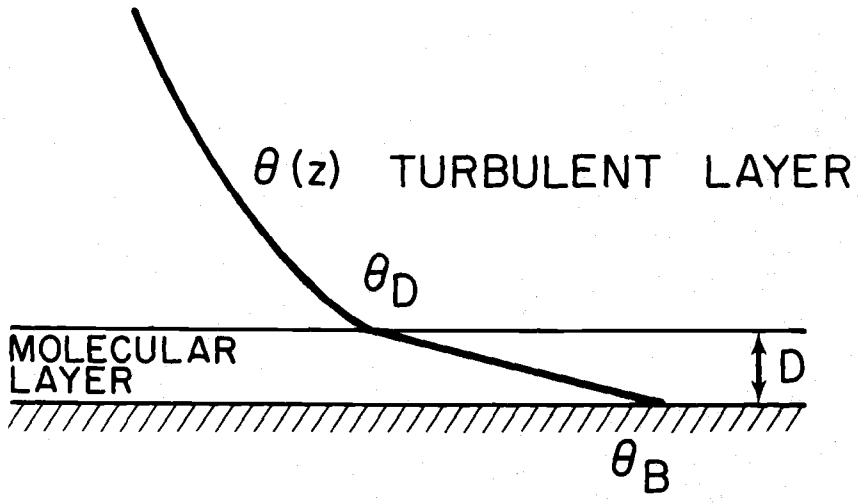

(a)

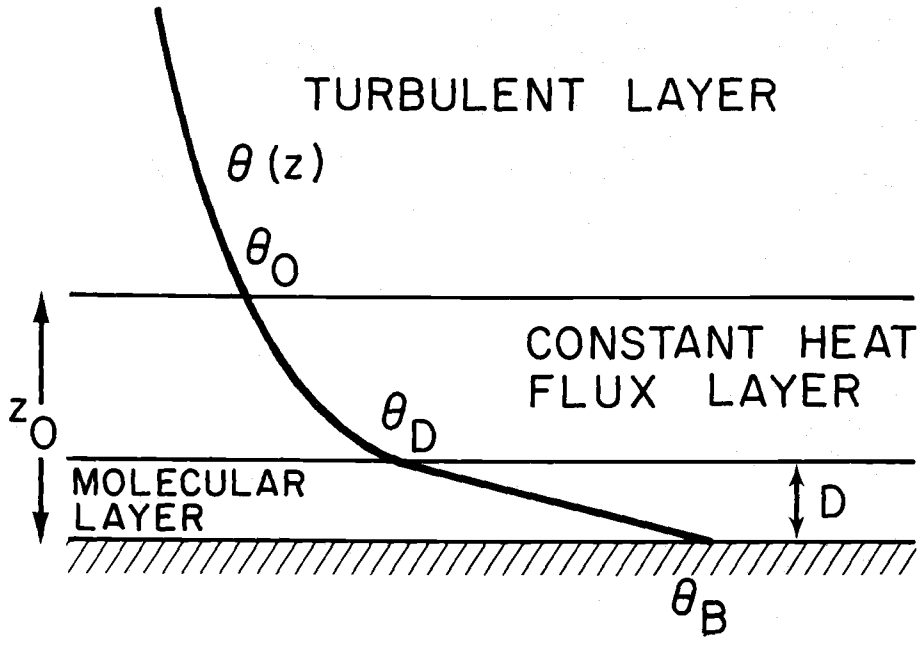

(b)

Figure 2.1. Idealized temperature profiles resulting from the imposition of a molecular layer. (a) $z_0 \leq D$. (b) $z_0 \geq D$.

for cases $z_0 \leq D$ and $z_0 \geq D$. The following conditions are imposed at the lower boundary, where unsubscripted variables are evaluated at z_0 or D (whichever is greater).

$$\theta_D - (DK_h/\kappa)\frac{\partial\theta}{\partial z} = \theta_B \qquad \text{for} \quad z_0 \leq D$$

$$\theta_0 - (m+1)(DK_h/\kappa)\frac{\partial\theta}{\partial z} = \theta_B \qquad \text{for} \quad z_0 \geq D$$

where

$$m = (\kappa/u_* kD\alpha_h)\ln(z_0/D) \tag{2-7}$$

$$U = \frac{u'_*}{k}\ln(z/z_0)$$

$$1.1\left(\tau\frac{\partial U}{\partial z} - \frac{\tau^{3/2}}{kz}\right) + \frac{3g}{T_0}\overline{\theta w} = 0$$

The condition on U requires that the velocity is unchanged from the upwind value; this is obviously true if applied at z_0 and approximately true if applied at D. The condition on τ arises from the stress conservation equation applied at the surface and is discussed further in Chapter 4. $W = 0$ at the lower boundary.

The introduction of the relevant length scale ν/u_*, which contains the velocity scale u_*, renders impossible a profitable non-dimensionalization of the complete problem. However, non-dimensionalization is useful in cases where heat is treated as a passive contaminant.

2.4 Computational Method

Details of the numerical scheme are presented in Chapter 6. Basically, finite differences are taken in the x-direction to reduce the Equations (2-1), (2-2), and (2-3) to second order equations of a linear form, and these are solved in the vertical using a highly accurate seventh order predictor-corrector. Progressive steps are taken in the downwind direction, using the previously computed profile to form x-derivatives. This method has distinct advantages over some other techniques.

(a) Accurate profiles are obtained very near the surface where second derivatives of temperature are expected to be large. Although the lower boundary condition on temperature could be enforced with a finite difference grid, the lowest derivative of temperature could be quite inaccurate.

(b) The step-by-step method in the x-direction eliminates the need for the storage of a large finite difference grid.

(c) The solution may be continued for any desired fetch. Boundary conditions may be changed at any step.

(d) Boundary conditions are easily implemented and very flexible. They may consist of specifying a value of the variable, its vertical derivative, or a linear combination of the two.

(e) There is no need to assume profile shapes near the surface, as is done by Taylor (1970).

3. HEAT AS A PASSIVE CONTAMINANT

Treating heat as a passive contaminant is desirable for several reasons. First, there are a minimum of complicating and controversial assumptions which may obscure the essential strength or weakness of the eddy diffusivity model and the numerical technique. Second, the results may be used as a baseline for comparison with more complicated formulations, those including stress and velocity changes. Last, and quite important, a non-dimensionalization is possible which allows the solution to hold for any temperature step and friction velocity with a given roughness length. Therefore, an extensive investigation is made into the passive contaminant case; Equation (2-1) is the only equation entering the solution, and a_h is constant. Non-dimensionalization is performed with length scale ν/u_*, velocity scale u_*, and temperature scale $\theta_B - \theta_A$. A tilde denotes quantities transformed by the non-dimensionalization.

$$\begin{aligned} \tilde{U} &= U/u_* \\ \tilde{z} &= zu_*/\nu \\ \tilde{\theta} &= (\theta-\theta_A)/(\theta_B-\theta_A) \end{aligned} \tag{3-1}$$

Since the roughness length must be expressed in terms of ν/u_*, each z_0 constitutes a separate case. The appearance of two elemental length scales restricts the generality of the solution. Although

this study is concerned with an abrupt increase in surface temperature, the non-dimensional results hold equally well for a sudden decrease in surface temperature. The general method employed here can be readily adapted for the treatment of water vapor, which must also pass through a molecular layer and might be considered a passive contaminant in a forced convection situation.

3.1 A Basic Solution Over a Flat Plate

It is attractive to first consider the problem over a flat plate since there is data on the molecular layer thickness. Laboratory data (Tennekes and Lumley, 1972) indicate a velocity profile over a flat plate, assuming an abrupt change from viscous to turbulent flow.

$$\begin{aligned} \tilde{U} &= \tilde{z}, & \tilde{z} &\leq 11 \\ \tilde{U} &= 2.5 \ln \tilde{z} + 5, & \tilde{z} &\geq 11 \end{aligned} \qquad (3\text{-}2)$$

If the simplicity of the two-layer model is accepted, there is a layer of thickness $11\nu/u_*$ on the surface where strong viscous forces inhibit turbulent motion. If turbulence is negligible, then heat, like momentum, must be transferred through the layer by molecular means. Thus, over a flat plate, the estimate $\tilde{D} = 11$ may be accepted with some confidence. In this case it will also be assumed that $a_h = 1$. From (3-2) it is seen that $\tilde{z}_0 = e^{-2}$. The downwind step was taken to be $\Delta\tilde{x} = 4000$ after tests showed $\Delta\tilde{x} = 1000$ was

not significantly more accurate.

After solution, a return to ordinary dimensional values may be obtained as shown in (3-3). The Richardson number is computed but is not allowed to influence a_h in this passive contaminant case.

$$\begin{aligned} U &= \tilde{U} \cdot u_* \\ \theta &= \tilde{\theta} \cdot (\theta_B - \theta_A) + \theta_A \\ H &= \tilde{H} \cdot u_* \cdot (\theta_B - \theta_A) \\ Ri &= \tilde{Ri} \cdot (g/T_0) \cdot (\theta_B - \theta_A) \nu / u_*^3 \end{aligned} \tag{3-3}$$

where

$$\tilde{H} = -\tilde{K}_n \frac{\partial \tilde{\theta}}{\partial \tilde{z}}$$

and

$$\tilde{Ri} = \left(\frac{\partial \tilde{\theta}}{\partial \tilde{z}}\right) / \left(\frac{\partial \tilde{U}}{\partial \tilde{z}}\right)^2$$

Subject to the transformations in (3-3), Figures 3.1, 3.2 and 3.3 give profiles of temperature, heat flux and gradient Richardson number at fetches of 2×10^4, 4×10^4, 1×10^5, 2×10^5, 3×10^5 and 4×10^5. For a friction velocity of 30 cm/sec these fetches would be about 1, 2, 5, 10, 15 and 20 meters. As an example, suppose $u_* = 30$ cm/sec and the temperature step is 20 centigrade degrees. Then referring to Figure 3.2, the surface heat flux at a fetch of five meters, $-K_h \frac{\partial \theta}{\partial z}$, would have a numerical value of $0.049 \times 20 \times 30 = 29$ which converts by a factor of 1.3 to 38 milliwatts/cm^2.

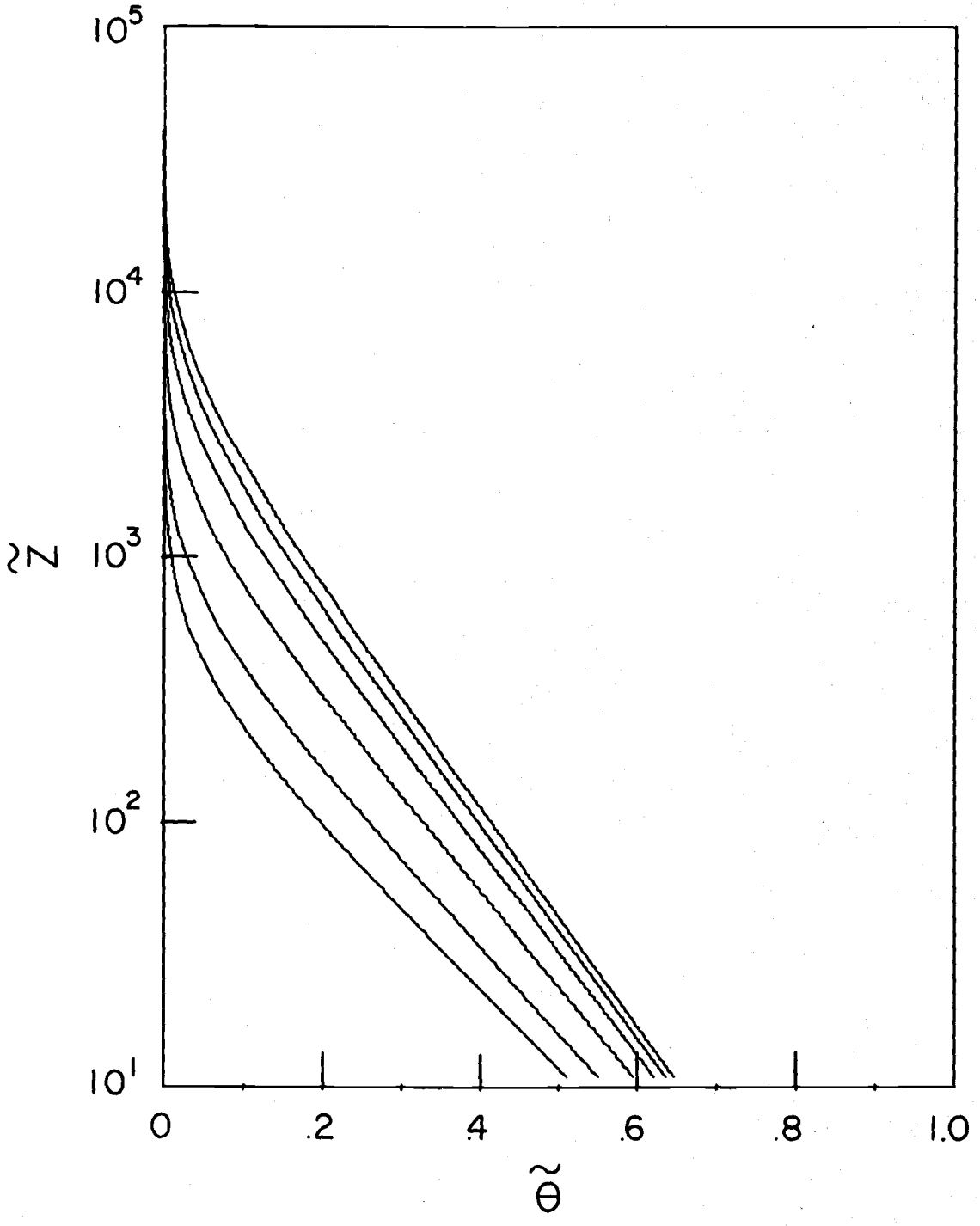

Figure 3.1. Temperature profiles at fetches of $\tilde{x}$ = 0.2, 0.4, 1.0, 2.0, 3.0, and 4.0 x 10^5 (temperature increasing with fetch). Flat plate.

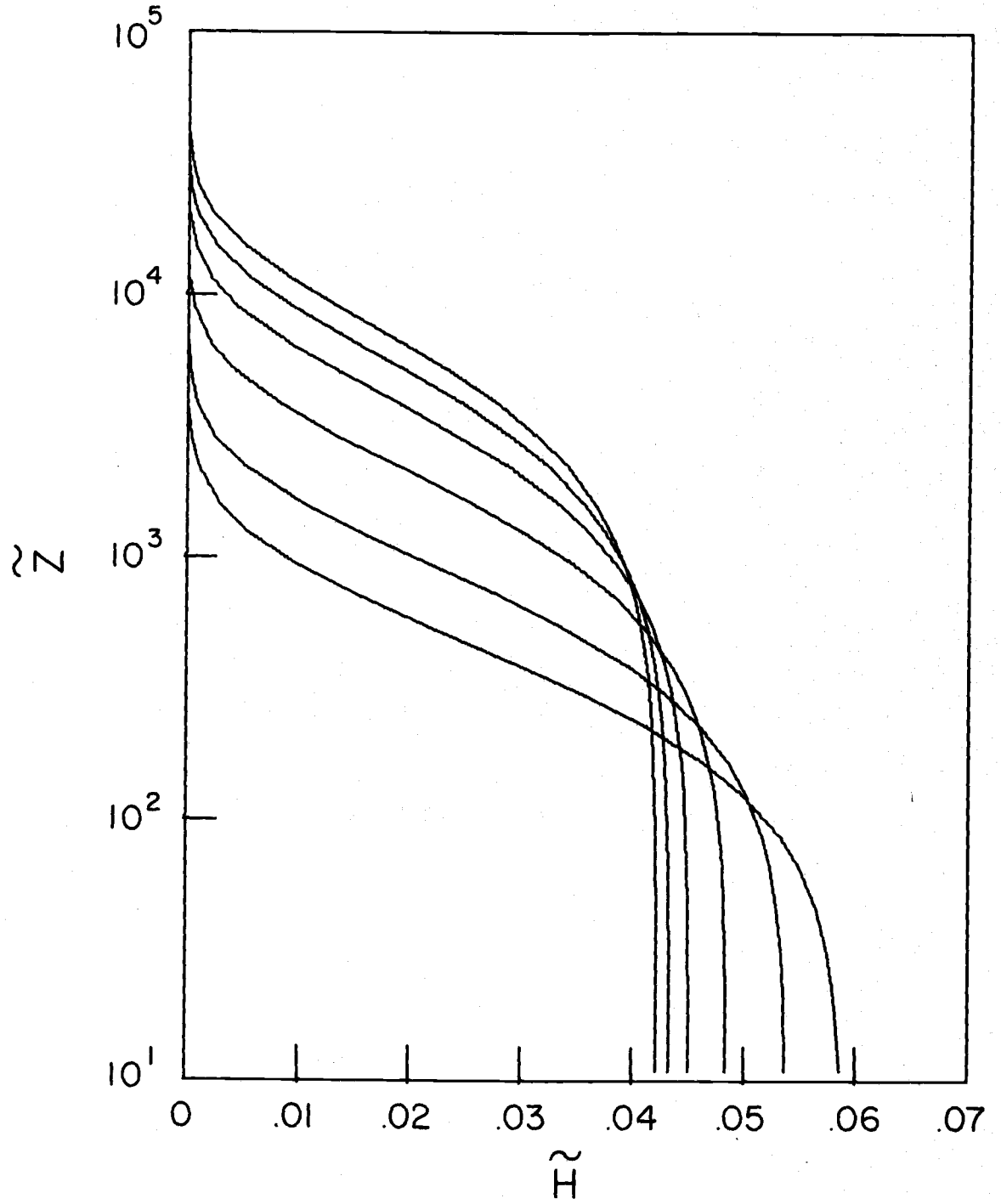

Figure 3.2. Heat flux profiles at fetches of $\tilde{x}$ = 0.2, 0.4, 1.0, 2.0, 3.0, and 4.0 x 10^5 (surface flux decreasing with fetch). Flat plate.

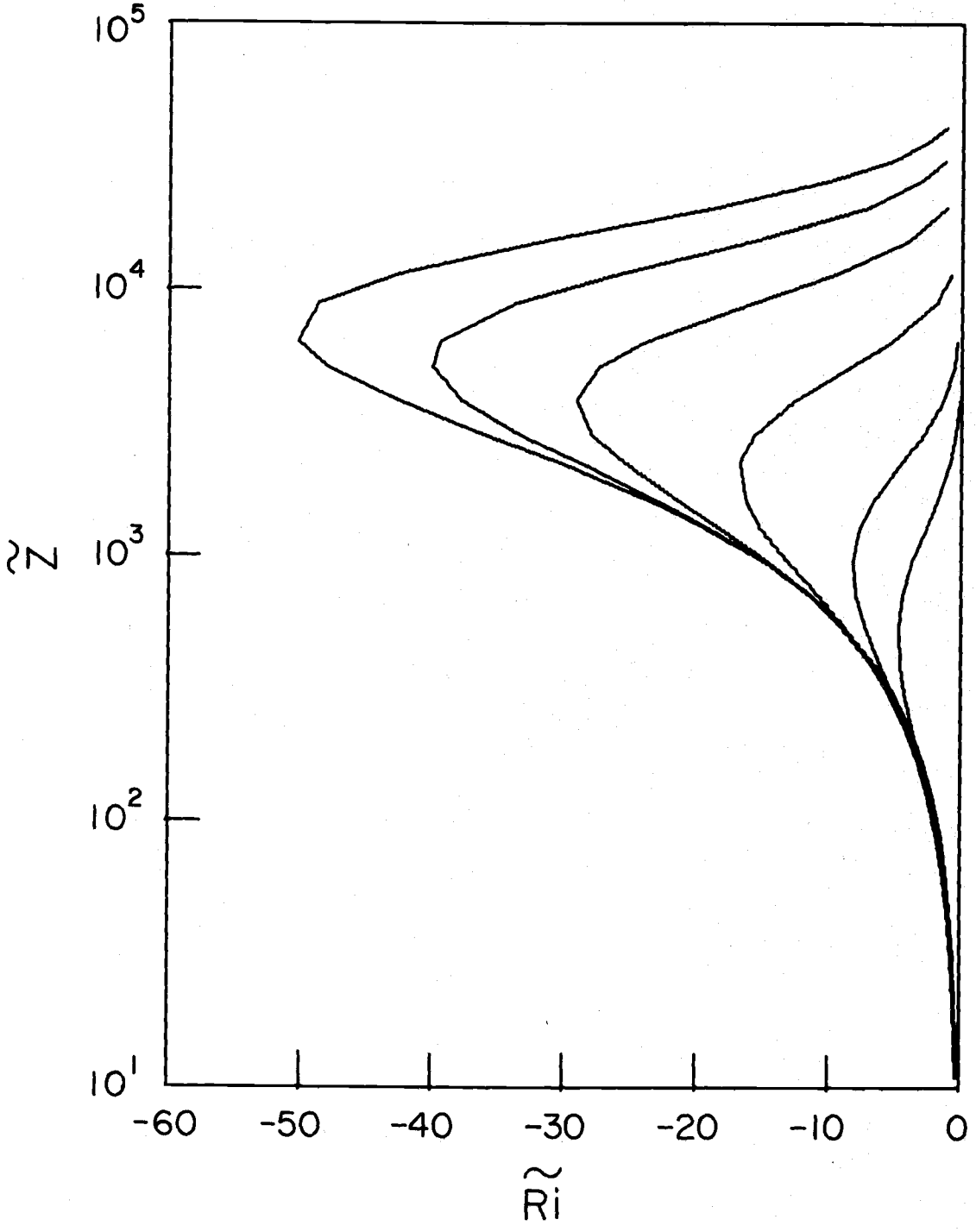

Figure 3.3. Gradient Richardson number profiles at fetches of $\tilde{x} = 0.2$, 0.4, 1.0, 2.0, 3.0, and 4.0 x 10^5 ($\tilde{Ri}$ decreasing with fetch). Flat plate.

Although not indicated in the figures, at $\tilde{x} = 4 \times 10^5$ it was assumed that the surface temperature returns to its original value, and the run was continued to $\tilde{x} = 5 \times 10^5$. Results show that less than 15 percent of the heat which had entered the air would return to the surface, and this would undoubtedly be less if buoyancy effects were considered.

Bau On Young et al. (1973) have performed wind tunnel experiments to study transfer processes from both a flat plate and a free water surface. Because this data is not geophysical, caution must be exercised in comparison with model results. For instance, in the wind tunnel, the measured $-\overline{uw}$ decreases rapidly with height, reaching zero at $\tilde{z} = 1800$ on a fetch of $\tilde{x} = 80,000$. This is in sharp contrast to the model which assumes a constant stress layer of unspecified depth. In any case, some basic model assumptions seem to be verified by the data for flat plate heat transfer. First, the law-of-the-wall velocity profile (3-2) holds below $\tilde{z} = 1000$. Second, the temperature profile behaves as though there is a surface molecular layer, although the thickness is about $16\ \nu/u_*$ (see Appendix B). This increased thickness is not explained fully by the dependence on Prandtl number. Third, α_h is near unity in the lower IBL. Fourth, the surface stress seems unaffected by heating and remains constant with fetch. At a fetch of $\tilde{x} = 80,000$, the measured non-dimensional heat flux is 0.040 versus a model prediction of 0.042,

using $a_h = 1$, $\tilde{D} = 16$. The wind tunnel data will be discussed further with respect to heat and vapor transfer over water surfaces.

3.2 Dependence of the Results on Model Parameters

In treating heat as a passive contaminant, the model contains three parameters, a_h, $\tilde{z}_0$ and $\tilde{D}$, whose values may affect the results. Figures 3.1, 3.2 and 3.3 give results of a single case, and such graphs could be generated for any case desired. In order to gain insight into how the parameters affect the surface heat flux predictions, a wide range of cases were considered to a moderate fetch of $\tilde{x} = 80,000$. The results are found in Tables 3.1, 3.2 and 3.3 and indicate a surprisingly small sensitivity of heat flux to the basic parameters of the model.

Table 3.1. Surface $\tilde{H}$ at $\tilde{x} = 80,000$ as a function of $\tilde{z}_0$.

$\tilde{z}_0$	$\tilde{H}$ $a_h = 1$, $\tilde{D} = 11$
e^{-2} (.14)	.04964
4.28	.04678
11.	.04580
100.	.04303

Table 3.1 shows surface $\tilde{H}$ as a function of roughness, where $\tilde{z}_0 = e^{-2}$ corresponds to a flat plate. There is a slight rise in $\tilde{H}$ as roughness decreases, but in the lead situation $\tilde{z}_0$ will generally

lie in the range 1 to 20, making the variation of $\tilde{H}$ with $\tilde{z}_0$ negligible.

Table 3.2 shows the surface $\tilde{H}$ as a function of a_h. Considerable change is possible in $\tilde{H}$ by increasing a_h, increasing the efficiency of turbulent heat transfer relative to momentum transfer. However, the largest values of a_h in the table appear to be physically improbable. Observations of a_h under near-neutral stratification lie in the range 1 to 1.35 (Businger et al., 1971).

Table 3.2. Surface $\tilde{H}$ at $\tilde{x} = 80,000$ as a function of a_h.

a_h	$\tilde{H}$ $\tilde{z}_0 = e^{-2}$, $\tilde{D} = 11$
1	.04960
1.5	.05953
2.	.06715
3.	.07662
4.	.08312

Table 3.3 gives surface $\tilde{H}$ as a function of $\tilde{D}$. It is clear that a very thick molecular layer should result in smaller heat flux, but it is seen that a very thin layer will also result in a smaller flux. The maximum heat flux occurs for D such that $K_h(D) = \kappa$, that is, for $\tilde{D} = 3.28$ when $a_h = 1$ and $\tilde{D} = 1.64$ when $a_h = 2$. Stated in simple terms, the heat flux will be largest when the largest available transfer coefficient is utilized. If D becomes very small,

K_h as formulated in this model will actually be less than κ, and a reduced heat flux will result. This behavior for small $\tilde{D}$ is purely an artifact of the model formulation and would be at variance with the physical situation. However, the reasonable estimates for $\tilde{D}$ are well above these critically small values. In a two-layered model, assuming an abrupt change from molecular to turbulent transfer, the molecular layer must be chosen large enough to encompass part of a transition layer. The choice of $\tilde{D} = 11$ was based on the thickness of a viscous layer necessary for the two-layered representation of the velocity profile over a flat plate. There appears to be no compelling reason at this time to choose a smaller value for $\tilde{D}$.

Table 3.3. Surface $\tilde{H}$ at $\tilde{x} = 80,000$ as a function of $\tilde{D}$.

$\tilde{D}$	$\tilde{H}$ $\tilde{z}_0 = e^{-2}$, $a_h = 1$	$\tilde{H}$ $\tilde{z}_0 = 11$, $a_h = 1$	$\tilde{H}$ $\tilde{z}_0 = 11$, $a_h = 2$
40	.02570	.02443	--
20	.03933	.03689	.04587
11	.04964	.04560	.06335
8	.05358	.04880	.07211
5	.05686	.05162	.08169
3.28	.05768	.05258	--
2	.05684	.05159	.09029
1.64	--	--	.09015
0.5	--	.04620	.08546

From Table 3.1, $\tilde{H}$ varies little with $\tilde{z}_0$; however, the height of the IBL increases significantly as $\tilde{z}_0$ increases. Figure 3.4 shows the isotherm $\tilde{\theta} = 0.001$ as a function of fetch for a wide range

of $\tilde{z}_0$, assuming $a_h = 1$ and $\tilde{D} = 11$. In a qualitative sense, Figure 3.4 indicates how much Figures 3.1, 3.2, and 3.3 should be stretched in the vertical to fit a rough case. The approximate 4/5 power law for IBL growth, which is mentioned by Elliott (1958), is confirmed here. Assigning an approximate slope to IBL growth depends on how the top of the IBL is defined, the roughness length, and the downwind distance involved. Considering flow over water for a fetch of tens of meters, the slope of the $\tilde{\theta} = 0.001$ isotherm is about 1/10, and the slope of the $\tilde{\theta} = 0.01$ isotherm is about 1/20.

3.3 The Badgley Data and Heat Flux Estimates

It is possible to calculate the average heat flux over a lead from the profiles of temperature and velocity at the upwind and downwind edges. Letting h be the height of the IBL at the end of a fetch of length f, conservation of heat implies

$$\int_0^h (\theta_A+\Delta\theta)(U_A+\Delta U)dz + \int_0^f \theta_A W(h)dx - \int_0^h \theta_A U_A dz = \int_0^f H(x,0)dx \tag{3-4}$$

where $\Delta\theta$ and ΔU are changes over the lead from the ambient θ_A and U_A. The second integral on the left may be rewritten using continuity,

$$\int_0^f W\theta_A dx = -\int_0^h \theta_A \int_0^f \frac{\partial U}{\partial x} dxdz = -\int_0^h \theta_A \Delta U dz \tag{3-5}$$

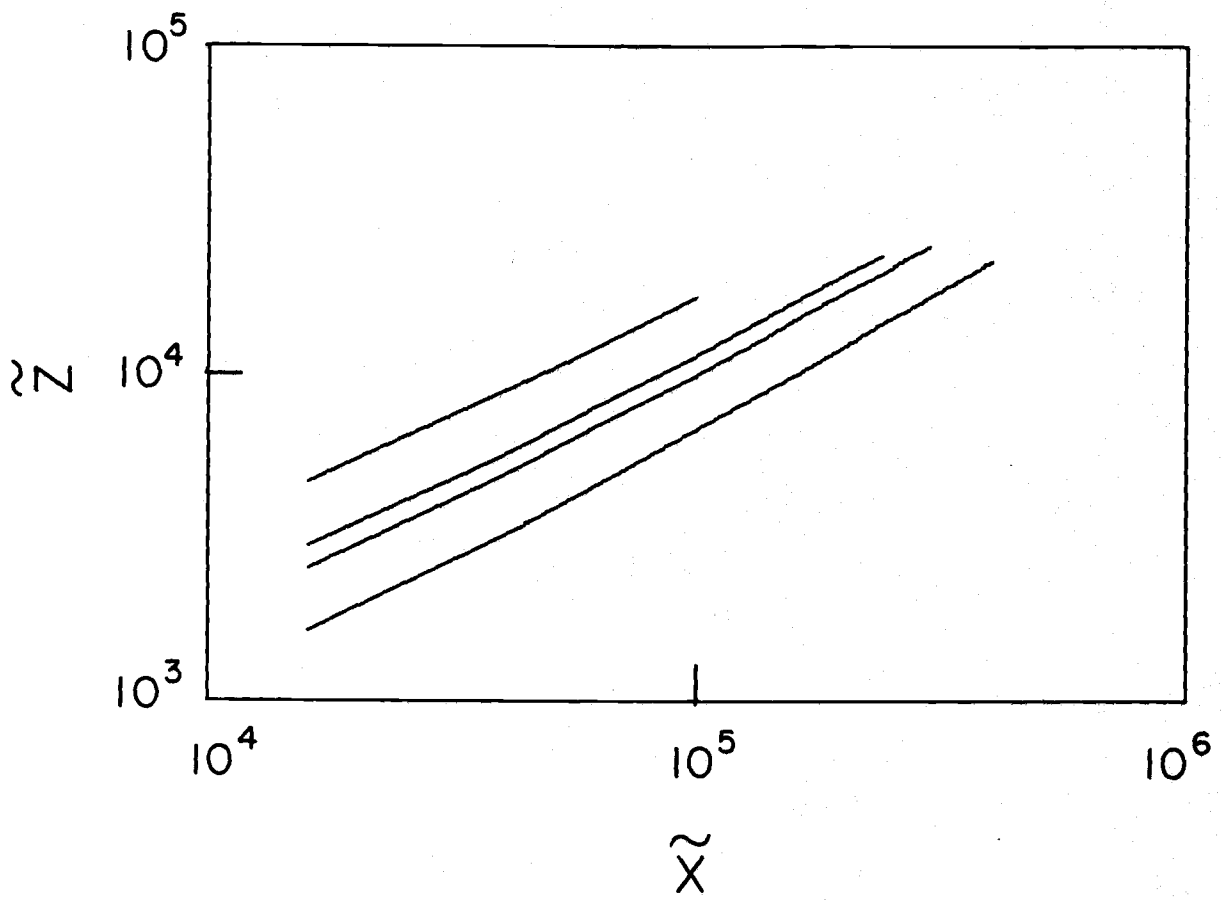

Figure 3.4. The isotherm $\tilde{\theta} = 0.001$ for surface roughness $\tilde{z}_0 = e^{-2}$, 4.28, 11 and 100 (IBL height increasing with $\tilde{z}_0$).

So then,

$$\int_0^f H(x,0)dx = \int_0^h \Delta\theta(U+\Delta U)dz \qquad (3\text{-}6)$$

Equation (3-6) provides a means of computing the total heat flux at the surface of the lead by knowing the temperature increase and velocity at all levels. In reality data will be taken at distinct levels, but the data points could reasonably be connected with logarithmic arcs, making possible a piecewise, closed integration of the right side of (3-6). Such a method of heat flux estimation will be termed the flow method.

Badgley (1966) reported measurements of temperature and velocity profiles at the downwind edge of a 20 meter artificial pond at Barrow, Alaska; the data is presented in Table 3.4. The integral of heat flux (3-6) was computed piecewise as described above; the results in Table 3.5 are presented for each level in order to emphasize that significant portions of the calculated flux are accounted for in the higher levels where temperature changes are slight. The temperature profile should be accurate to 0.01°C to obtain accurate flux estimates. If, for instance, 0.1°C is subtracted from each non-zero $\Delta\theta$ in Table 3.4, the calculated heat flux will drop 15%. Thus, any bias between the upwind and downwind sensors could substantially alter the results. Despite its potential inaccuracy, the flow method is attractive because it provides an average heat flux over the lead and does not

Table 3.4. Badgley data at 20 meter fetch.

Height cm	θ_A	$\Delta\theta$	$U_A + \Delta U$
0	-26.5	24.8	0
5	-27.0	5.6	160
10	-27.2	3.8	195
20	-27.2	2.1	215
40	-27.2	1.6	230
60	-27.2	1.3	250
80	-27.2	0.9	265
100	-27.2	0.7	275
150	-27.2	0.5	290
200	-27.2	0.3	320
300	-27.2	0.2	360
400	-27.2	0.0	390

Table 3.5. Integral (3-6) computed between each level assuming logarithmic profiles between Badgley's data points.

Level (cm)	Excess Heat Flow (milliwatts)
0- 5	5754
5- 10	5330
10- 20	7608
20- 40	10561
40- 60	8997
60- 80	7297
80-100	5589
100-150	10897
150-200	7821
200-300	10901
300-400	4585
0-400	85344

rely on assumptions concerning a_h, D or z_H. The average heat flux computed from Badgley's data is 42.7 mw/cm^2 over the 20 meter fetch.

Badgley, using the "aerodynamic method," estimates a heat flux at 20 meters of 29.1 mw/cm^2 (18.2 Kcal/cm^2 per month). This estimate seems consistent with that from the flow method, reflecting a drop of heat flux with fetch. However, for the purpose of computing the heat flux, Badgley assumes $z_0 = z_H$, taken as 0.02 cm over water. Under the conditions of the Badgley experiment this would set z_H to about $2\nu/u_*$, a value which is in direct conflict with the supposition of a molecular sublayer for heat (see Section 3.5).

3.4 Temperature Profiles Generated by the Model under Conditions of the Badgley Experiment

Badgley's (1966) experimental data, consisting of temperature and velocity profiles at a 20 meter fetch over an artificial pond, are the best available. The ambient air is at -27.2°C while the water is at -1.7°C. The wind profile shown in Figure 3.5 is well approximated below 1.5 meters by a logarithmic expression with $u_* = 16$ cm/sec and $z_0 = 0.096$ cm (in this case about equal to $11\,\nu/u_*$). The above values define θ_A, θ_B, u_* and z_0 which will be used to form the initial and boundary conditions in the model for any dimensional case which seeks to simulate the Badgley experiment. Above

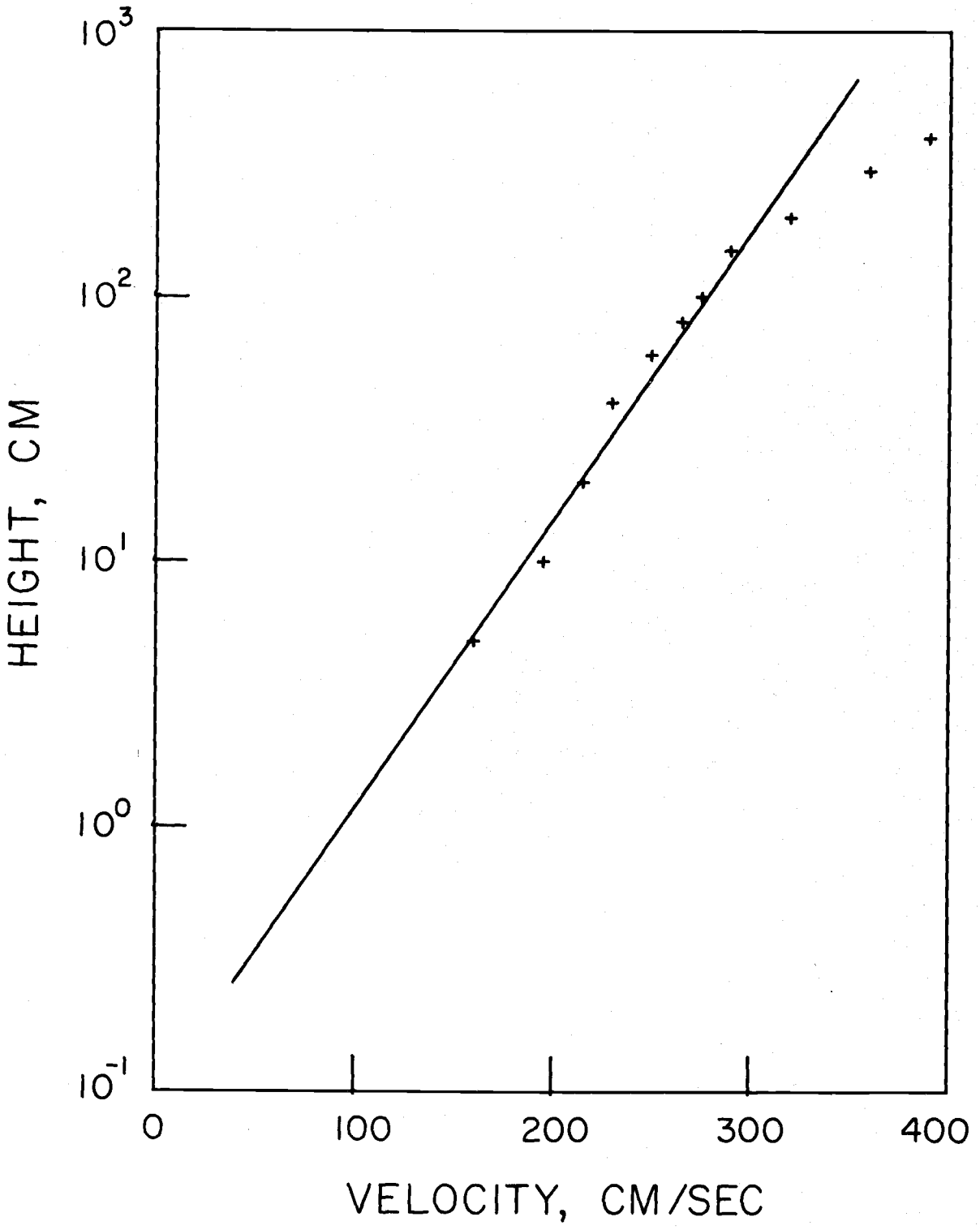

Figure 3.5. The Badgley wind data and the log-profile used for the model initial condition.

1.5 meters the wind data deviates from the log-profile so as to indicate stable stratification. For simplicity this deviation was not incorporated into the model initial conditions, since it was above the region of most radical change in the IBL. It is commonly accepted that z_0 over water is about 0.023 cm (Kondo et al., 1973); thus it is possible that the Badgley wind profile at 20 meters reflects a larger upwind roughness or the effect of stability.

Figure 3.6 presents the Badgley temperature profile at 20 meters and results of the model using $\alpha_h = 1$ and $\alpha_h = 2$ and two different lower boundary conditions. Condition 1, the lower condition advocated in this paper, enforces an equality between molecular and turbulent heat fluxes at the top of the molecular sublayer. Condition 2 sets the temperature at the roughness length to the surface temperature (Taylor, 1970). The surface heat fluxes corresponding to Figure 3.6 are given in Table 3.6 and are generally 10 to 15 percent lower than the average over the lead. Condition 1 imposes a theoretical maximum on the flux, about 65 mw/cm^2 in the Badgley case, so the rise in flux is less dramatic than for Condition 2 as α_h increases. There are two reasons for preferring Condition 1 over Condition 2. First, for this one temperature profile, Condition 1 produces a much better fit, especially at low levels. The turbulent layer under Condition 1 senses, not the surface temperature, but a temperature substantially reduced by a molecular layer. The second reason for

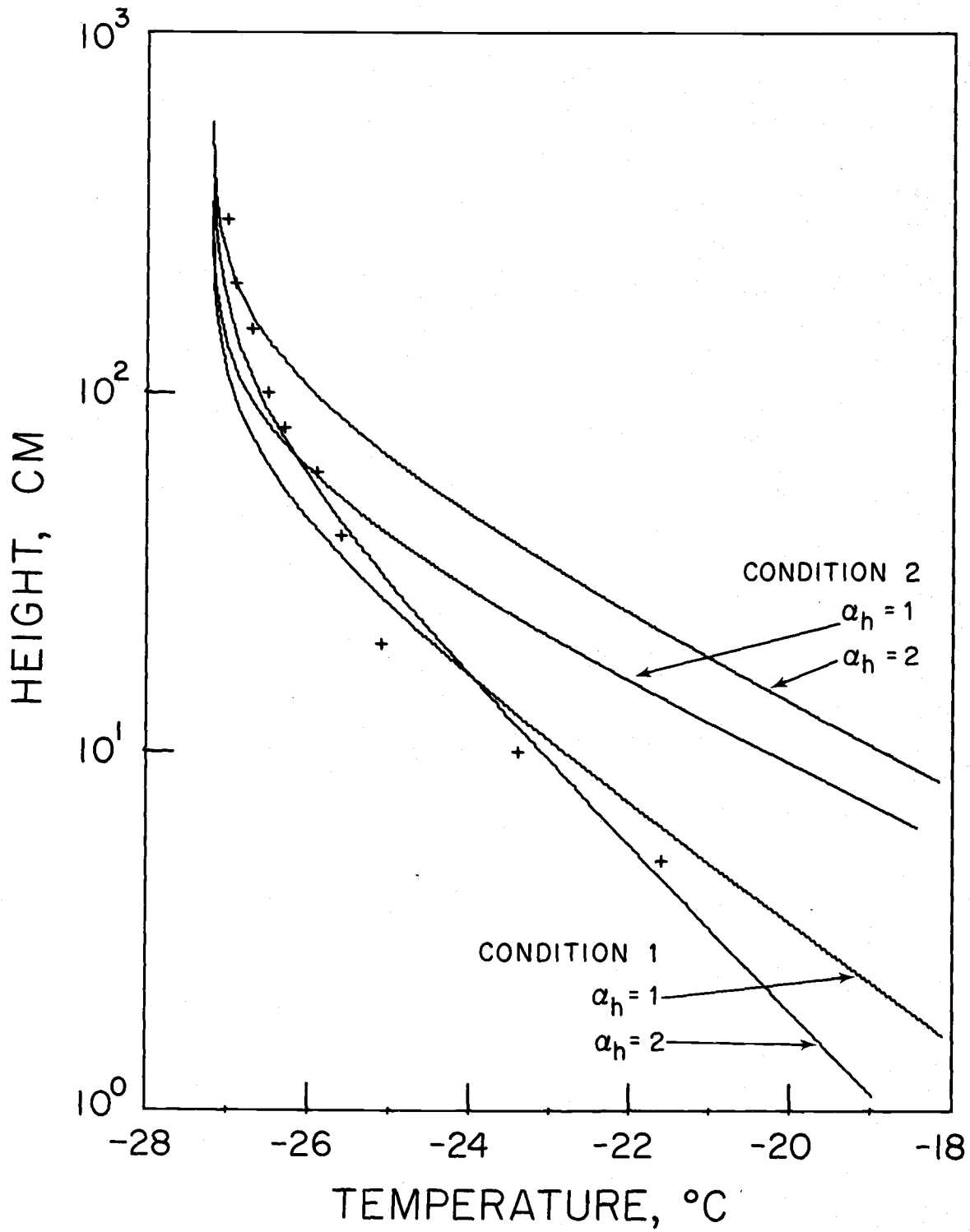

Figure 3.6. The Badgley temperature data and model results.

preferring Condition 1 is found in the behavior of the temperature profile with increasing a_h. It is a reasonable expectation that higher surface heat flux will be coincident with colder air adjacent to a warm surface, under any given boundary condition. Whereas heat flux increases with a_h under both Conditions 1 and 2, only under Condition 1 is this increase accompanied by a colder air adjacent to the surface. In fact, under Condition 2 the behavior of the temperature profile is opposite to expectation, showing increased air temperature at all levels with increased heat flux. Therefore, use of Condition 2 produces a model inconsistent with the concept of a surface molecular layer. Even if the assumed z_0 is reduced so that the model under Condition 2 would fit the data in Figure 3.6, this inconsistency would remain. Furthermore, in Section 3.5 it is shown that z_H should scale with ν/u_*, in contrast to z_0 which is approximately independent of u_*.

Table 3.6. Surface heat fluxes corresponding to Figure 3.6.

Condition	a_h	Flux (mw/cm^2)
1	1	22.1
1	2	31.5
2	1	33.6
2	2	61.7

In view of the relatively good fit of the temperature data when treating heat as a passive contaminant, it may be possible to obtain reliable heat flux estimates by refining the estimate of D and choosing a suitable constant value of a_h. In reality, a_h is a function of Ri and hence z (Businger et al., 1971). It may be that this dependence could explain why the model predicts higher temperatures at low levels and lower temperatures at high levels as compared to the data in Figure 3.6.

3.5 A Relation between D, z_H and a_h

In a two-layer model with molecular layer of thickness D, there will be a relation between D and the roughness parameter of the variable under consideration, temperature or velocity. In the case of temperature, the relation will also include a_h. A constant flux layer will exist near the surface where a logarithmic temperature profile is expected to hold just above the molecular layer.

$$\theta(z) = \theta(D) - \frac{H}{a_h u_* k} \ln (z/D) \tag{3-7}$$

Defining z_H such that $\theta(z_H) = \theta_B$ leads to

$$\tilde{z}_H = \tilde{D} \exp(-a_h \tilde{D} \nu k/\kappa) \tag{3-8}$$

The corresponding expression for momentum over a flat plate is

$$\tilde{z}_0 = \tilde{D} \exp(-k\tilde{D}) \qquad (3\text{-}9)$$

Data has shown that $\tilde{z}_0 = e^{-2}$ so that $\tilde{D} = 11$ for a two-layer momentum model. In the case of temperature, (3-8) implies a locus of $(a_h, \tilde{D})$ for a single value of $\tilde{z}_H$. Figure 3.7 displays such loci over a wide range of $\tilde{z}_H$; this figure provides a ready reference once $\tilde{z}_H$ are experimentally determined and also some indication of the magnitude of $\tilde{z}_H$ to be expected. For example, if the two-layer temperature model is essentially correct and a_h is greater than unity, then it is seen that $\tilde{z}_H$ will not exceed 1.1. Accurate determination of $\tilde{z}_H$ would require a large vertical gradient in temperature, a situation likely to occur only following an abrupt and substantial change in surface temperature.

If $\tilde{z}_H$ is determined from a low level temperature profile and an independent measurement of heat flux, $\overline{\theta w}$, is made, then a_h and $\tilde{D}$ will be determined. The procedure will be illustrated here using the lowest data points of the Badgley profile (Table 3.4). For illustrative purposes, the Badgley heat flux estimate of 29.1 mw/cm^2 is adopted as though it were an independent measurement of $\overline{\theta w}$, and the friction velocity is taken as 16 cm/sec based on the Badgley velocity profile. The temperature profile in the turbulent layer is written

$$\theta(z) = -1.7 + A \ln(z/z_H) \qquad (3\text{-}10)$$

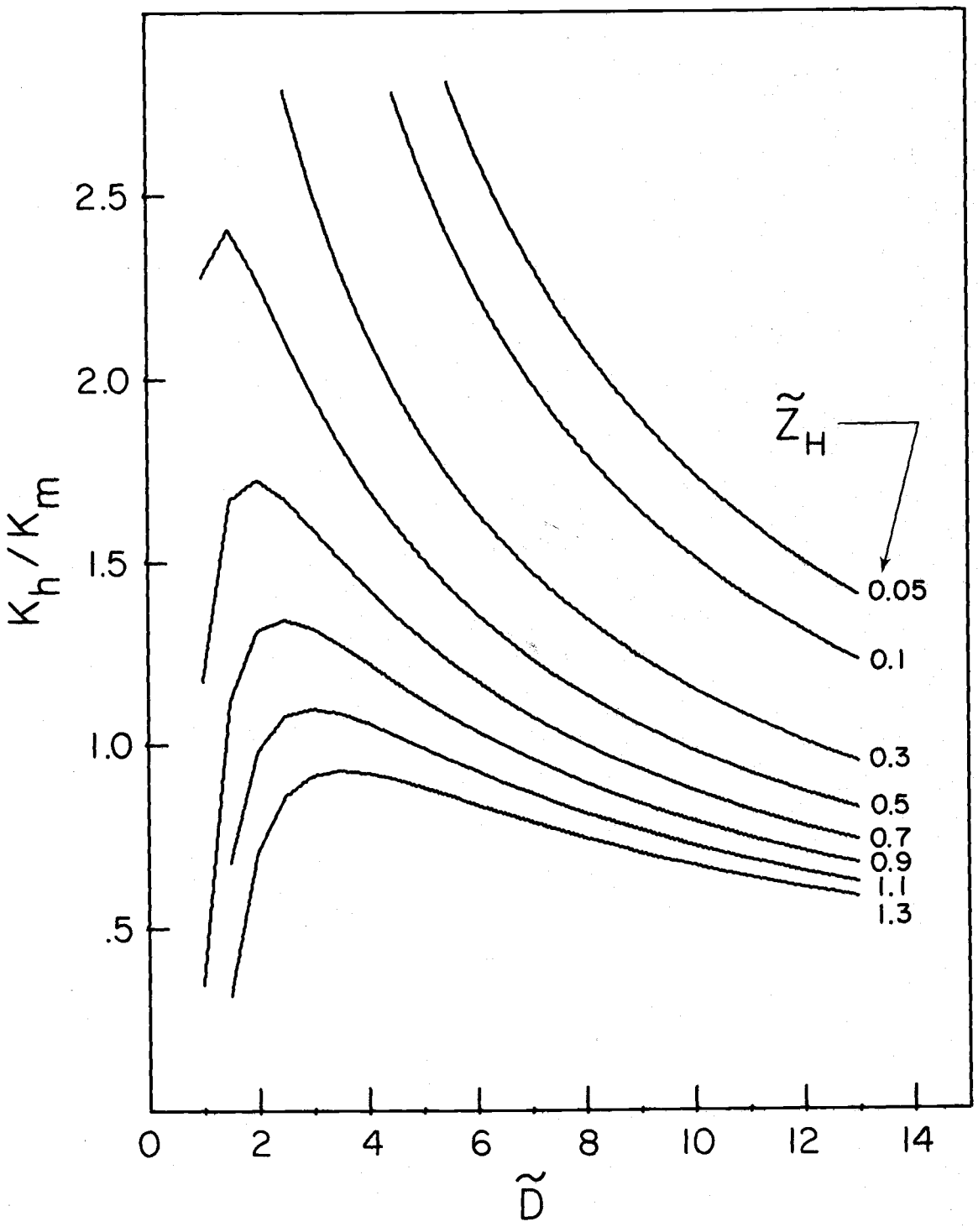

Figure 3.7. The relation between α_h, $\tilde{z}_H$ and $\tilde{D}$.

where

$$A = -H/\alpha_h k u_* \tag{3-11}$$

and A may be determined by any two points.

$$A = (\theta(z_1)-\theta(z_2))/\ln(z_1/z_2) \tag{3-12}$$

The temperature roughness parameter is then determined.

$$z_H = z_1 \exp(-(\theta(z_1)+1.7)/A) \tag{3-13}$$

Results of calculations using (3-8), (3-11), (3-12) and (3-13) are presented in Table 3.7.

Table 3.7. Triads of $\tilde{z}_H$, $\tilde{D}$ and α_h based on the Badgley experiment.

z_1, z_2 (cm)	A	$\tilde{z}_H$	α_h	$\tilde{D}$
5, 10	-2.597	.268	1.35	8.38
5, 20	-2.525	.216	1.38	8.80
10, 20	-2.453	.164	1.42	9.36

A pairwise determination was made in order to point out the difficulty in calculating $\tilde{z}_H$ accurately, even though the temperature gradient is large and the lower points are virtually along the same logarithmic arc (see Figure 3.6). The values of α_h are close to those found by Businger et al. (1971) while the corresponding $\tilde{D}$ are somewhat smaller than the value for momentum. When using a

particular set of $(\alpha_h, \tilde{D})$ in the numerical model, the only result which is guaranteed is that $\tilde{z}_H$ will be maintained according to (3-8). However, using $\alpha_h = 1.38$ and $\tilde{D} = 8.8$ in the model gave a heat flux of 28.2 mw/cm^2 at 20 meters fetch. In other words, the model predicted a heat flux very close to the one assumed in order to determine α_h and $\tilde{D}$. This internal consistency in the theory spurs the hope that a pair of α_h and $\tilde{D}$ may be found which will allow the model to accurately predict heat flux in the lead situation.

The above analysis assumed the Badgley flux estimate was independent in order to illustrate a procedure to be used when more data is gathered. A more straight forward approach might be to accept $\alpha_h = 1.35$ based on Businger et al. (1971). The temperature profile would then imply a flux of about 29 mw/cm^2, (3-8) will collapse to a simple relation between $\tilde{D}$ and $\tilde{z}_H$, and $\tilde{D}$ will be estimated at about 9. At this point, however, revision of the value of $\tilde{D}$ is unwarranted because of the little data available. From Table 3.3 it is seen that changing $\tilde{D}$ from 11 to 9 in the model would increase the predicted heat flux less than 5%.

Wind tunnel data (Bau On Young, 1973) over a free water surface exhibit major differences from those taken over a flat plate (see Appendix B). The measured value of α_h is about 2, and the temperature profiles indicate that the molecular layer has a thickness of about $6\,\nu/u_*$. In fact, the temperature profiles do not in all cases

agree with the concept of a molecular sublayer. However, over a water surface, profiles might be distorted by latent heat release or a divergence of the radiative flux. Non-dimensional heat fluxes measured in the wind tunnel average 0.079, whereas the model with $a_h = 2$ and $\tilde{D} = 6$ yields $\tilde{H} = 0.078$. There is some increase in surface stress with fetch, but it is not clear whether this is due to increased surface roughness or buoyancy effects. Ultimately, the success of the eddy diffusivity model as a predictor rests in establishing universal values of the basic model parameters, a_h and $\tilde{D}$. Experimental data is needed to show if indeed one set of these parameters is always applicable to a given situation.

3.6 The Independence of z_0 and z_H on Slightly Rough Surfaces

Some models (Elliott, 1958; Taylor, 1970) have used a lower boundary condition equivalent to asserting that z_0 and z_H are identical. On the other hand, it has been a basic tenet of this study that the near-surface transfer processes for heat and momentum are dissimilar, and thus there is no foundation for asserting a relation between the roughness parameters. Arguments in favor of the latter proposition, as well as comparative model results, have been presented. However, since the issue is of such importance, additional data will be examined. Recently Garratt and Hicks (1973) have summarized a large number of simultaneous z_0 and z_H measurements

which indicate that the roughness parameters are not only unequal but probably independent for $Re_*(u_*z_0/\nu)$ less than about 50. This range of Re_* would include most atmospheric flows over water.

Garratt and Hicks point out that if one assumes additivity of the molecular and eddy diffusivities,

$$K_h = a_h u_* k z + \kappa \tag{3-14}$$

then

$$z_H = \kappa / a_h u_* k \tag{3-15}$$

Before concluding that this is a reasonable estimate, it should be noted that the corresponding result for momentum is

$$z_0 = \nu / u_* k \tag{3-16}$$

Expression (3-16) is derived by assuming that molecular viscosity becomes the dominant mechanism for momentum transfer at the surface; such a circumstance would seem to imply the modeling of flow over a flat plate. However, the roughness length for a flat plate is at least an order of magnitude smaller than that given in expression (3-16), and therefore, one might suspect also that (3-15) would substantially overestimate the magnitude of z_H. Indeed, based on the Badgley data, Table 3.7, this seems to be the case.

Figure 3.8 is an adaptation of Figure 2 of Garratt and Hicks, showing the bands encompassing data gathered from numerous sources. Also shown is the line which results from (3-15). Atmospheric flows over water will have $Re_* < 50$, where Re_* and $\ln(z_0/z_H)$ maintain a single valued relation. However, this relation by no means implies that there is a relation between z_0 and z_H.

It might generally be assumed that z_H scales with the length scale ν/u_*. So,

$$z_H = C\nu/u_* \tag{3-17}$$

where C is some constant. Dividing both sides of (3-17) by z_0 and taking logarithms,

$$\ln(z_0/z_H) = \ln(10) \cdot \log_{10}(Re_*) - \ln(C) \tag{3-18}$$

No relation between z_0 and z_H is implied. Plotted on Figure 3.8, (3-18) will be a line with (linear) slope of $\ln(10)$. Thus, the assumption that z_H is independent of z_0 and inversely proportional to u_* will result in a family of parallel lines, of which line (a) in Figure 3.8 is just one. Because the general data trend follows the same slope, the assumptions on z_H may be deemed correct. The constant of proportionality C in (3-18) will control the ordinate of the line, and the value $C \approx 3.3$ from (3-15) could be reduced to $C \approx 1$ while still producing a line within the data band. However, use

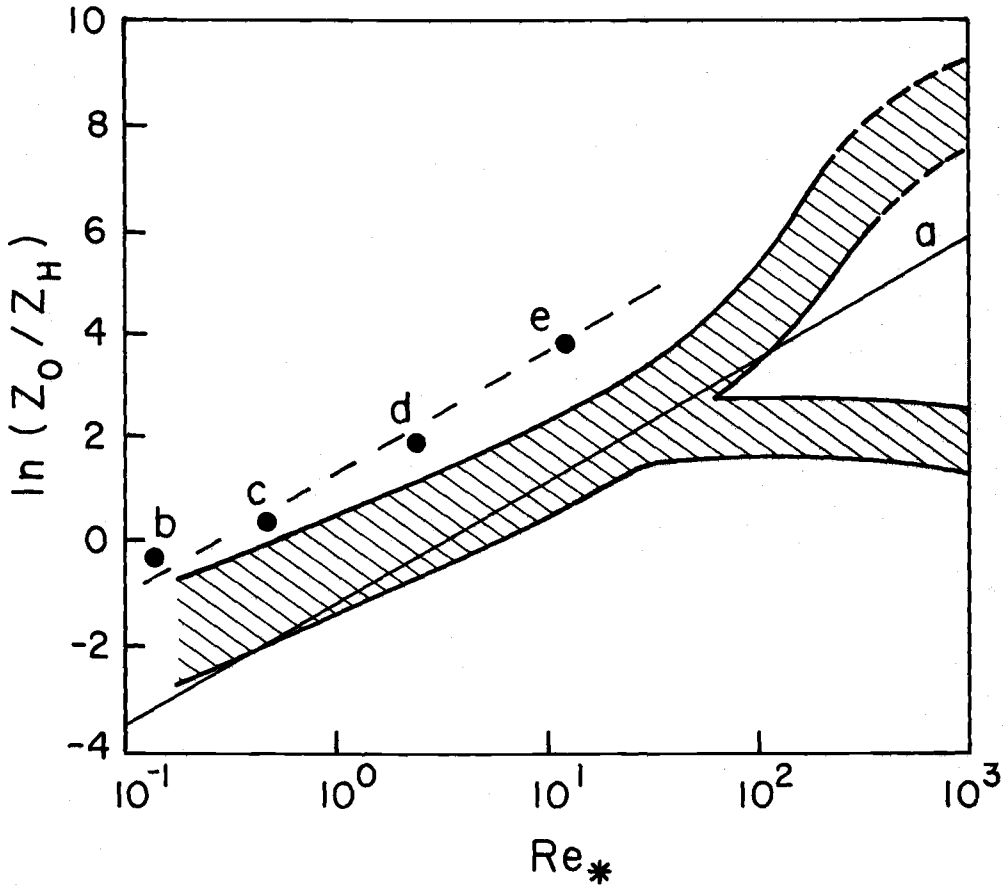

Figure 3.8. Bands encompassing data from simultaneous z_0 and z_H measurements. Line (a) expresses (3-15) with $a_h = 1$. Adapted from Garratt and Hicks (1973). Points b, c, d and e are computed by the present author based on the data of Bau On Young (1973) and Badgley (1966).

of $C \approx 0.2$ indicated by the Badgley data, Table 3.7, is not supported by the data compiled by Garratt and Hicks.

Additional points in Figure 3.8 have been calculated by the present author from the available data which was taken following an abrupt increase in surface temperature. Points b, c and d are based on the wind tunnel data of Bau On Young et al. for a flat plate (b) and free water surfaces with friction velocities of 18.2 cm/sec (c) and 36.5 cm/sec (d). The point e is based on Badgley's data over an artificial lead. The dashed line is parallel to line (a) and indicates independence of z_0 and z_H.

There seems to be a conflict between the newly computed points and the previous data. It should be recognized that the data compiled by Garratt and Hicks were taken under conditions approaching horizontal homogeneity; the largest temperature gradients resulted from changes of only two degrees between the surface and 10 meters height. The difficulty in determining z_H even with a large near-surface gradient has been demonstrated in Table 3.7. The very width of the data band in Figure 3.8 attests to this difficulty, reflecting a factor of seven in the determination of z_H. A question remains as to why the estimates of z_H indicated by the data band are systematically higher than those based on the temperature-change experiments.

4. CHANGES IN STRESS AND ALTERATION OF THE WIND PROFILE

4.1 The Stress Conservation Equation

Development of a method for modeling stress and velocity changes seems particularly difficult, principally because the appearance of a stress dissipation term in Equation (2-3) which is unknown in terms of mean quantities. Before proceeding, it is well to imagine the type of stress and velocity profiles which may result over a lead. Assuming a constant stress layer with a logarithmic wind profile initially and no change in surface roughness, it is clear that there will be increases in stress near the surface. There would be two simple stress profiles possible; the first would be monotonically decreasing from the surface to the top of the IBL, while the second would have a maximum at an intermediate level. Convective plumes would tend to overturn the flow in the IBL, bringing higher velocities to low levels and lower velocities to high levels. This type of velocity redistribution would be consistent with a stress profile having an intermediate maximum. Figure 3.5 presents the wind data from Badgley's experiment with the logarithmic profile assumed in the model for initial conditions. An S-shaped alteration of the wind profile may be indicated, but, since no initial profile is given by Badgley, no direct comparisons are possible between the data and model results. Ignored

in this study is the possibility that a roughness change may contribute to the velocity changes. It is likely that roughness would decrease from ice to open water, although the change is expected to be small for Badgley's data.

Taylor (1970) presents numerical solutions of the horizontal momentum, heat and continuity equations for a case considering only a surface temperature change. In Taylor's method, stress is computed indirectly using universal relationships holding under conditions of horizontal homogeneity. The resulting stress profiles appear unstable near the top of the IBL and wind velocity shows increases at all levels. Although it is difficult to avoid the assumption of horizontal homogeneity completely, for instance in choosing an empirically determined constant, it is probably unwise to make it a cornerstone of the theory, since the situation being studied is distinctly inhomogeneous. The inclusion of a stress conservation equation seems advisable.

Peterson (1969) transformed the turbulent energy equation to a stress equation by using the empirical relation that stress is approximately 0.16 of turbulent energy in the boundary layer. Although Peterson was concerned with a roughness change only, a buoyancy production term could be added giving Equation (4-1).

$$U \frac{\partial \tau}{\partial x} + W \frac{\partial \tau}{\partial z} = C_1 \tau \frac{\partial U}{\partial z} - \epsilon + \frac{\partial}{\partial z} \left(K \frac{\partial \tau}{\partial z} \right) + C_2 \frac{g}{T_0} \overline{\theta w} \qquad (4\text{-}1)$$

with $C_1 = C_2 = 0.16$ and $\epsilon = C_1 \tau^{3/2}/kz$. Before any judgement is made on the appropriate values of the constants C_1 and C_2, it is interesting to look at the reduced moment equation (2-3). The mechanical production term will be rewritten using $\overline{w^2} = -1.1\ \overline{uw}$ (Lumley and Panofsky, 1964), although some recent data (Haugen et al., 1971) suggest that $\overline{w^2} = -1.7\ \overline{uw}$. Monin and Yaglom (1972, p. 667) point out that the eddy viscosity tensor K_{ij} has significant off diagonal terms and so

$$\overline{\theta u} = -K_{xz} \frac{\partial \theta}{\partial z} - K_{xx} \frac{\partial \theta}{\partial x} \qquad (4\text{-}2)$$

where

$$K_{xz}/K_{zz} \approx -3$$

$$K_{xx} \approx K_{zz} = K_m$$

This author has verified that the second term on the right of (4-2) will be negligible compared to the first in the Badgley lead situation. Thus Equation (2-3) may be written as (4-1) with $C_1 = 1.1$ and $C_2 = 3$; presumably under neutral, homogeneous conditions $\epsilon = C_1 \tau^{3/2}/kz$. The moment equation therefore would have production and dissipation terms an order of magnitude larger than those in the equation derived by Peterson. The difficulty in adapting the turbulent energy equation as a stress equation lies in ascribing rates of production in the same ratio as the quantities themselves. Two reservoirs may have storage

in a fixed ratio but that implies nothing about the flows in and out of them.

There is additional support for using the higher values of C_1 and C_2 in that the observed non-dimensional wind shear for small z/L may be derived from the reduced moment equation. In near neutral conditions with $\epsilon = C_1 \tau^{3/2}/kz$ and taking a constant flux layer, Equation (4-1) reduces to

$$C_1 [u_*^2 \frac{\partial U}{\partial z} - \frac{u_*^3}{kz}] + C_2 \frac{g}{T_0} \overline{\theta w} = 0 \qquad (4\text{-}3)$$

which becomes

$$\phi_m = 1 - (\frac{C_2}{C_1}) \frac{z}{L} \qquad (4\text{-}4)$$

Observations by Businger et al. (1971) set C_2/C_1 at about 3, for unstable stratification and small z/L. This ratio is consistent with the above individual values which will be retained, although a slight adjustment of C_2 may be justified so that C_2/C_1 would agree exactly with the data. This computation also implies that the very near surface constant flux layer following a change in surface conditions will have a log-linear profile and Equation (4-3) should be used to state the lower boundary condition on stress as given in (2-7).

4.2 The Roughness Change Re-examined

In view of the relative success of Peterson (1969) and Shir (1972) in fitting the data of Bradley (1968), the presumption of a radically higher value for C_1 should be tested in the roughness-change problem. It is not the purpose here to make a complete analysis but only to determine the influence of the magnitude of C_1 on the surface stress following an abrupt change in surface roughness. The equations and boundary conditions used are those of Peterson; only the numerical technique differs. The stress equation is

$$U \frac{\partial \tau}{\partial x} + W \frac{\partial \tau}{\partial z} = C_1 \tau \left[\frac{\partial U}{\partial z} - \frac{\tau^{1/2}}{kz} \right] + \frac{\partial}{\partial z} \left(K \frac{\partial \tau}{\partial z} \right) \qquad (4\text{-}5)$$

while the horizontal momentum equation is (2-2). Shir's approach was somewhat different, using the vorticity equations with $C_1 = 0.22$. Letting $M = \ln(z_0'/z_0)$, where the prime indicates upwind roughness, cases were run to moderate fetch for $M = -4.82$ and $M = +4.82$, the smooth-to-rough and rough-to-smooth cases corresponding to the Bradley data. The problem is non-dimensionalized by the larger of z_0 and z_0'. Figure 4.1 shows the results of the cases run; the vertical scale has been chosen to accentuate the differences in the curves, and should not obscure the fact that the curves are quite similar. It should be recalled that Bradley found near-equilibrium

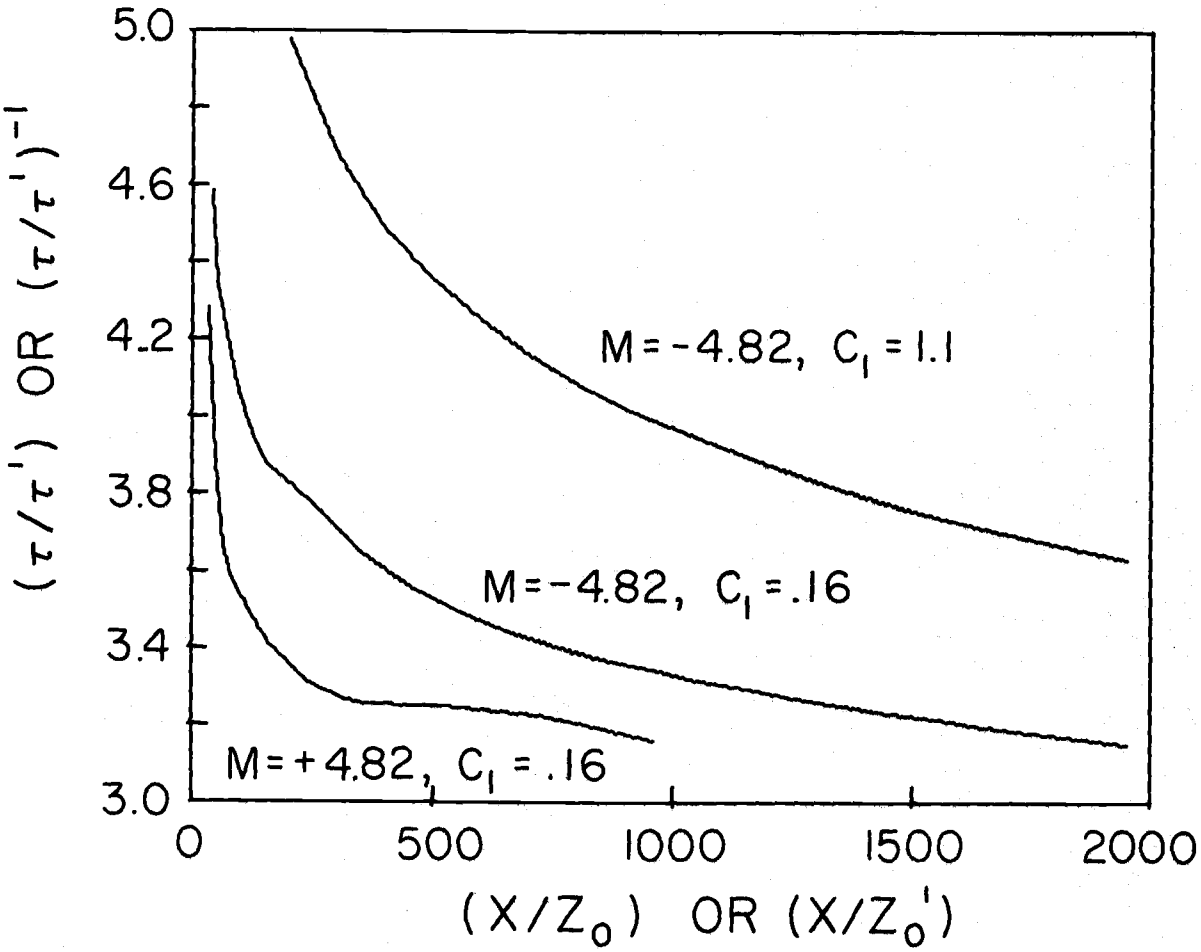

Figure 4.1. Non-dimensional surface stress (inverse of surface stress) as a function of x/z_0 (x/z_0') for smooth-to-rough (rough-to-smooth) case M = -4.82 (M = +4.82). Roughness change only.

values $\tau/\tau' = 3.1$ and 0.32 for $M = -4.82$ and 4.82 respectively, at fetches of 1000 and 1600.

For the smooth-to-rough case with $C_1 = 0.16$ there is good agreement with the data and previous models. Use of $C_1 = 1.1$, gives stress predictions about 15% higher after a moderate fetch of 2000, although the curves appear to be converging. It thus seems that a smaller value of C_1 is indeed desirable in the smooth-to-rough case.

For the rough-to-smooth case with $C_1 = 0.16$ the equilibrium stress value is again approached but more rapidly than in either the data or Shir's results. Comparison with Peterson's results suggests that he had computational difficulties in this case, predicting smaller stress values. Shir had supposed that his agreement with Bradley's data was due to use of the vorticity equations. The case was not run with $C_1 = 1.1$ because of prohibitive computer time requirements. The numerical method developed for the temperature problem is very inefficient when applied to the roughness change problem.

It is no accident that the equilibrium values of τ and τ^{-1} are nearly the same for M of equal magnitude and opposite sign. Equation (4-5) may be transformed to an equation in τ^{-1}

$$U \frac{\partial \tau^{-1}}{\partial x} + W \frac{\partial \tau^{-1}}{\partial z} = C_1 \tau^{-1} \left[\frac{\tau^{1/2}}{kz} - \frac{\partial U}{\partial z} \right]$$

$$+ \frac{\partial}{\partial z} \left(K \frac{\partial \tau^{-1}}{\partial z} \right) + 2 \frac{\partial \tau}{\partial z} \frac{\partial \tau^{-1}}{\partial z} / \frac{\partial U}{\partial z} \qquad (4\text{-}6)$$

The last term on the right of (4-6) is a second order term in the stress gradient, which should be small near the surface. It has the same magnitude as the small part of $\frac{\partial K}{\partial z} \frac{\partial \tau^{-1}}{\partial z}$ in the diffusion term.

$$\frac{\partial K}{\partial z} = \frac{\partial \tau}{\partial z} / \frac{\partial U}{\partial z} - \tau \left(\frac{\partial U}{\partial z} \right)^{-2} \frac{\partial^2 U}{\partial z^2} \qquad (4\text{-}7)$$

Equations (4-5) and (4-6) are highly similar. Remembering that the velocities and transfer coefficient scale with $\tau^{1/2}$, the values predicted for τ from Equation (4-5) due to a sudden increase in $\frac{\partial U}{\partial z}$ (smooth-to-rough) should be similar to those predicted for τ^{-1} from Equation (4-6) due to a sudden decrease in $\frac{\partial U}{\partial z}$ (rough-to-smooth).

These numerical experiments suggest that C_1 affects the rate at which the surface stress approaches its equilibrium value but does not alter the value approached. Higher C_1 produce slower convergence. Large changes in the value of C_1 make relatively minor changes in the predicted stress. However, for $M = -4.82$ a value of about 0.2 seems to best fit Bradley's data. For M of equal magnitude and opposite sign, the equilibrium stress predictions

will be recipricals.

The previous analysis points up the difficulty in applying an equation which holds under homogeneous conditions to the change-of-terrain problem. Examining Equation (4-5) vis-a-vis the stress moment equation (2-3), it is apparent why a single value of C_1 is not appropriate in the roughness-change problem. The $C_1\tau$ factor on the right side of (4-5) is more correctly $\overline{w^2}$, which would tend to change slowly. When surface roughness suddenly increases, τ becomes large because the same vertical velocity fluctuations are in the presence of an increased velocity gradient. In terms of the new τ, $\overline{w^2}$ is small and hence a small value of C_1 will provide a more accurate representation in the transition region. When the roughness suddenly decreases, a higher value of C_1 would be better. It is believed that $C_1 = 1.1$ is a proper average value, but is inaccurate when dealing with very large roughness changes. Because of the interrelation in the various moment equations, there would be a distinct advantage in carrying the entire set in the calculations. For the heat problem the situation is different. There is no sudden, step change in the velocity gradient or stress, and for this reason the use of $C_1 = 1.1$ should be more acceptable.

This section has sought to demonstrate how assumptions, which are reasonable under horizontally homogeneous conditions, may be in error when applied to the change-of-terrain problem.

4.3 The Dissipation of Stress

The word "dissipation" used here is a carry-over from its use with the turbulent energy equation. The dissipation term is a sink term in the $\overline{uw}$ moment equation arising from the pressure-velocity correlation; the sink is not viscous dissipation, but rather it is erasure due to the onset of isotropy at the low frequency end of the inertial subrange.

The assumed, explicit form for dissipation

$$\epsilon = C_1 \tau^{3/2}/kz \tag{4-8}$$

has some essential properties. First it equals mechanical production in the constant flux layer of the neutral atmosphere. Second, after the change in surface temperature, it will equal total production (mechanical and buoyant) if the velocity profile is log-linear in the near-surface constant flux layer. These two properties alone make (4-8) desirable since they would promote the transition from one equilibrium state to another. Whether or not (4-8) represents dissipation accurately in the transition region is not immediately evident.

The computational method developed primarily to treat the heat equation was found inadequate to solve (4-1) with (4-8), when any substantial heat flux was present. For this reason an implicit form for ϵ was sought which would not introduce a strong non-linearity

into the equation, and thus render it unsolvable by the developed method. It was perhaps fortunate that this difficulty arose since it led to greater physical insight into the behavior of (4-8) in the transition region.

Most of the IBL is a transition region where production and dissipation of stress are out of balance. The approximate balance that existed has been disrupted by a change in surface characteristics, and a new equilibrium is being sought. In order to formulate an acceptable implicit dissipation term, emphasis is placed on the nature of production and dissipation and their imbalance in the IBL. Production of stress occurs on large scales while its destruction takes place on small scales. There is a time delay within a parcel of air between a production increase and the corresponding dissipation adjustment, and this delay translated into a down-stream distance. While following a fluid element, the central question which must be answered is: If an abrupt increase occurs in stress production, how long will it take for the dissipation to rise to the same level?

Tennekes and Lumley (1972) discuss the various time scales of turbulence in detail. Given a length scale l and a velocity scale u, turbulent energy dissipation is about u^3/l. This implies that a significant portion of the energy of large scale eddies is lost indirectly to dissipation in one turn-over time (l/u). The energy of the large scale eddies must be passed down the energy cascade and start

arriving at the dissipation level. If extra energy were added at large scales, the dissipation would adjust on this time scale. The same scale will be adopted for stress. In the boundary layer, the length scale will be $0.4z$ while the velocity scale will be $\sqrt{-uw}$; the time scale t' is formed from their quotient. It is assumed that for a parcel of air moving with the mean flow the time rate of change of dissipation will be proportional to the net production (production minus dissipation) and inversely proportional to the local time scale. Using P for total production,

$$\frac{d\epsilon}{dt} = \frac{A(P-\epsilon)}{t'} \tag{4-9}$$

Once the constant of proportionality has been set, (4-9) provides an implicit ϵ which may be numerically implemented. The form insures a smooth transition from one equilibrium state to another. In addition, the form is consistent with intuitive ideas about the adjustment of ϵ in the transition region. However, by taking the time derivative of (4-8), the same behavior of ϵ in the transition region is evidenced.

$$\frac{d\epsilon}{dt} = \frac{3}{2} C_1 \frac{\tau^{1/2}}{kz} \frac{d\tau}{dt} \tag{4-10}$$

In (4-10), $t' = kz/\tau^{1/2}$ and $d\tau/dt$ is the sum of terms on the right side of (4-1). Thus (4-8) implies that ϵ changes at a rate

proportional to the sum of net production and divergence of stress flux. If the diffusion term is ignored, (4-9) and (4-10) are the same representation. In the Arctic lead problem, with no roughness change, the diffusion term is not relatively large, and the implicit and explicit forms are similar in the transition region. However, if the implicit ϵ were used in the roughness change problem, the diffusion term should be included in (4-9) since it is dominant (Peterson, 1972).

The implicit form for ϵ was implemented in this study, with the constant A taken (arbitrarily) as 2.24; this means that ϵ will rise at a rate so as to eradicate 90% of the net production in t'. From (4-10) the constant of proportionality is suggested as 1.65, although there is no compelling reason to accept it. The value of the constant will affect the magnitude of stress changes but not the general shape of the resulting profiles, and, since there are no data on stress changes in the lead situation, there is no reason to argue over an exact value of A. The magnitude of stress changes in the model will vary as $\exp(-A)$.

4.4 Effect of Stress Changes on Heat Flux

Viewed in the context of Equation (2-1)-(2-4), increased stress will cause higher surface heat flux. From (3-3), heat flux scales with u_* and the temperature step. When treating heat as a passive

contaminant, surface heat flux will normally decrease with fetch, as is seen in Figure 3.2. However, if stress builds up enough, this natural trend may be overpowered, and heat flux will even increase slightly with fetch. Under the conditions of the Badgley data, numerical experimentation with the model has shown that heat flux will show a slight increase with fetch if the stress increases more than 25% in 20 meters.

Such a circumstance may not be unreasonable as buoyancy effects begin to take hold; in fact Miyake's (1965) data, taken at both 10 and 20 meters, indicate a concave upward growth of the IBL, and such behavior would carry a strong implication of increasing heat flux with fetch or strong dependence of α_h on Ri. Within the numerical model, however, there seems to be considerable resistance to dramatic increases in heat flux, since heat flux scales with u_* and not stress. Therefore, if a doubling of local stress seems improbable, it is unlikely that a model including stress changes would predict a heat flux more than 40% higher than one which treats heat as a passive contaminant. It is likely that stress and velocity changes are small and hence play only a minor role in determining the turbulent heat flux from the lead.

4.5 A Simulation including Stress Changes

For a full lead simulation, the basic set of equations is (2-1), (2-2), (2-4) and (4-1) using the implicit stress dissipation term. Non-dimensionalization of the equations is always desirable in order to portray a class of solutions easily. However, this problem has interrelated velocity and length scales, a circumstance which precludes a profitable non-dimensionalization of any equation containing a dimensional constant such as gravitational acceleration. Therefore, the model results are dimensional and reflect the conditions of the Badgley lead experiment; the temperature step is 25.5 degrees, and the initial friction velocity is 16 cm/sec.

In all cases where heat was considered a passive contaminant, it was assumed that a_h is constant. Businger et al. (1971) give an empirical relation between a_h and z/L under horizontally homogeneous conditions,

$$a_h = 1.35(1-9z/L)^{1/2}/(1-15z/L)^{1/4} \qquad (4-11)$$

For the small range of z/L experienced in the Badgley experiment, (4-11) is approximated simply as

$$a_h = 1.35(1-z/L) \qquad (4-12)$$

Furthermore, expression (4-12) is approximated in the full simulation

by setting $z/L = Ri$ (Businger et al., 1971). Von Karman's constant has been set at 0.4 throughout this study and is retained at the same value for consistency, although Businger linked $a_h \approx 1.35$ with $k = 0.35$. If the smaller value of k were used, the estimate of u_* from the velocity profile would be smaller, and the predicted heat flux would drop accordingly. However, such refinements are unwarranted in view of the data accuracy.

Figures 4.2 through 4.6 give profile results at fetches of 5, 10, 15 and 20 meters. The heat flux profiles in Figure 4.3 show how increasing stress overpowers the natural tendency for surface flux to decrease with fetch (compared with Figure 3.2). At 20 meters, the surface heat flux is 28.1 mw/cm^2. If the stress is held constant, the flux prediction is 26.3 mw/cm^2; if in addition a_h is taken to be a constant 1.35, the flux drops to 26.0 mw/cm^2. Thus the dependence of a_h on z/L reflected in (4-12) has little impact on heat flux predictions, while stress changes may be important.

The stress profiles are given in Figure 4.5 and are characterized by a maximum at an intermediate level. It may be of some concern that the maximum value of the stress profile shows an approximate linear increase with fetch. Even though the buoyancy production decreases with height, the time scale increases and allows the net production to act longer. The diffusion term may eventually check the growth of stress; profiles of divergence of diffusion, net

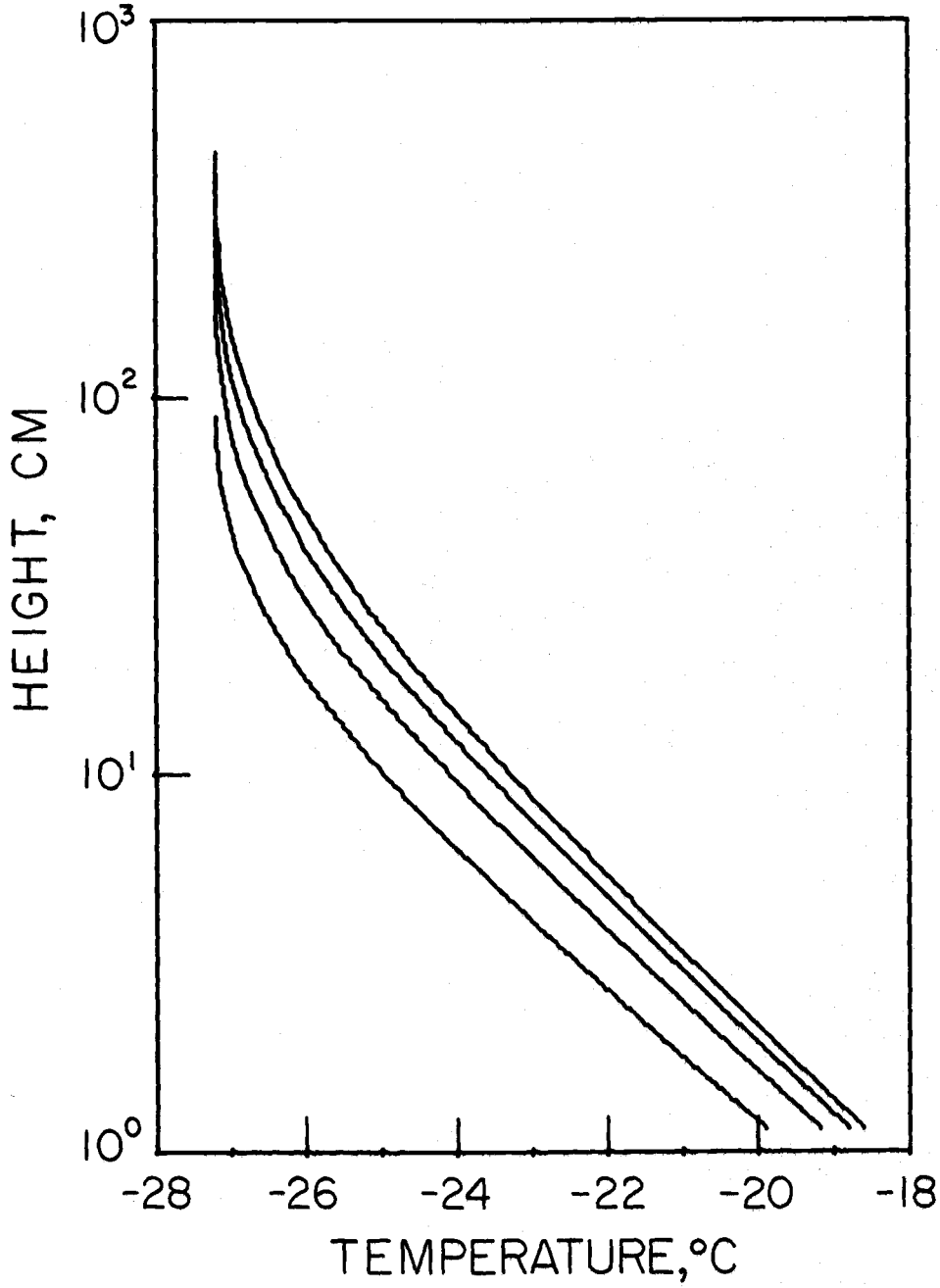

Figure 4.2. Temperature profiles at 5, 10, 15 and 20 meters. Model results using Badgley conditions.

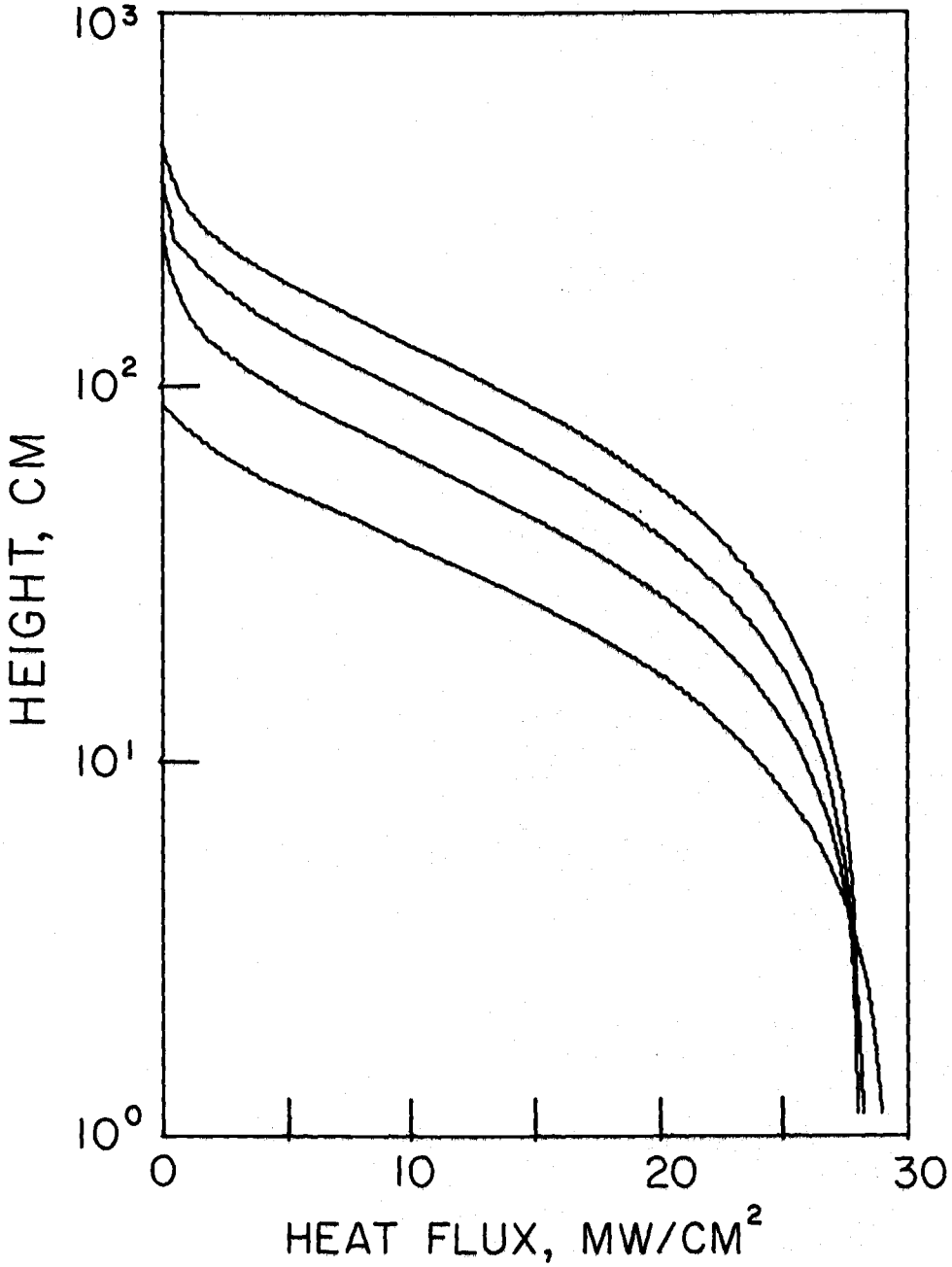

Figure 4.3. Heat flux profiles at 5, 10, 15 and 20 meters. Model results using Badgley conditions.

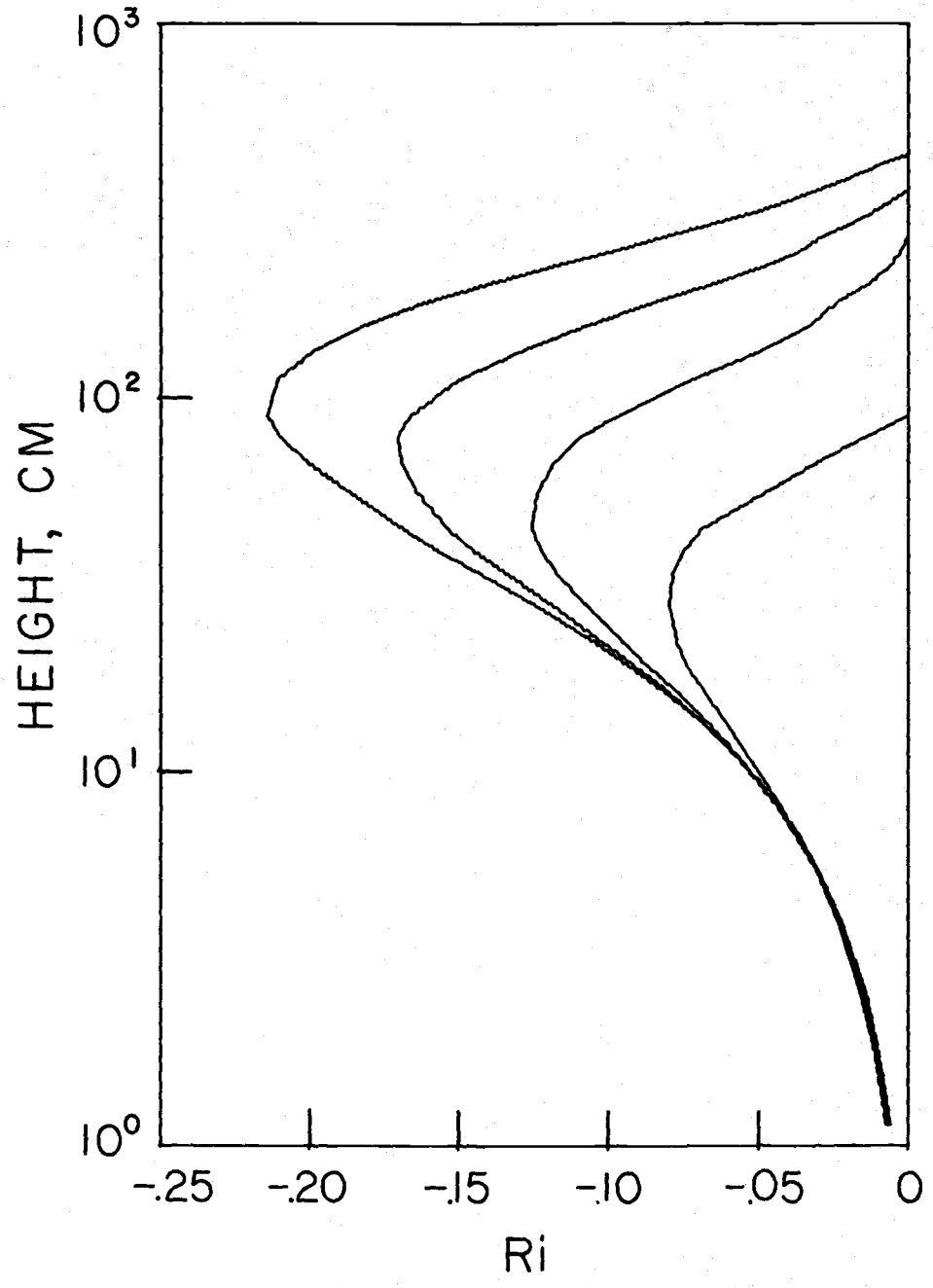

Figure 4.4. Gradient Richardson number profiles at 5, 10, 15 and 20 meters. Model results using Badgley conditions.

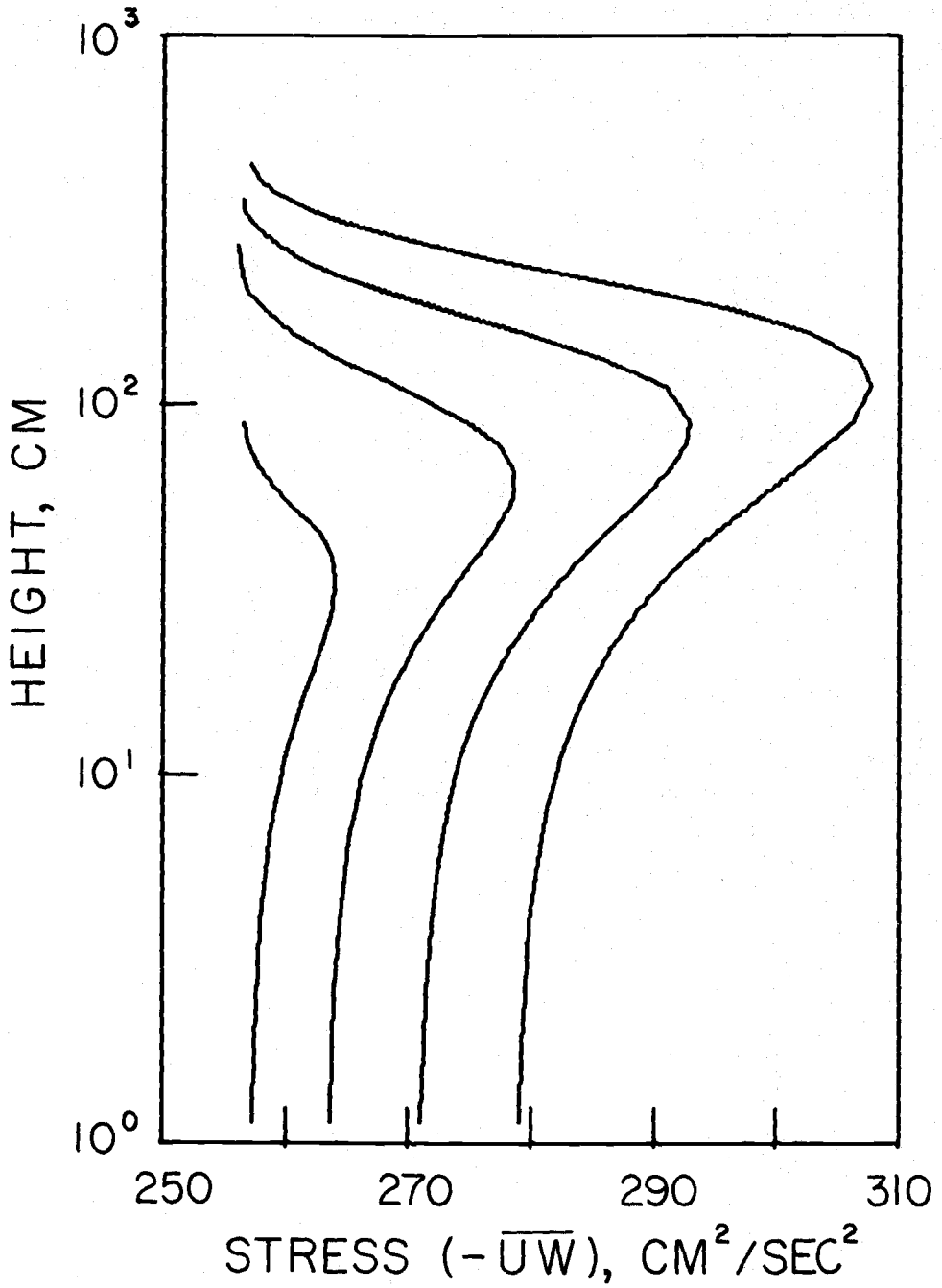

Figure 4.5. Stress profiles at 5, 10, 15 and 20 meters. Model results using Badgley conditions.

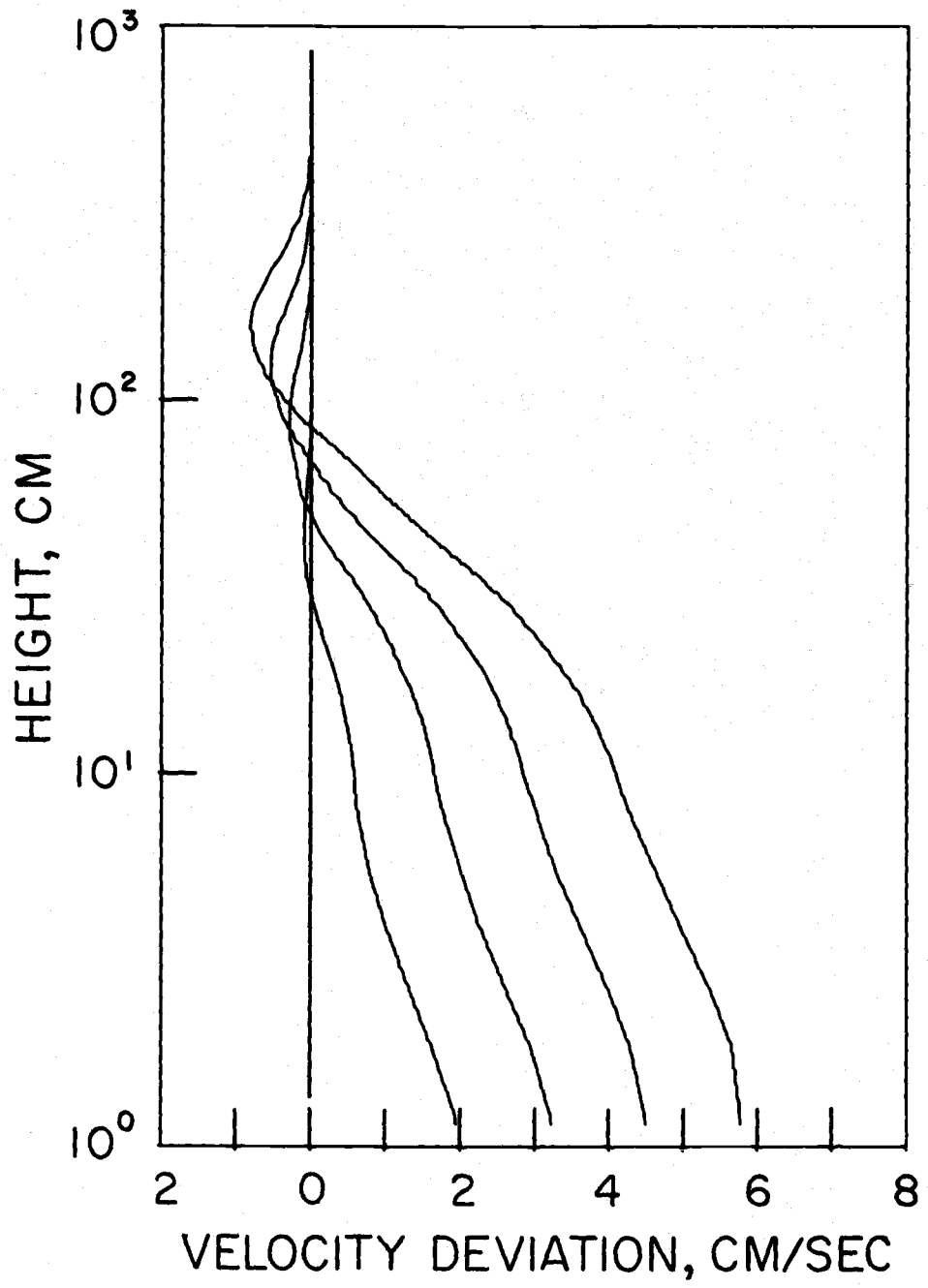

Figure 4.6. Deviation of velocity from the initial logarithmic profile at 5, 10, 15 and 20 meters. Model results using the Badgley conditions.

production, and advection of stress at 20 meters are given in Figure 4.7. It should again be emphasized that there are no data against which the model may be judged; even if the stress profiles are accurate in general shape, the magnitude of the stress changes are influenced by the choice of A in (4-9). Stress changes may indeed be small over the Arctic lead, and therefore have little influence on the surface heat flux.

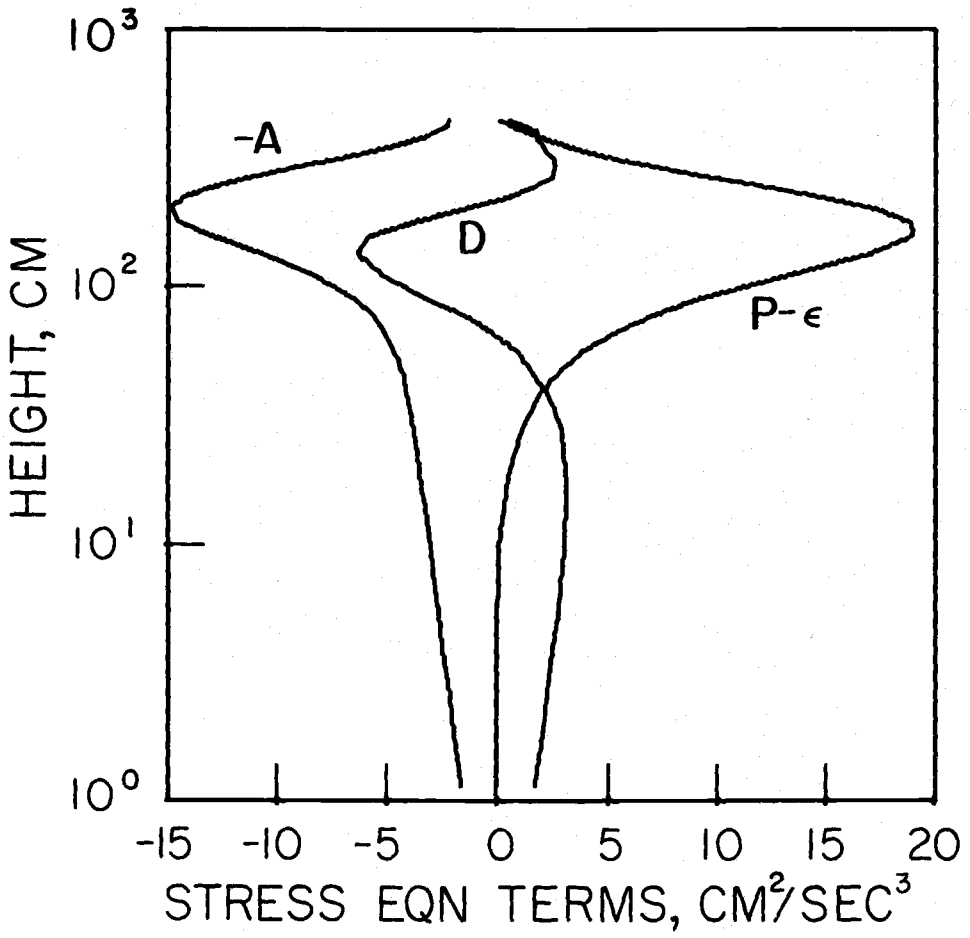

Figure 4.7. Profiles of stress equation terms at 20 meters: advection, A; divergence of turbulent flux, D; net production, P - ϵ. Model results using Badgley conditions.

5. THE LATENT HEAT FLUX

5.1 A Simple Estimate of the Latent Heat Flux

Up to this point only the sensible turbulent heat flux has been considered. Although vapor pressures are low at the temperatures found over Arctic leads, the latent heat flux may be significant. The equation for water vapor in the turbulent layer is

$$U \frac{\partial q}{\partial x} + W \frac{\partial q}{\partial z} = \frac{\partial}{\partial z} (K_e \frac{\partial q}{\partial z}) \qquad (5-1)$$

Water vapor is assumed to be a passive contaminant, and (5-1) is of the same form as the heat equation (2-1). In addition, vapor, like heat, must be transferred across a surface molecular sublayer. It is the objective of this section to use the similarities between heat and vapor transfer in order to arrive at estimates of the latent heat flux and provide insight into when and where condensation, or steaming, may occur over Arctic leads. The results of this section are qualitative, relying on the previous work for sensible heat transfer. An explicit solution of the vapor equation, with effects of condensation, is found in the second section of this chapter.

Before proceeding, several relationships and constant values should be set forth. The heat of vaporization will be taken as 595 calories per gram of water at 0° C. Internally in the program, the

vapor pressure e, will be in units of mm Hg, and is related to specific humidity by $q = 0.622e/760$. The air density at 0° C is 1.29×10^{-3} gm/cm^3.

If the simplifying assumption is made that the turbulent and molecular transfer coefficients for water vapor are identical to those for heat, then the non-dimensional results in Chapter 3 may be interpreted as results for water vapor also. If $a_h = a_e = 1$, then Figure 3.1 may as well represent water vapor profiles over a flat water surface. The scaling would be by $q_B - q_A$, where q_B would be the saturation value at θ_B. Likewise, Figure 3.2 gives non-dimensional flux profiles which may be converted to latent heat flux profiles under the proper scaling and conversion factors. Because of the dependence of vapor pressure on temperature, a dimensionalization is always necessary to establish the proper scaling for vapor. The dimensionalization used here for illustrative purposes will again represent the conditions of the Badgley experiment. The non-dimensional surface flux at a 20 meter fetch is 0.0417 which converts by the factor $1.3u_*(\theta_B - \theta_A)$ to a sensible heat flux of 22.1 mw/cm^2, already shown in Table 3.6. The conversion for latent heat flux is by $3.2u_*(q_B - q_A) \times 10^3$. Assuming the ambient air contains no water vapor, the latent heat flux will be 8.0 mw/cm^2. If the ambient air is saturated, the latent flux will be about 10% less. Thus it is seen that in rather typical conditions for an Arctic lead the latent heat flux may

constitute 25% of the total heat flux.

It is interesting to contemplate the flux scaling factors set forth in the previous paragraph. Considering the lead situation where $\theta_B = -1.7°C$, there will be a maximum and minimum possible latent heat flux depending on whether or not the ambient air is dry or saturated. As θ_A approaches θ_B, the sensible heat flux necessarily goes to zero, as does the latent heat flux if the ambient air is saturated. However, if the ambient air is dry, the latent heat flux will be invariant with θ_A. Thus, if the temperature step is small over a lead, less than about ten centigrade degrees, the latent heat flux may exceed the sensible flux, depending on the ambient relative humidity.

Turning away from the lead situation for a moment, it is apparent that the latent heat flux will always be predominant for higher surface temperatures. In view of the above scaling factors, a given temperature step will yield the same sensible heat flux irrespective of the absolute temperatures. However, the latent flux behaves much differently due to a nearly exponential increase in vapor pressure with temperature, and this behavior will be illustrated using a temperature step of 25 centigrade degrees and assuming the ambient air is saturated. Taking surface temperatures of 25°C, 50°C and 75°C, the latent heat flux will be approximately 1.7, 6 and 18 times the sensible heat flux. This observation is certainly important when dealing with

temperate zone problems, such as predicting heat transfer from cooling ponds. In such cases the latent flux must be treated carefully since it will overshadow the sensible flux.

In this idealized approach, assuming the transfer of heat and vapor to be identical, insight is possible into the conditions which promote condensation, or steaming, over an Arctic lead. Under this approach, a single non-dimensional profile may be transformed to either a temperature profile or vapor profile through multiplication by the appropriate step change and addition of the result to the ambient profile. Thus, if at a given point the temperature has increased by a certain fraction of the temperature step, the vapor content will have increased by the same fraction as the vapor step. Using the Badgley experiment conditions, this simplified relation between air temperature and vapor pressure is illustrated in Figure 5.1 for several different ambient relative humidities. Also shown in the saturation vapor pressure so that the temperatures associated with supersaturation are evident. Figure 3.6 gives a dimensional profile of temperature at a 20 meter fetch, $\alpha_h = 1$ with Condition 1, which may be used to determine the depth of the condensation region. As can be seen from the two figures, condensation is restricted to a shallow surface layer except when the ambient relative humidity approaches 100%. If the ambient relative humidity is 50%, condensation is confined to the lower 20 centimeters.

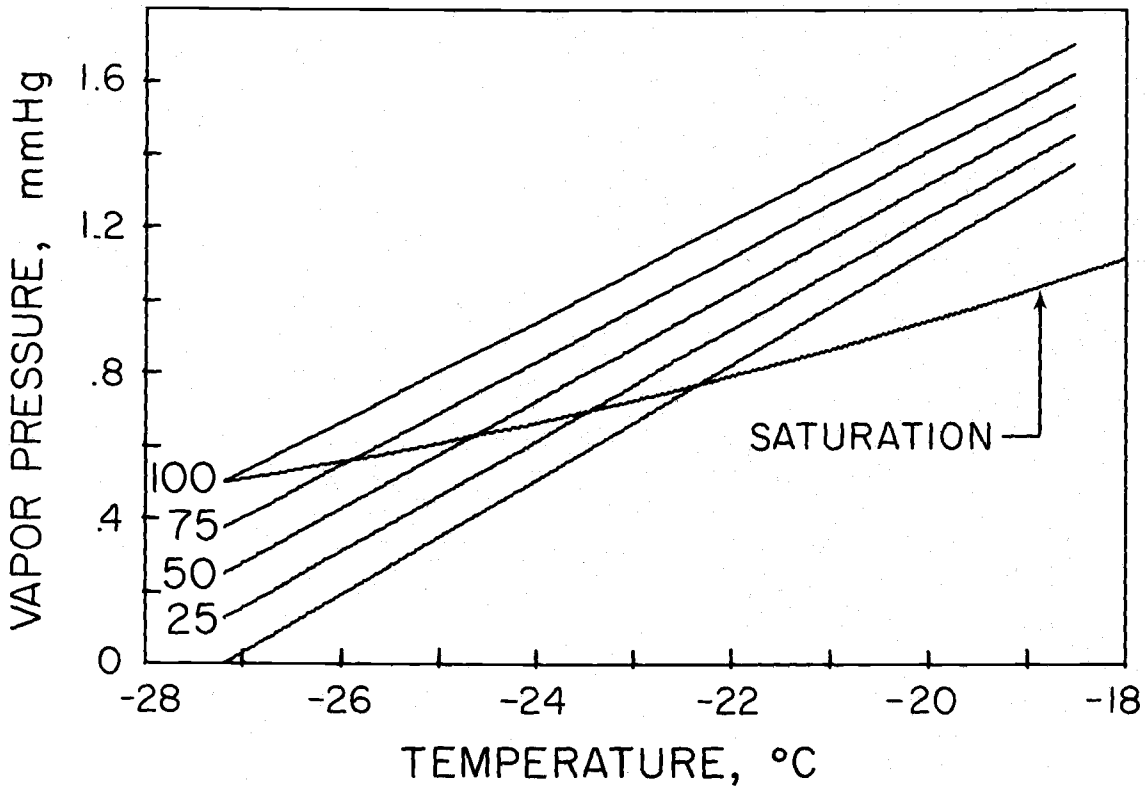

Figure 5.1. A simplified relation between air temperature and vapor pressure changes under the Badgley conditions, assuming ambient relative humidities of 0, 25, 50, 75 and 100 percent.

Because of the simplifying assumptions used in this discussion, there is good reason to expect condensation will be restricted to the lower portion of the IBL, no matter what ambient relative humidity conditions exist. First, it may be best to choose $a_h = 1.35$, and this will tend to increase temperatures at upper levels, thus lowering relative humidities there. Second, the saturation vapor pressure over ice is less than over water. Even if the ambient air is saturated over ice, it will be only about 75% saturated over water. Third, the large supersaturations displayed in Figure 5.1 will not exist. Condensation will act as a sink for water vapor in the low levels, and hence impede the transfer of vapor to the upper levels of the IBL. The only refinement of the assumptions which may increase vapor content is the setting of the molecular diffusivity of water vapor to its proper value, about 25% larger than that for heat.

Although condensation may be restricted to a relatively thin surface layer, the condensate itself may diffuse upward and be visually evident throughout the IBL.

Saunders (1964) uses the same assumption of similarity between heat and vapor transfer to predict the critical air-water temperature difference necessary for the onset of steaming; typical values of 11 to 15 centigrade degrees, depending on ambient relative humidities, are basically confirmed by observation. Saunders found that the critical temperature difference is subject to several degrees variation

depending on the salinity of the water, and this is striking in view of a vapor pressure depression of only two percent at ocanic salinities. The saturation vapor pressures in the present study were calculated from fresh water expressions, and therefore model results on condensation may be in error when the temperature difference is near critical. However, the latent heat flux scales by the vapor pressure step and hence is affected little by salinity influences. Condensation is an interesting visual phenomenon but probably not very important in determining the surface latent heat flux, as is seen in the next section. Relative to this study, Saunders' work is important in showing that observationally confirmed predictions concerning vapor concentration are possible by assuming similarity of conductivity and diffusivity. Thus, use of a single non-dimensional profile for heat and vapor may indeed be acceptable for some purposes.

5.2 A Simulation Including Condensation

This section deals with a dimensional simulation under the Badgley experiment conditions. Condensation will occur when the relative humidity exceeds 100%. The equation for condensate, supercooled water, is

$$U \frac{\partial c}{\partial x} + W \frac{\partial c}{\partial z} = \frac{\partial}{\partial z} (K \frac{\partial c}{\partial z}) \qquad (5\text{-}2)$$

The pertinent equations in the model are (2-1), (5-1) and (5-2).

Sensible heat, water vapor and condensate are all treated as passive contaminants with the proviso that they may interact through condensation. Once condensate is formed it is not allowed to re-evaporate. The boundary conditions on (5-1) are analogous to those for temperature, recognizing that there must be molecular transfer of vapor from the surface. The boundary conditions on condensate assume there is no vertical flux at the surface or top of the IBL. It is assumed that $a_h = 1.35$ and $a_e = 1.0$. The ambient relative humidity is taken to be 50% over ice.

On each step in fetch, the temperature and vapor profiles are predicted as though the quantities are independent passive contaminants. Then, at the points where the relative humidity exceeds 100%, vapor is removed while simultaneously introducing the equivalent latent heat and condensate; the resulting relative humidity is 100% at the revised temperature. This is an incremental method of portraying a continuous process.

Profiles of vapor and condensate concentration, as well as relative humidity, are shown in Figure 5.2 for a 20 meter fetch. The corresponding surface latent heat flux is 8.9 mw/cm^2; the sensible flux is 24.8 mw/cm^2. Condensation, indicated by a 100% relative humidity, is restricted to the lower 7 centimeters, although condensate diffuses much higher and may be visually evident depending on the droplet size and lighting conditions. Profiles of temperature and

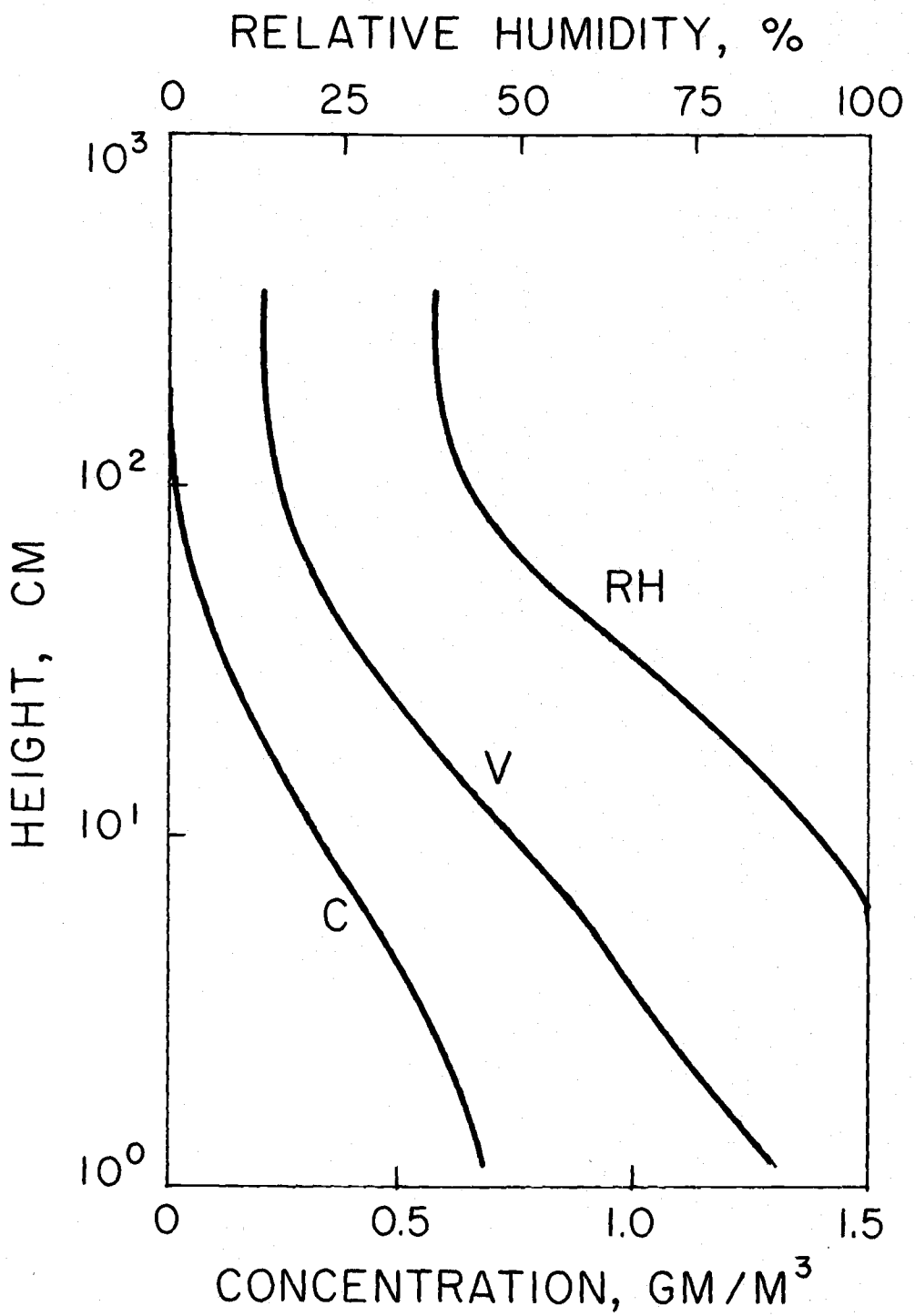

Figure 5.2. Profiles of condensate (C), water vapor (V) and relative humidity (RH, upper scale) at 20 meters. Model results using Badgley conditions.

sensible heat flux show slight perturbations caused by latent heat release. For instance the heat flux profile increases to 27.8 mw/cm^2 at the top of the condensation layer. However, the profiles are highly similar to those already presented and are omitted here.

Badgley's (1966) estimate of latent heat flux over the artificial lead is 4.8 mw/cm^2, significantly lower than the model prediction.

Wind tunnel data (Bau On Young et al., 1973) over a free water surface includes vapor concentration data. The measured near-surface a_e is about 1.1, and the concentration profiles indicate a molecular layer with thickness about 10 ν/u_*. Non-dimensional concentration fluxes measured in the wind tunnel average about 0.047, very nearly the same as predicted by the model. It has been assumed that the effective thickness of the molecular layer should be the same for heat and vapor. This may not be true.

6. DEVELOPMENT OF THE MODEL AND COMPUTATIONAL METHOD

6.1 Choice of a Numerical Technique

A model consists of three important elements: a set of equations describing the natural phenomenon, proper boundary conditions and a numerical technique which offers a practical and accurate method of solution. These three elements of the model are interrelated. The choice of a certain set of equations may dictate the use of a specific numerical technique which, in turn, may influence the solution. For example, the Navier-Stokes equations in three dimensions may be solved completely using a relaxation method on a finite difference grid. Only subgrid scale activity must be parameterized using an eddy transfer coefficient and mean gradients. This approach seems attractive at first glance and has achieved success in dealing with the planetary boundary layer (Deardorff, 1970, 1972). The Arctic lead problem, however, deals with a very thin surface layer within which gradients of velocity and temperature change rapidly. The use of finite differences in the vertical tends to inaccurately portray the gradients. Since the boundary conditions may easily involve gradient expressions, these also will be disrupted. The inaccuracy is systemic, dependent on the choice of technique, and not computational. Yet there is no other numerical method available if the full set of

turbulent equations is to be solved. Thus, delineation of the numerical technique and the implications of its use may be equally important as the more common concerns of the equations and boundary conditions.

If the full set of equations is not used, it must be pared down using appropriate assumptions to exclude insignificant terms and form terms which reflect time averaging. The reduction of the turbulent equations to a solvable set generally involves the introduction of undetermined constants. The notion that any empirical data may be fit by choosing certain values of these constants is not really true. It would be a remarkable discovery if a relatively simple equation were found to fit any curve by adjustment of several constants. A given equation can fit only certain general shapes. However, the numerical modeler must be conservative in how much he asserts about his model. If a certain choice of constant values leads to agreement with a single set of experimental results, then there is a possibility that no essential terms have been excluded from the equations and the boundary conditions are correct. As more data can be fit with the same constant values, increased confidence can be placed in the model as an accurate description of the natural phenomenon, and use of the model for prediction may be contemplated. In this research the number of undetermined constants was kept at an absolute minimum, and the values assigned were within ranges clearly prescribed by empirical evidence. Where a wide range could conceivably be assigned, different

values were tested to determine the effect on the solution. The simplest approach in reduction of the turbulent equations is to introduce eddy transfer coefficients to model the Reynold's flux terms, and consider the problem in only two dimensions. This approach was used because it was felt that no previous model had satisfactorily treated even this simple case, particularly with regard to lower boundary conditions.

The Equations (2-1) through (2-4) are partial differential equations in two dimensions. They could be solved on a finite difference net, but such a technique would have major disadvantages. First, vertical derivatives would tend to be inaccurately depicted near the surface. Second, the finite difference net requires considerable computer storage if fine grid spacing is desired. Third, the physical dimensions of the problem would be rigidly determined at the outset by setting the size of the net. However, by turning away from the finite difference net, each of these disadvantages may be overcome. The equations may be reduced to ordinary differential equations in z by using a finite difference representation of the x-derivative. In the downwind direction the gradients will generally be small, except at the actual surface discontinuity. The available computer storage may then be concentrated on points along just two vertical profiles, one at the fetch under consideration and the other at the immediate upwind fetch. Progressive steps are taken in the downwind direction, using the

previously computed profile to form x-derivatives. The dimensions of the problem are unrestricted since the downwind steps may continue indefinitely and the solution in the vertical may be extended in response to IBL growth.

The basic equations of the model for U, θ and τ may be reduced to ordinary second order differential equations with a linear appearance. The equations are not really linear since the coefficients are functions of the variables being solved. However, by treating the equations as linear and cycling through the set several times for each step in fetch, a convergent solution is possible. The equations solved in the model are given below: the equations for water vapor and condensate are analogous to that for temperature and are omitted for brevity.

For velocity (2-2) becomes

$$\frac{\partial^2 U}{\partial z^2} + \frac{1}{K_h}\left[\frac{\partial K_h}{\partial z} - W\right]\frac{\partial \theta}{\partial z} - \left[\frac{U}{\Delta x \cdot K_n}\right]\theta = -\frac{U\theta}{\Delta x \cdot K_h} \qquad (6\text{-}1)$$

For temperature (2-1) becomes

$$\frac{\partial^2 \theta}{\partial z^2} + \frac{1}{K}\left[\frac{\partial K}{\partial z} - W\right]\frac{\partial U}{\partial z} - \left[\frac{U}{\Delta x \cdot K}\right]U = -\frac{UU_2}{\Delta x \cdot K} \qquad (6\text{-}2)$$

Equation (2-3) for stress was transformed under appropriate assumptions to (4-1). If the explicit form (4-8) for dissipation is

taken, the equation becomes

$$\frac{\partial^2 \tau}{\partial z^2} + \frac{1}{K}\left[\frac{\partial K}{\partial z} - W\right]\frac{\partial \tau}{\partial z} + \frac{1}{K}\left[1.1\,\frac{\partial U}{\partial z} - 1.1\,\frac{\tau^{1/2}}{kz} - \frac{U}{\Delta x}\right]\tau$$

$$= \frac{-U\tau^2}{\Delta x \cdot K} - \frac{3g}{K \cdot T_0}\,\overline{\theta w} \qquad (6\text{-}3)$$

Due to computational instability, this equation could not be solved when treated as a linear equation if any substantial thermal production was present. However, in treating the roughness-change only, this formulation was successful. Apparently the appearance of $\tau^{1/2}$ in the coefficient of τ makes the equation strongly non-linear and thus not amenable to treatment as a linear equation. So in the lead simulation a different approach was taken, writing (4-1) as

$$\frac{\partial^2 \tau}{\partial z^2} + \frac{1}{K}\left[\frac{\partial K}{\partial z} - W\right]\frac{\partial \tau}{\partial z} - \left[\frac{U}{\Delta x \cdot K}\right]\tau$$

$$= \frac{1}{K}\left[\frac{-U\tau^2}{\Delta x} - 1.1\tau\,\frac{\partial U}{\partial z} - \frac{3g}{T_0}\,\overline{\theta w} + \epsilon\right] \qquad (6\text{-}4)$$

where the dissipation term is implicit and bears resemblance to the explicit form in (6-3).

The transformation of the stress equation to a linear form is actually an inefficient procedure, employed because the computer subroutines had already been developed to accurately solve the

temperature and velocity profiles near the surface. In the lead situation, the stress profiles will not have large derivatives, and it is more efficient to solve (6-3) by transforming to

$$[1.1\frac{\partial U}{\partial z} - \frac{U}{\Delta x}]\tau - \frac{1.1\tau^{3/2}}{kz} + \frac{3g}{T_0}\overline{\theta w} + \frac{U\tau^2}{\Delta x} + \frac{\partial}{\partial z}(K\frac{\partial \tau}{\partial z}) = 0 \qquad (6-5)$$

which may be solved as an algebraic equation in τ by Newton's Method. This was done in test cases, and results agree within 10 percent of those obtained by (6-4). This agreement is important since it shows that the explicit form (4-8) yields results similar to those of the implicit form (4-9), where the constant A in (4-9) was taken as 1.65 for the purpose of this direct comparison.

In summary, (6-1), (6-2) and (6-4) formed the basic set of second order differential equations used in the lead situation. For the roughness-change only, the set was (6-1) and (6-3). The equations are solved in the vertical subject to boundary conditions applied at the surface and the top of the IBL. The numerical method assumes that the equations are linear, and, since they are not, several cycles through the set are required for each step in fetch. The cycling procedure is illustrated in Figure 6.1.

6.2 Solution to the Two-Point Boundary Value Problem

Let L be a linear differential operator.

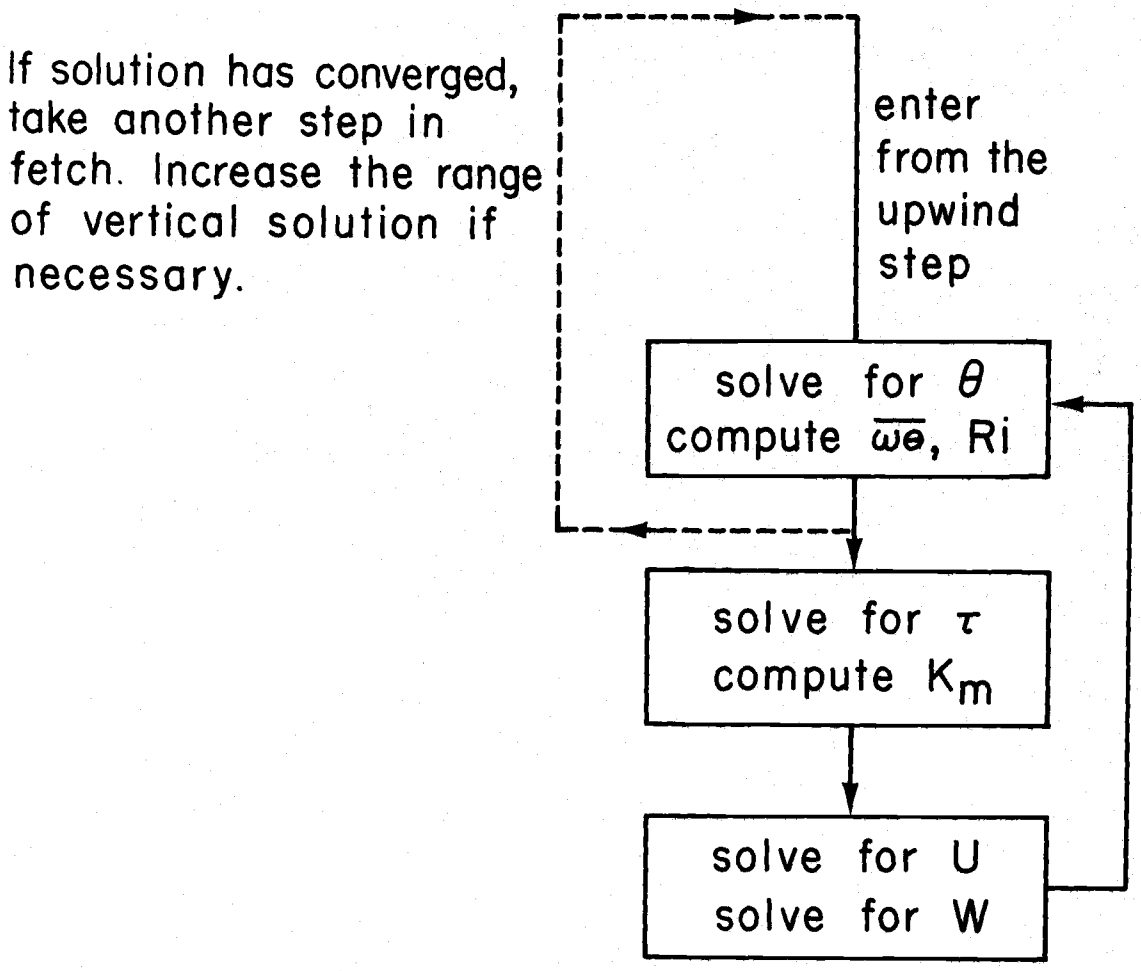

Figure 6.1. Method of cycling through the equations for temperature, stress, velocity and continuity.

$$Ly = y'' + p(z)y' + q(z)y = r(z) \tag{6-6}$$

defined on the interval (a, b). General boundary conditions are

$$a_0 y(a) - a_1 y'(a) = \alpha \tag{6-7}$$

$$b_0 y(b) - b_1 y'(b) = \beta \tag{6-8}$$

A solution may be found by solving the two independent initial value problems

$$Ly_1 = r(z), \quad y_1(a) = -c_1\alpha, \quad y_1'(a) = -c_0\alpha \tag{6-9}$$

$$Ly_2 = 0, \quad y_2(z) = a_1, \quad y_2'(z) = a_0 \tag{6-10}$$

where

$$a_1 c_0 - c_1 a_0 = 1 \tag{6-11}$$

By linearity, the combination

$$y = y_1 + sy_2 \tag{6-12}$$

will satisfy the differential equation in (6-9) and the condition (6-7) for any s provided that (6-11) is obeyed. Thus if s may be chosen so that (6-8) is satisfied then (6-12) will constitute the solution to the two-point problem. That is, choose

$$s = (\beta - b_0 y_1 - b_1 y_1')/(b_0 y_2 - b_1 y_2') \tag{6-13}$$

at $z = b$.

Mathematically the solution of the two-point boundary value problem is relatively simple and is detailed by Keller (1968). However, implementation of the solution on a digital computer must be carefully approached. A generalized subroutine has been developed to solve (6-6) subject to the boundary conditions (6-7) and (6-8). The skeleton of the subroutine is the routine MILNE1 from the OSU Program Library, a seventh order predictor-corrector for solving sets of simultaneous second order linear differential equations with initial value boundary conditions. The nature of the geophysical problem under consideration required extensive modification of MILNE1.

In the change-of-terrain problem the solution must begin very close to the surface. The subroutine, in order to establish starting values, must take three steps closer to the surface than where the lower boundary condition is imposed. Since the equations are undefined on the surface, very small vertical increments must be used initially. However, the retention of such small steps as the solution recedes from the surface is both wasteful and unnecessary to retain reasonably accuracy; the step size may be periodically increased as the solution progresses in z. Most routines, like the original MILNE1, make a total restart when the step size is changed, discarding all information except the current value of the function and its derivative. This is quite inefficient since the seventh order routine

predicts ahead based on the function and its first and second derivatives at the previous seven steps. In solving the lead problem, it was decided that the step size would double every 16 steps up to some maximum number of doublings. In order to utilize previous information, the solution and its derivatives were retained at the previous 14 points at all times. When the step size was doubled, every other retained value would become one of the seven previous values so far as the new step size was concerned. The transition by this method was extremely smooth.

It should be specifically pointed out that the subroutine spends most of its time solving the simultaneous initial value problems (6-9) and (6-10). Only at the very end does it compute s by (6-13) and form the solution to (6-6) subject to (6-7) and (6-8) by linear combination. Computations must be completed over the entire interval (a, b) before any part of the two-point solution may be examined.

The linear combination (6-12) may be difficult to form in practice on a computer because of loss of significant digits. As the z-coordinate increases, the solutions to (6-9) and (6-10) diverge rapidly. Since the solution to the two-point problem is finite, temperature for instance, (6-12) eventually becomes the difference of two very large numbers. Hence, although it may be perfectly feasible to form s by (6-13), the combination (6-12) will become impossible at large z due to loss of significance.

A restart procedure has been developed to prevent the loss of significant digits in the formation of the two-point solution. As an example suppose that the upper boundary condition requires a given functional value at the top of the IBL. The boundary condition (6-8) is specialized by taking $b_0 = 1$ and $b_1 = 0$; that is, the solution is required to have value β at $z = b$. The solutions to (6-9) and (6-10) are computed over the entire interval (a, b) and the first point c at which

$$|y_1(c)-\beta| > 10^4 \qquad (6-14)$$

is noted. The tolerance here is chosen based on the quantities being solved--temperature, stress and velocity--all of order 10^3. If the proper initial conditions could be guessed exactly, $y_1(b)$ would equal β, so the condition (6-14) signals that y_1 has begun to diverge. After computations are completed on (a, b), s is calculated from (6-13) and the solution is formed by (6-12) up to the point c indicated by (6-14). Since y and β are of order 10^3, $y_1(c)$ and $sy_2(c)$ are of order 10^4. The combination (6-12) at c then represents the subtraction of two numbers of order 10^4 to get a number of order 10^3. It is clear that the formation of the two-point solution cannot proceed much beyond c without loss of accuracy, since the initial value solutions are rapidly diverging. Instead the solution is restarted by adopting $y(c)$ and $y'(c)$ as the initial

values in (6-9) and $a_0 = a_1 = 1$ in (6-10); computations are then made over the interval (c, b). This procedure is repeated until the two-point solution may be formed over the entire interval (a, b) without loss of significance. In practice, only two restarts were required in any of the problems dealt with here.

6.3 Imposition of the Upper Boundary Condition

The imposition of the upper boundary condition (6-8) is restricted to taking either b_0 or b_1 to be zero. Either the function or its derivative is forced to a certain value.

Temperature: At the top of the IBL, the conditions $\theta = \theta_A$ and $\frac{\partial \theta}{\partial z} = 0$ should hold simultaneously. There are three possible ways to enforce (6-8).

$$b_0 = 1, \quad b_1 = 0, \quad \beta = \theta_A \tag{6-15}$$

$$b_0 = 0, \quad b_1 = 1, \quad \beta = 0 \tag{6-16}$$

$$b_0 = 1, \quad b_1 = 1, \quad \beta = \theta_A \tag{6-17}$$

Scheme (6-15) would insure that $\theta(b) = \theta_A$, whereas scheme (6-16) would insure $\frac{\partial \theta}{\partial z}(b) = 0$. Scheme (6-17) would enforce neither of these conditions exactly. Because $\frac{\partial \theta}{\partial z}$ is used to calculate the vertical heat flux, it is highly desirable to use scheme (6-16). Otherwise it will be very difficult to bring the heat flux profiles to zero even

at great height, and it is clear why this is so. Since K_h increases with height, even a $\frac{\partial\theta}{\partial z}$ so small as to be physically meaningless will produce a substantial heat flux by the simple calculation $H = -K_h \frac{\partial\theta}{\partial z}$. Unlike scheme (6-15), scheme (6-16) will allow $\theta(b)$ to differ from θ_A, but by taking b large enough the difference may be reduced to any desired level. In the case of stress and velocity it is not nearly as important how (6-8) is enforced.

Stress: In the case of stress, the derivative was forced to zero at the top of the IBL.

$$b_0 = 0, \quad b_1 = 1, \quad \beta = 0 \tag{6-18}$$

Velocity: At the top of the IBL, the wind profile should join with the original logarithmic profile.

$$b_0 = 1, \quad b_1 = 0, \quad \beta = \frac{u'_*}{k} \ln(b/z'_0) \tag{6-19}$$

Criteria for Increasing b: For each profile, both the function and its derivative should return to their ambient values at the top of the IBL. However, only one of these conditions is forced mathematically, while the other may be nearly stratified if b is large enough. As the IBL grows in the downwind direction, b is increased when either of the following criteria are violated.

$$\left| \frac{\theta(b)-\theta_A}{\theta_B-\theta_A} \right| < 0.0007 \qquad (6\text{-}20)$$

$$\left| \frac{\tau(b)-(u'_*)^2}{(u'_*)^2} \right| < 0.006 \qquad (6\text{-}21)$$

In the full lead simulation it was usually (6-21) which was responsible for increasing the range of vertical integration.

Water Vapor: The flux of water vapor should be zero at the top of the IBL.

$$b_0 = 0, \quad b_1 = 1, \quad \beta = 0 \qquad (6\text{-}22)$$

Condensate: The flux of condensate should be zero at the top of the IBL.

$$b_0 = 0, \quad b_1 = 1, \quad \beta = 0 \qquad (6\text{-}23)$$

6.4 Imposition of the Lower Boundary Condition

In its full form, the lower boundary condition (6-7) asserts a linear relation between the function and its derivative. The condition is satisfied by choosing the proper initial conditions to the problems (6-9) and (6-10). Whenever $a \neq 0$, the constants c_0 and c_1 are required to satisfy (6-11), and these constants could be chosen at random. However, it should be recognized that the equation in (6-9) is the same as (6-6); it is, therefore, desirable that $y_1(a)$ and $y'_1(a)$

be estimates of $y(a)$ and $y'(a)$. In this way $y_1(z)$ will not diverge as rapidly and fewer restarts will be necessary. The best available estimates, to be denoted with subscript e, are the results for $y(a)$ and $y'(a)$ on the previous calculation, either at the upwind step or on the previous cycle at the current fetch. In practice only one of $y_1(a)$ and $y_1'(a)$ is estimated since (6-7) gives a relation between the two. The height a, at which the lower condition is applied, is the lowest extent of the turbulent boundary layer, either the top of the molecular sublayer or the roughness length.

Temperature: It is in applying the lower boundary condition on temperature that the generality of (6-7) is best appreciated. The lower condition asserts that the turbulent heat flux at a must equal the molecular heat flux through the molecular sublayer, and this translates into a linear relation between $\theta(a)$ and $\theta'(a)$.

$$\kappa\theta(a) - (m+1)DK_h\theta'(a) = \kappa\theta_B \qquad (6\text{-}24)$$

where $m = (\kappa/u_* kD)\ln(z_0/D)$ and $m = 0$ for $z_0 \leq D$. The constants c_0 and c_1 need not be formally computed since (6-24) forces a relation between the estimated temperature and its derivative.

$$
\begin{aligned}
y_1(a) &= \theta_e \\
y_1'(a) &= \kappa(\theta_e - \theta_B)/DK_h(m+1) \\
y_2(a) &= DK_h(m+1) \\
y_2'(a) &= \kappa
\end{aligned}
\tag{6-25}
$$

Stress: The stress on the surface is related to the velocity gradient; specifically it is the root of the stress conservation equation (4-3). If this root is taken for $y_1(a)$, then $y_2(a)$ must be zero so that (6-12) will give the proper value for $\tau(a)$. So then $a_0 = 1$, $a_1 = 0$, $c_1 = -1$ and α is the root of (4-3).

$$
\begin{aligned}
y_1(a) &= \alpha \\
y_1'(a) &= (\partial\tau/\partial z)_e \\
y_2(a) &= 0 \\
y_2'(a) &= 1
\end{aligned}
\tag{6-26}
$$

Velocity: At the bottom of the turbulent layer, the velocity is assumed to be constant, a necessary condition if applied at the roughness length. No restriction is placed on the velocity gradient. The constants involved are $a_0 = 1$, $a_1 = 0$, $c_1 = -1$ and $\alpha = U(a)$.

$$
\begin{aligned}
y_1(a) &= \alpha \\
y_1'(a) &= (\partial U/\partial z)_e \\
y_2(a) &= 0 \\
y_2'(a) &= 1
\end{aligned}
\tag{6-27}
$$

Water Vapor: The condition on vapor is analogous to that for heat, asserting an equality between molecular and turbulent fluxes at the top of a molecular sublayer.

$$\psi q(a) - (m+1)DK_e q'(a) = \psi q_B \tag{6-28}$$

where $m = (\psi/u_* k D\alpha_e)\ \ln(z_0/D)$ and $m = 0$ for $z_0 \leq D$.

$$\begin{aligned} y_1(a) &= q_e \\ y_1'(a) &= \psi(q_e - q_B)/DK_e(m+1) \\ y_2(a) &= DK_e(m+1) \\ y_2'(a) &= \psi \end{aligned} \tag{6-29}$$

Condensate: There is no flux of condensate at the surface.

$$\begin{aligned} y_1(a) &= c_e \\ y_1'(a) &= 0 \\ y_2(a) &= 1 \\ y_2'(a) &= 0 \end{aligned} \tag{6-30}$$

6.5 The Formulation of Stress Dissipation

It was assumed that the time rate of change of dissipation (ϵ) would be proportional to the difference between total production (P) and dissipation and inversely proportional to the local turbulent time scale (t'). Then, if $\epsilon = \epsilon_0$ and $P = P_0$ at $t = 0$,

$$\epsilon = P_0 - (P_0 - \epsilon_0) \exp(-A \cdot \Delta t / t') \qquad (6\text{-}31)$$

is used to predict ahead one step in fetch ($\Delta t = \Delta x / U$). If it is proposed that 90% of the current net production ($P - \epsilon$) will be eradicated in t', then the constant of proportionality will be $\ln(10)$. Total production, the sum of mechanical and buoyancy production, is computed on each step, and the average net production is substituted in the right side of (6-4).

$$\frac{1}{\Delta t} \int_0^{\Delta t} (P - \epsilon) dt = \frac{t'(P_0 - \epsilon_0)}{A \cdot \Delta t} [1 - \exp(-A \cdot \Delta t / t')] \qquad (6\text{-}32)$$

7. A DISCUSSION OF THE SECOND MOMENT EQUATIONS

7.1 The Desirability of the Heat Flux Equation

Recently there has been interest in solving the complete set of first and second moment equations (Lumley and Khjeh-Nouri, 1973; Rao et al., 1974; Mellor, 1973), and this method deserves consideration in the Arctic lead problem. Use of the second moment equations would allow partial avoidance of the eddy diffusivity assumption; the equations of second moments contain third moments, fluxes of second moments, which must be approximated in terms of second moments. There is involved here what Lumley terms an "article of faith," that the approximation of third moments in the second moment equations will be acceptable, just as the approximation of second moments in the mean equations has proved acceptable for many purposes. It may also be hoped that by removing the approximation to the third moments the prediction of mean quantities will be more accurate. It would be overly ambitious at this point to adopt a large set of moment equations, even in two dimensions. More in tune with the basic philosophy of this study would be the consideration of a simple set of moment equations, preferably those which would remove the central objections to the eddy diffusivity model. It should be recalled that a moment equation has already been employed in this model, the $-\overline{uw}$ equation.

A central objection to the eddy diffusivity model, discussed in the first six chapters, is that the assumed forms for K_m and K_h may not hold in the lead situation. While empirical expressions are well known for conditions of horizontal homogeneity, their use in the transition region of the IBL may not be justified. It would therefore be prudent to adopt the $\overline{\theta w}$ equation; the heat flux would then be computed directly from a conservation equation, providing a basic alternative to the eddy diffusivity approach. A set of equations might include those for $\overline{\theta w}$, $\overline{\theta^2}$ and θ.

Mellor (1973) has adopted a set of seven moment equations to study the constant flux layer of the atmosphere and was successful in predicting empirically confirmed expressions for ϕ_h and ϕ_m. This work will be used as a starting point and referred to extensively. Mellor presents equations for $\overline{\theta w}$ and $\overline{\theta^2}$.

$$\frac{D\overline{\theta w}}{Dt} = -\frac{\partial}{\partial z}(\overline{ww\theta}) + \overline{p\frac{\partial \theta}{\partial z}} + \frac{g}{T_0}\overline{\theta^2} - \overline{w^2}\frac{\partial \theta}{\partial z} \qquad (7\text{-}1)$$

$$\frac{D\overline{\theta^2}}{Dt} = -\frac{\partial}{\partial z}(\overline{w\theta\theta}) - 2\overline{w\theta}\frac{\partial \theta}{\partial z} - 2\kappa\overline{\frac{\partial \theta}{\partial x_k}\frac{\partial \theta}{\partial x_k}} \qquad (7\text{-}2)$$

In Equation (7-1), the pressure correlation term serves as a sink or dissipation term, erasing $\overline{\theta w}$ by transferring fluctuations into the other components. Mellor sets

$$\overline{p\frac{\partial\theta}{\partial z}} = -\frac{q}{3\ell_2}\overline{\theta w} \tag{7-3}$$

where $q = (u^2+v^2+w^2)^{1/2}$ and $\ell_2 = kA_2z$. Equation (7-2) contains a molecular dissipation term which Mellor sets as

$$2\kappa\frac{\partial\theta}{\partial x_k}\frac{\partial\theta}{\partial x_k} = \frac{2q}{\Lambda_2}\overline{\theta^2} \tag{7-4}$$

where $\Lambda_2 = kB_2z$. Mellor sets the values of A_2 and B_2 based on various observed relations between moments in the constant flux layer under near neutral conditions. Mellor in fact restricts his model to the horizontally homogeneous constant flux layer, and so (7-1) and (7-2) reduce to

$$-\overline{w^2}\frac{\partial\theta}{\partial z} + \frac{g}{T_0}\overline{\theta^2} - \frac{q}{3\ell_2}\overline{\theta w} = 0 \tag{7-5}$$

$$-\overline{w\theta}\frac{\partial\theta}{\partial z} - \frac{q}{\Lambda_2}\overline{\theta^2} = 0 \tag{7-6}$$

It is a reasonable belief that whatever moment equation is considered it should reduce to some readily recognizable, observationally derived relation under conditions of horizontal homogeneity and small z/L. Thus it was seen that the second moment equation for stress reduced to the expression for non-dimensional wind shear. Likewise it will be shown here that the equation for $\overline{\theta w}$ reduces to the expression for

the non-dimensional temperature gradient. In a sense then the stress and heat flux equations are principal equations in duplicating the observed relations of fluxes to mean gradients in the constant flux layer; the other moment equations serve to perturb these principal equations at large $|z/L|$.

The following computations utilize approximations which hold for small z/L.

$$\begin{aligned} \overline{w^2} &= C_1 u_*^2 \\ q &= C_2 u_* \\ \overline{\theta w} &= -a_h u_* k z \frac{\partial \theta}{\partial z} \end{aligned} \tag{7-7}$$

Under (7-7), (7-6) becomes

$$\overline{\theta^2} = \left(\frac{B_2 a_h k^2}{C_2}\right) z^2 \left(\frac{\partial \theta}{\partial z}\right)^2 \tag{7-8}$$

Then, substituting (7-8) into (7-5) and using (7-7), the $\overline{\theta w}$ equation transforms to an expression for the non-dimensional temperature gradient.

$$\phi_h = \frac{C_2}{3A_2C_1} + \frac{z}{L}\left(\frac{B_2}{a_h C_2 C_1}\right) \tag{7-9}$$

The values of the groups of constants in (7-9) may be assigned from Businger's data (1971).

$$C_2/3A_2C_1 = 0.74 \tag{7-10}$$

$$B_2/a_h C_2 C_1 = 3 \tag{7-11}$$

It would be reasonable to take $C_1 = 1.1$ and $a_h = 1.35$, whence (7-11) implies $B_2/C_2 = 4.45$. In (7-8) the coefficient becomes 0.97, and so the temperature variance equation states the familiar relationship (Lumley and Panofsky, 1964)

$$\overline{\theta^2} \approx z^2 \left(\frac{\partial \theta}{\partial z}\right)^2 \tag{7-12}$$

From (7-10), $C_2/A_2 = 2.45$. The individual values for C_2, A_2 and B_2 could be introduced, but that is unnecessary since the above ratios must be maintained. There is a tautology expressed here. A model, using the $\overline{\theta w}$ equation as the only second moment equation, will reproduce Businger's ϕ_h if z/L remains small; the model will behave in this manner precisely because the reduced moment equation is the empirical expression for the non-dimensional temperature gradient. Mellor showed something more significant, that Businger's ϕ_h would be well approximated over a wide range of z/L by taking a larger set of moment equations.

7.2 A Simple Test Case

For a test case, the simplest possible set of equations is chosen, those for $\overline{\theta w}$ and θ. This model will be similar to the passive

contaminant model studied in Chapter 3 except a_h will seek its own value in the transition region of the IBL. The buoyancy production term is excluded from the heat flux equation, since heat is treated as a passive contaminant. Subject to the previous discussion and using an eddy diffusion term for the third moment in (7-1), the set is

$$U \frac{\partial \overline{\theta w}}{\partial x} = \frac{\partial}{\partial z}\left(K \frac{\partial \overline{\theta w}}{\partial z}\right) - 1.1 u_*^2 \frac{\partial \theta}{\partial z} - \frac{0.815 u_* \overline{\theta w}}{kz} \qquad (7\text{-}13)$$

$$U \frac{\partial \theta}{\partial x} = \frac{\partial}{\partial z}\left(K_h \frac{\partial \theta}{\partial z}\right) \qquad (7\text{-}14)$$

where

$$K_h = \overline{\theta w} \Big/ \frac{\partial \theta}{\partial z} \qquad (7\text{-}15)$$

Before undertaking the solution it is well to consider what is to be gained by using the above set, which is similar to the set used in the roughness change problem, Section 4.2, and behaves in a similar manner. Looking at the heat flux equation (7-13) when the surface discontinuity is encountered, there will be an abrupt change in the temperature gradient giving rise to a production in heat flux. Production results in an increase in $\overline{\theta w}$ over a period of time. Therefore, $\overline{\theta w}$ will tend to lag behind $\frac{\partial \theta}{\partial z}$, and K_h given by (7-15) will tend to be smaller than assumed in the eddy diffusivity model. Thus, a_h may be expected to be less than its equilibrium value. Since an equilibrium layer may be assumed at the surface, it is proper

to force $\alpha_h = 1.35$ there. Furthermore, there is a distinct numerical problem in computing (7-15) near the top of the IBL where the expression becomes indeterminant. The atmosphere at the top of the IBL is in equilibrium so that α_h is forced to 1.35 there also. In addition, the $\overline{\theta w}$ equation will assure that α_h will return to 1.35 at intermediate levels as the surface equilibrium layer grows. Therefore, because of constraints which are both logical and necessary, heat flux predictions of this model will differ little from the passive contaminant model explored in Chapter 3, when using $\alpha_h = 1.35$.

The model was run under the conditions of the Badgley lead experiment. The surface heat flux at 20 meters of fetch was within one percent of that predicted by the passive contaminant, eddy diffusivity model. Values of α_h in the transition region of the IBL dropped as low as 0.7 near the upwind edge of the lead.

In view of the numerical experimentation in Chapter 3, it is not surprising that alteration of the turbulent equations in the model makes little difference in the predicted heat flux. The solution for heat flux is strongly determined by the lower boundary condition on temperature. No matter how the turbulent transport is formulated, heat must always be diffused through the molecular layer on the surface.

8. WINDLESS CONVECTION

8.1 An Equation for the Heat Flux

It is apparent that the model is inadequate for predicting heat transfer as the mean wind tends to zero, since the heat flux scales with u_*. Under windless conditions over a heated surface, there will be a significant upward heat transfer due to buoyant plumes. The model may be thought of as holding when turbulence is forced by a near-surface shear. As u_* approaches zero, the buoyancy forces assume a greater relative importance. The transition between forced and free convection would seem difficult to describe with the eddy diffusivity approach. However, it is well to look at the limiting case of windless convection; the heat transfer in such a case would set a lower bound on the predicted heat flux as u_* goes to zero. A criterion for model applicability may be defined.

An equation for the upward sensible heat flux over a smooth heated surface may be formed by combining two assumptions set forth by previous authors: (1) There is a molecular sublayer on the surface with thickness dependent on g/T_0, H and κ (Townsend, 1959). (2) The temperature gradient in the turbulent zone is dependent on g/T_0, H and z (Priestly, 1959). In this study the temperature dependent constants will correspond to the lead situation.

A fundamental feature of this investigation will be inclusion of a molecular sublayer at the surface. As in the model, the assumption of a molecular sublayer is necessary for prediction of heat flux and tends to minimize the variations in the predictions as undetermined constants are chosen over a range indicated by experimental data. Under assumption (1) the thickness of the molecular sublayer is given by

$$D = B(\kappa^3 T_0 / gH)^{1/4} \tag{8-1}$$

where B is a constant. Data of Townsend (1959) clearly show this formulation holds for three different heat fluxes. From Townsend's data, this author concludes that B is about 2 and certainly lies in the range 1.5 to 2.5. This layer is so thin that laboratory measurements of its thickness should be applicable to the atmosphere. The data of Townsend show that at least 1/3 of the total temperature decrease occurs across the molecular sublayer, typically having a thickness of only 0.2 cm. As with the model, the assumption of a molecular sublayer makes a tremendous difference in the temperature sensed by the turbulence at the lower boundary.

Assumption (2) leads to the familiar temperature gradient expression.

$$\frac{\partial \theta}{\partial z} = -C(g/T_0)^{-1/3} H^{2/3} z^{-4/3} \tag{8-2}$$

where C is constant. The corresponding transfer coefficient may be written as

$$K_h = Az^n \tag{8-3}$$

where $n = 4/3$ and

$$A = C^{-1}(gH/T_0)^{1/3} \tag{8-4}$$

The form of K_h will be slightly altered to provide consistency with the idea of a molecular sublayer. Within the sublayer, viscous forces are assumed to preclude all turbulent motion; above D there will be a blending of molecular and turbulent transfer.

$$K_h = \kappa + A(z-D)^n \tag{8-5}$$

It is the purpose of this chapter to predict heat flux using the transfer coefficient (8-5) and a flux-equality lower boundary condition.

The expression for the temperature gradient

$$\frac{\partial \theta}{\partial z} = -H/(\kappa + A(z-D)^n) \tag{8-6}$$

may be integrated from D to h, where h is a height at which reference temperature θ_h is taken. Using the expression for the molecular heat flux

$$H = \kappa(\theta_B - \theta_D)/D \tag{8-7}$$

(8-6) yields

$$\Delta\theta - DH/\kappa = \int_D^h \frac{H dz}{\kappa + A(z-D)^n} \qquad (8\text{-}8)$$

where $\Delta\theta = \theta_B - \theta_h$.

Equation (8-8) is an equation in H which may be solved by Newton's iterative method. The solutions are dependent on setting the values of the parameters C, B, $\Delta\theta$, h and n. Basic values of these parameters will be chosen since a base solution is needed in order to judge the relative effects of changing one value while holding the others the same.

The value of B has already been discussed, n is dictated by the dimensional argument and h may be chosen as any conveinent measurement height. Based on data, Priestly (1959) found $C = 1.07$ in (8-2). On the other hand, Dyer (1965) found a much smaller $C = 0.83$. Deardorff and Willis (1967) make a theoretical estimate of $C = 1.22$ for parallel plate convection at very high Rayleigh number.

There is some controversy about the value of n, equivalent to questioning the dimensional reasoning leading to (8-2). Experimental evidence does not clearly support the existence of temperature gradients with a $-4/3$ power dependence on height. However, it seems that atmospheric measurements in the absence of wind are lacking; instead reliance must be placed on small scale laboratory measurements or atmospheric measurements taken in the presence of considerable wind shear. Townsend (1959), using an open-topped box heated from below,

found a best fit of the temperature profiles indicated $n = 2$, with a possible range from 1.3 to 2.5. Deardorff and Willis (1967) make horizontally averaged temperature measurements in a convection chamber and could not find a single value of n which would suffice over any significant height interval. However, the data suggested that a $n = 4/3$ regime may develop near the lower boundary as the Rayleigh number increases. The failure of Townsend to find such a regime, since in the open box much higher Rayleigh numbers could be achieved, was attributed to use of a single temperature probe near the center of the box. In order to determine if $n = 4/3$ under windless conditions in the atmosphere, Deardorff and Willis proposed an open box field experiment, but such an experiment has apparently never been carried out. To further add complexity to the choice of n, atmospheric measurements taken in the presence of wind shear indicate $n = 3/2$ (Dyer, 1965; Businger et al., 1971) over a broad range of z/L. Dyer, however, found that $n = 4/3$ was acceptable for z/L in the limited range -.02 to -0.6.

Considering the above discussion, basic values of the parameters in (8-8) will be taken as

$$C = 1.07\ (0.83, 1.22)$$

$$B = 2.0\ (1.5, 2.5)$$

$$\Delta\theta = 25.5^{\circ}C\ (5, 45) \qquad (8\text{-}9)$$

$$h = 1000\ cm\ (200, 6000)$$

$$n = 4/3\ (4/3, 2.0)$$

Values in parentheses indicate the range over which each parameter will be varied in order to assess the impact on the solution. The basic $\Delta\theta$ was chosen as that from the Badgley lead experiment; therefore the results may be compared to dimensional results of the model. The solution of (8-8) with the basic parameter values will give a heat flux prediction for the Badgley lead if the wind were to go to zero. Of course in the windless case the lead is considered to be an infinite plane, and the effects of air advecting from the sides and rising over the lead are not considered. An analogous procedure for the prediction of latent heat transfer under windless conditions may be easily formulated.

8.2 Heat Flux Predictions

Solutions of (8-8) subject to (8-9) are presented graphically in Figures 8.1-8.5. Each parameter of (8-9) is varied while holding all others at their basic values.

Figure 8.1 shows that variation of C from 0.83 to 1.22 results

results in a 20 percent decrease in the predicted flux. C^{-1} plays a role similar to a_h in the model as is seen in (8-4).

The value of B, which determines the thickness of the molecular sublayer, also has a significant influence on the predicted flux. As B goes from 1.5 to 2.5 in Figure 8.2, the flux decreases by 21 percent.

If the assumptions concerning molecular sublayer thickness and temperature gradient are correct, the heat flux will be found in Figure 8.3 for a range of $\Delta\theta$. The flux prediction is dependent on experimental determination of the constants C and B. The dashed lines in Figure 8.3 indicate solutions using pairs of constants which maximize (C = 0.83, B = 1.5) and minimize (C = 1.22, B = 2.5) the predicted flux.

It may be noted that if C is known, then measurement of the temperature gradient will give the heat flux by (8-2).

$$H = C^{-3/2}(g/T_0)^{1/2}\left(\frac{\partial\theta}{\partial z}\right)^{-3/2}z^2 \qquad (8\text{-}10)$$

However, the estimation of heat flux by (8-10) would be inconvenient at best. Measurement of temperature gradient would have to be made over open water; it would be just as well to measure $\overline{\theta w}$ directly. Under the method described in this Chapter, a single air temperature measurement made over the ice surrounding a large open lead would

suffice to predict the heat flux under windless conditions. Such a procedure is supported by Figure 8.4 which shows the minor influence of h on the solution. Above a few meters height, the temperature would be at a nearly constant, ambient value.

Choosing a value of n other than 4/3 is inconsistent with the assumption that the temperature gradient depends on g/T_0, H and z. However, other values of n have been mentioned, and Figure 8.2 shows the influence of n on the predicted heat flux.

8.3 A Criterion for Model Applicability

Since the heat flux predicted by the model will go to zero with u_*, there must be a minimum u_* below which the model fails to accurately predict the flux under a given heating intensity. In the Badgley lead experiment, $u_* = 16$ cm/sec and the model predicts a heat flux of about 26 mw/cm^2 at a 20 meter fetch assuming heat is a passive contaminant. If u_* drops over such a lead, the flux will drop proportionately, and at $u_* = 5.5$ cm/sec the heat flux predicted by the model will equal that predicted for the windless case, 9.2 mw/cm^2. Further decrease in u_* would render the model inapplicable, since the flux predicted for windless conditions is a minimum flux for the lead. If buoyancy effects were included in the Badgley simulation, the minimum u_* for model applicability would tend to be even less.

One way of looking at the transition from free to forced convection is to concentrate on the molecular sublayer. It has been demonstrated that the thickness of the sublayer is an important factor in determining the heat flux, and two formulations for the thickness have been introduced depending on relevant scaling parameters. Starting with a windless state, (8-1) will give the molecular sublayer thickness. On the other hand, (A-12) will give the thickness in the presence of wind shear. As u_* rises from zero, the thickness from (A-12) will decrease. Setting the ratio of (A-12) to (8-1) equal to one and rearranging terms,

$$D/L = B^4 k(\kappa/\nu)^3/(7.1)^3 \approx 0.048 \qquad (8\text{-}11)$$

where L is the Monin-Obukhov length. D/L may be viewed as a stability parameter. For D/L larger than the critical value indicated by (8-11), the numerical model should not be applied. For a lead situation with H in the broad numerical range 1 to 25, the transition value of u_* will lie in the range 2.4 to 5.4 cm/sec.

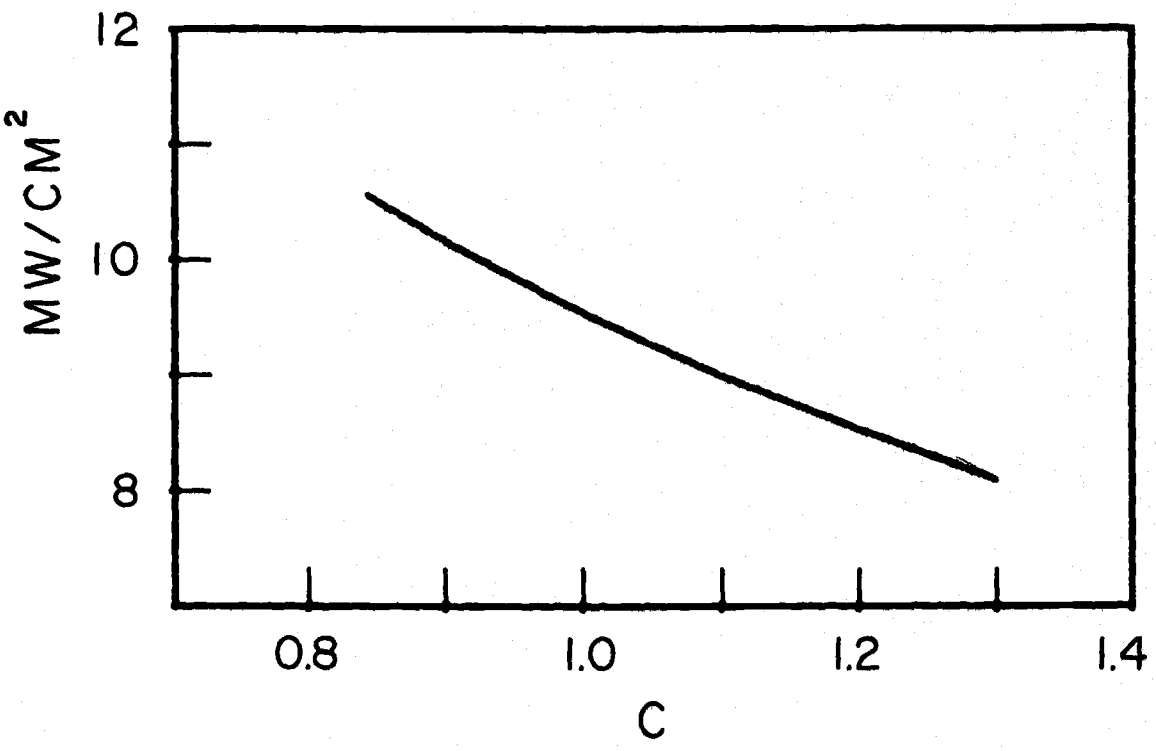

Figure 8.1. Predicted heat flux as a function of C. Windless convection.

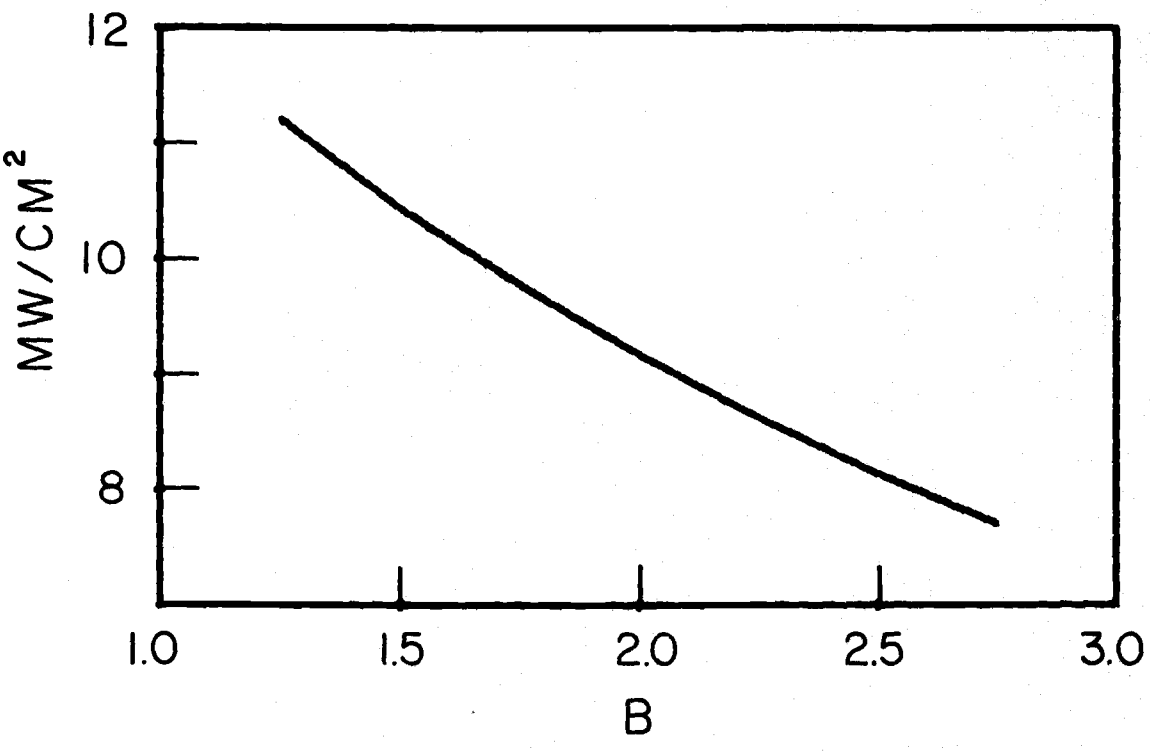

Figure 8.2. Predicted heat flux as a function of B. Windless convection.

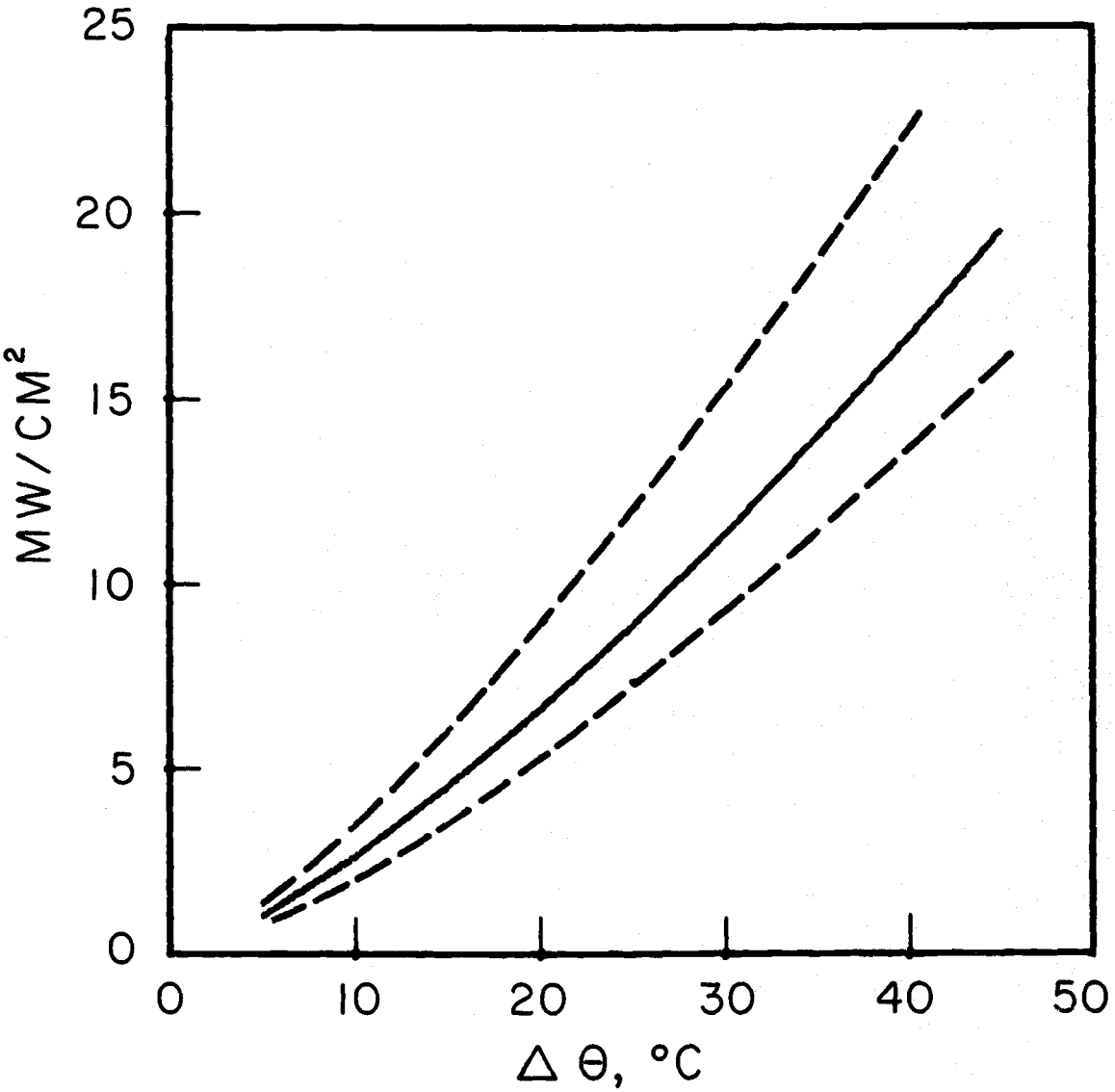

Figure 8.3. Predicted heat flux as a function of the temperature difference between the surface and 10 meters. Dashed lines give solutions using extreme values of the constants B and C. Windless convection.

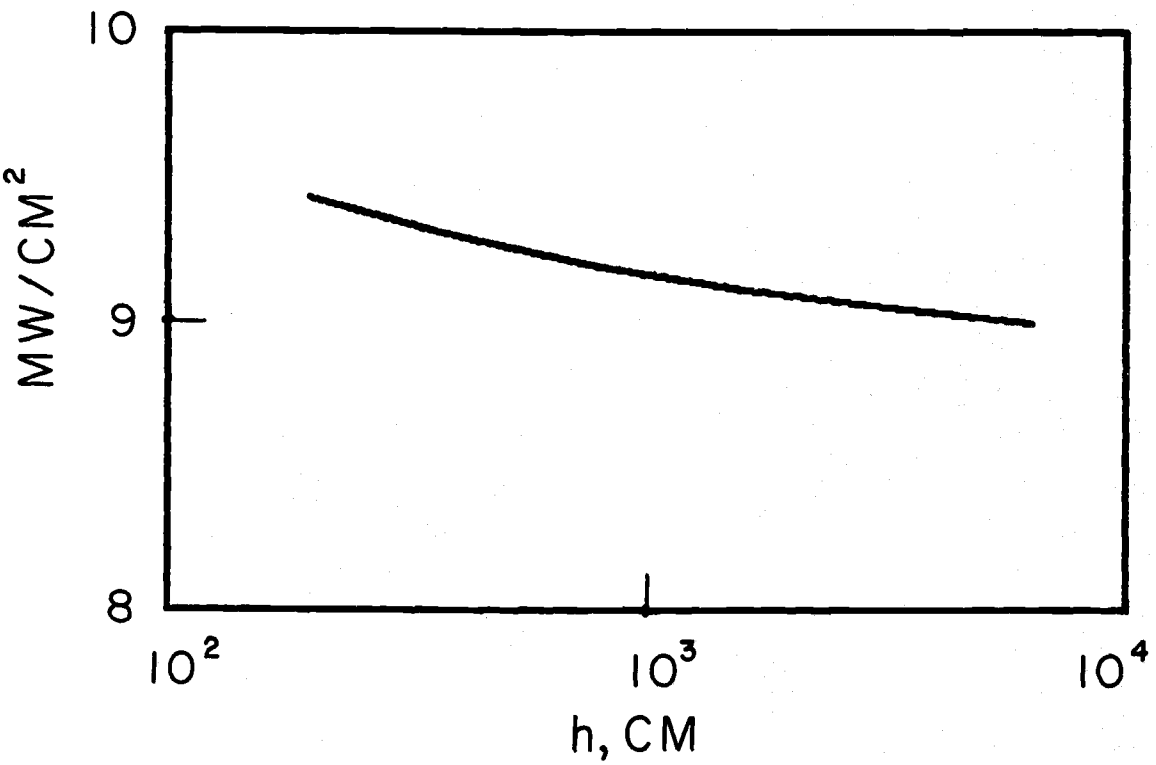

Figure 8.4. Predicted heat flux as a function of h, the height where an ambient temperature is assumed. Windless convection.

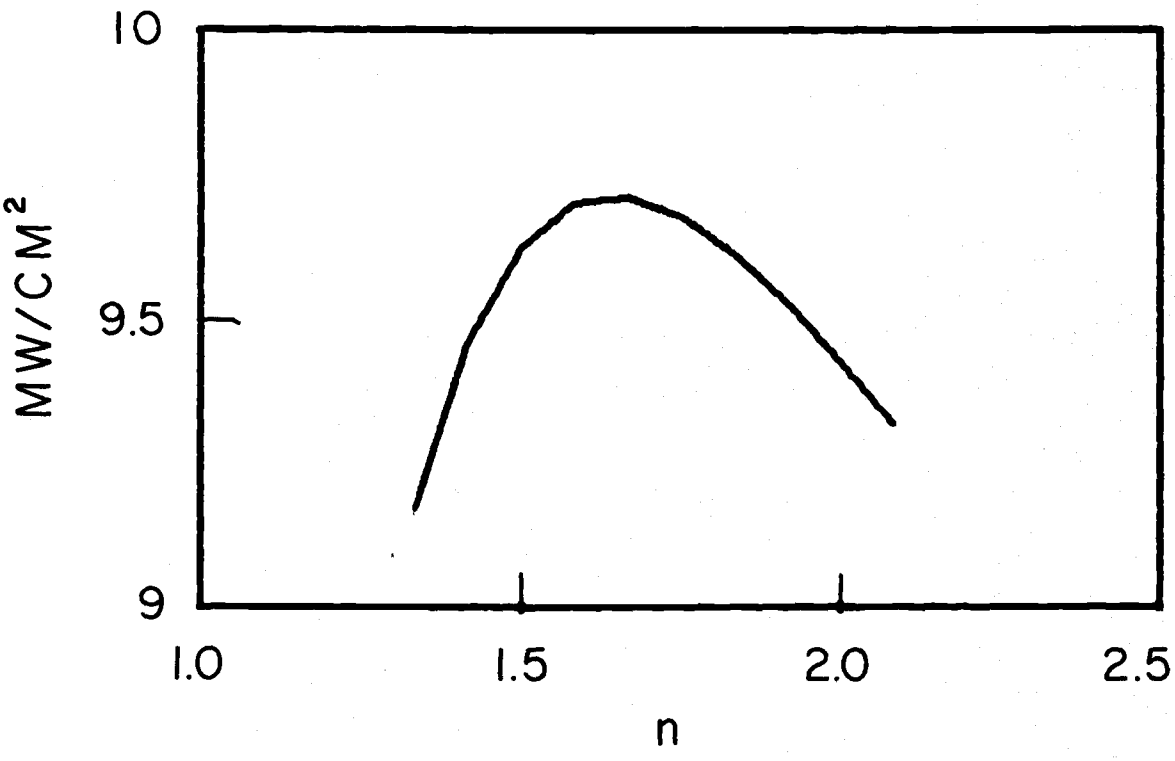

Figure 8.5. Predicted heat flux as a function of n. Windless convection.

9. SUMMARY AND CONCLUSIONS

A two-dimensional, eddy diffusivity model has been developed to simulate the Arctic lead situation, idealized as neutrally stratified flow encountering an abrupt increase in surface temperature and vapor pressure. An important feature of the model is expressed in the lower boundary conditions. Heat and water vapor must be transferred by molecular means through a thin, surface sublayer. The lower boundary condition, designated Condition 1, enforces equality of molecular and turbulent fluxes at the top of the molecular sublayer. The thickness of the sublayer is assumed to scale with ν/u_*. Another lower boundary condition, designated Condition 2, asserts equality between the roughness parameters for heat, vapor and momentum, and is evaluated because of its use by previous authors.

The appropriateness of Condition 1 as opposed to Condition 2 is verified in several ways. First, profiles of temperature in a geophysical experiment and both temperature and vapor concentration in a wind tunnel experiment seem to confirm the existence of a molecular sublayer. Second, the use of Condition 2, $z_0 = z_H$, leads to a model whose temperature profiles behave in a manner inconsistent with the concept of a molecular sublayer. Increased turbulent transfer efficiency results in higher heat flux predictions but not reduced near-surface temperatures, as must be expected if the surface transfer is

molecular. Third, data from a wide variety of sources indicate that z_0 and z_H are not only unequal but also independent on slightly rough surfaces. This should be expected since z_H would scale with ν/u_* while z_0 is independent of u_*, at least for flows over a rigid, rough surface.

The effective thickness of the molecular sublayer lies in the range $6\ \nu/u_*$ to $16\ \nu/u_*$, based on available data. As a basic value, the sublayer thickness, D, was taken as $11\ \nu/u_*$ for both heat and water vapor. Increasing D from $11\ \nu/u_*$ to $16\ \nu/u_*$ would decrease the heat flux prediction by about 12% when $a_h = 1$. Similarly, decreasing D from $11\ \nu/u_*$ to $6\ \nu/u_*$ would increase the heat flux prediction by about 10%. From available data, a suitable constant value of a_h for the lead situation lies between 1 and 1.4. Increasing a_h from 1 to 1.4 would increase the heat flux by about 18%. Use of a constant a_h is not strictly correct, since there is a stability dependence. However, use of an empirical expression for a_h, dependent on Ri, alters the heat flux prediction less than 2% for the Badgley lead conditions, although larger differences may be expected for lower wind speeds. Within expected ranges over water, z_0 has a negligible effect on heat flux predictions. The slope of IBL is about 1/20 at a fetch of twenty meters.

Because of the close anology between heat and vapor transfer, both in terms of the lower boundary conditions and the similar transfer

coefficients, much of the work done specifically for heat may be used to draw conclusions about vapor (e.g., the effect of basic model parameters, α_e, D and z_0, on the non-dimensional flux predictions).

The latent heat flux over a lead will usually be significant. It is possible for the latent flux to exceed the sensible flux if $(\theta_B - \theta_A)$ is less than 10°C. For $(\theta_B - \theta_A) = 25°C$, the latent flux is about 30% of the sensible flux and is proportionately smaller as the ambient temperature decreases. Condensation will likely occur when $(\theta_B - \theta_A)$ exceeds a critical value of about 15°C. The actual condensation zone will be quite shallow, growing with a slope of 1/300, versus 1/20 for the IBL. Condensate may be visible throughout the IBL due to turbulent diffusion. Condensation is visually impressive but has little influence on the surface vapor flux.

Changes in stress, induced over the lead by thermal production, may have an influence on heat flux magnitude. Predicted stress profiles are characterized by a maximum at an intermediate level, consistent with the expected overturning of air within the IBL. The model predicts that heat flux would increase by approximately 10% if stress changes are considered, an increase larger than that suggested by wind tunnel data (Bau On Young et al., 1973). Data are needed to indicate stress changes over a lead. However, for prediction of surface heat flux, it may be acceptable to treat heat as a passive

contaminant and incorporate the buoyancy influences into α_h and D.

The use of additional second moment equations and specifically the $\overline{\theta w}$ equation seems of little advantage, at least in small scale leads where z/L remains small. Surface heat flux predictions are overwhelmingly determined by the lower boundary condition on temperature proposed in this dissertation. Use of the $\overline{\theta w}$ equation will not significantly alter the surface heat flux, although there will be some alteration of the profiles higher in the IBL. Near the upwind edge of the lead, such a model predicts substantially reduced values of α_h at intermediate levels in the IBL. If such dramatic behavior of α_h were observationally confirmed, the inclusion of a $\overline{\theta w}$ equation would be warranted.

The numerical model is not meant to be applicable for low wind speeds since the predicted heat flux goes to zero with the friction velocity. Assuming a free convection temperature profile and a molecular layer thickness dependent on κ, g/T_0 and H leads to a prediction of sensible heat flux in the absence of wind. This flux is the minimum possible flux over the lead and is approximated by $0.224\Delta\theta + 0.00515(\Delta\theta)^2$ mw/cm^2, where $\Delta\theta$ is the temperature difference between the water and the air at 10 meters height. At very low wind speeds, the flux prediction of the model will be less than that for windless convection. In such a case, the model must be deemed inapplicable.

Within the suggested range for model parameters, the non-dimensional heat flux at a fetch of $80,000\ \nu/u_*$ (7 meters for $u_* = 16$ cm/sec) lies between 0.050 and 0.078, convertible by $1.3\, u_*(\theta_B - \theta_A)$ to mw/cm^2. The non-dimensional vapor flux lies in the lower half of the same range, convertible by $3.2u_*(q_B - q_A) \times 10^3$ to mw/cm^2. The fluxes at this particular fetch are about 15% higher than fluxes at a fetch three times as long. The ranges of flux predictions reflect maximum uncertainties in the values of basic model parameters. The predictive capability of the model must ultimately rest on empirically establishing values of D, a_h, a_e and z_0 which hold over the Arctic lead.

BIBLIOGRAPHY

Badgley, F.I.: Heat budget of the surface of the Arctic Ocean. Proceedings, Symposium on Arctic Heat Budget and Atmospheric Circulation, Lake Arrowhead, RAND-UCLA, 267-277, 1966.

Bau On Young, M., Hsu, E.Y. and Street, R.L.: Air-Water Interactions: the Nature of Turbulent Heat, Mass, and Momentum Transfer Mechanisms in the Air Boundary Layer. Technical Report No. 163, Dept. of Civil Engineering, Stanford Univ., Sept. 1973.

Bradley, E.F.: A micrometeorological study of velocity profiles and surface drag in the region modified by a change in surface roughness. Quart. J. Roy. Meteor. Soc. 94:361-379, 1968.

Businger, J.A., Wyngaard, J.C., Izumi, Y. and Bradley, E.F.: Flux-profile relationships in the atmospheric surface layer. J. Atmos. Sci. 28, 181-189, 1971.

Coantic, M. and Seguin, B.: On the interaction of turbulent and radiative transfers in the surface layer. Boundary-Layer Meteorology 1:245-263, 1971.

Deardorff, J.W.: A Three-dimensional numerical investigation of the idealized planetary boundary layer. Geophysical Fluid Dynamics 1, 377-410, 1970.

Deardorff, J.W.: Numerical investigation of the neutral and unstable planetary boundary layers. J. Atmos. Sci. 29, 91-115, 1972.

Deardorff, J.W. and Willis, G.E.: The free-convection profile. Quart. J. Roy. Meteor. Soc. 93:166-175.

Dyer, A.J. The flux-gradient relation for turbulent heat transfer in the lower atmosphere. Quart. J. of the Roy. Meteor. Soc. 91:151-157, 1965.

Elliott, W.P.: The growth of the atmospheric internal boundary layer. Trans. Amer. Geophy. Union 39, 1048-1054, 1958.

Garratt, J.R. and Hicks, B.B.: Momentum, heat and water vapour transfer to and from natural and artificial surfaces. Quart. J. Roy. Meteor. Soc. 99, 680-687, 1973.

Haugen, D.A., Kaimal, J.C. and Bradley, E.F.: An experimental study of Reynolds stress and heat flux in the atmospheric surface layer. Quart. J. Roy. Meteor. Soc. 97:168-180, 1971.

Keller, H.B.: Numerical Methods for Two-Point Boundary Value Problems, Blaisdell Publishing Co., 1968.

Kondo, J., Fujinawa, Y. and Naito, G.: High-frequency components of ocean waves and their relation to the aerodynamic roughness. J. of Physical Oceanography 3, 197-202, 1973.

Lumley, J.L. and Khjeh-Nouri, 1973: Computational modeling of turbulent transport. Presented at Second IUTAM-IUGG Symposium on Turbulent Diffusion in Environmental Pollution, 8-14 April 1973, Cholottesville, VA (to be published in Advances in Geophysics).

Lumley, J.L. and Panofsky, H.A.: The Structure of Atmosphere Turbulence. Interscience Publishers, 1964.

Mellor, G.L.: Analytic prediction of the properties of stratified planetary surface layers. J. Atmos. Sci. 30:1061-1069, 1973.

Miyake, M.: Transformation of the Atmospheric Boundary Layer over Inhomogeneous Surfaces. Scientific Report, Office of Naval Research, Contract No. 477(24), (NR307-252), 1965.

Monin, A.S. and Yaglom, A.M.: Statistical Fluid Mechanics: Mechanics of Turbulence, Volume 1. MIT Press, 1971.

Panchev, S. and Donev, D.: Wind profile and vertical motions above an abrupt change in surface roughness and temperature. Boundary-Layer Meteorology 2, 52-63, 1971.

Peterson, E.W.: Modification of mean flow and turbulent energy by a change in surface roughness under conditions of neutral stability. Quart. J. Roy. Meteor. Soc. 95, 561-575, 1969.

Peterson, E.W.: Relative importance of terms in the turbulent-energy and momentum equations as applied to the problem of a surface roughness change. J. Atmos. Sci. 29, 1470-1476, 1972.

Priestly, C.H.B.: Turbulent Transfer in the Lower Atmosphere. The Univ. of Chicago Press, 1959.

Rao, J.C., Wyngaard, J.C. and Cote, O.R.: The structure of the two-dimensional internal boundary layer over a sudden change of surface roughness. J. Atmos. Sci. 31, 738-746, 1974.

Saunders, P.M.: Sea smoke and steam fog. Quart. J. Roy. Meteor. Soc. 90, 156-165, 1964.

Schlichting, H.: Boundary Layer Theory. McGraw-Hill, 1960.

Shir, C.C.: A numerical computation of air flow over a sudden change of surface roughness. J. Atmos. Sci. 29, 304-310, 1972.

Sverdrup, H.U.: On the evaporation from the oceans. Journal of Marine Research 1, 3-14, 1937.

Taylor, P.A.: A model of air flow above changes in surface heat flux, temperature and roughness for neutral and unstable conditions. Boundary-Layer Meteorology 1, 18-39, 1970.

Tennekes, H. and Lumley, J.L.: A First Course in Turbulence. MIT Press, 1972.

Townsend, A.A.: Temperature fluctuations over a heated horizontal surface. J. Fluid Mech. 5:209-241, 1959.

APPENDIX A

The purpose of this appendix is to present and compare four different lower boundary conditions on temperature, two of which have appeared in the main body of the thesis. Condition 1 is the primary condition used in the dissertation and represents one simple way of including molecular transfer near the surface. On the other hand, Condition 2 assumes no explicit molecular transfer. Conditions 3 and 4 represent alternative methods of implementing molecular transfer at the surface. Each lower boundary condition will be cast in the form (6-7), and the expression for $\tilde{z}_H$ will be given. The model will be run under the Badgley experiment conditions, treating heat as a passive contaminant with $a_h = 1.35$.

Condition 1. This condition results in a two-layered model with an abrupt change from molecular to turbulent transfer. There will be a discontinuity in the temperature gradient at the top of the molecular sublayer. The eddy transfer coefficient is

$$K_h = a_h u_* k z \tag{A-1}$$

The temperature roughness parameter is related to a_h and D.

$$\tilde{z}_H = \tilde{D} \exp(-a_h k \nu \tilde{D}/\kappa) \tag{A-2}$$

The lower boundary condition applied at $z_0 \geq D$ is

$$\theta_0 - \frac{K_h D}{\kappa}\left[1+\frac{\kappa}{D a_h u_{*k}}\ln(z_0/D)\right]\frac{\partial\theta}{\partial z} = \theta_B \qquad \text{(A-3)}$$

From flat plate momentum data an estimate of $\tilde{D}$ for this formulation is $\tilde{D} = 11$.

Condition 2. This condition does not provide for molecular transfer near the surface. The eddy transfer coefficient is (A-1). The roughness parameters for momentum and temperature are equal, and the surface temperature is found at z_0.

$$\tilde{z}_H = \tilde{z}_0 \qquad \text{(A-4)}$$

$$\theta_0 = \theta_B \qquad \text{(A-5)}$$

Only when z_0 is small enough to be found on Figure 3.7 will this condition be consistent with the concept of a molecular layer.

Condition 3. There is a blending of molecular and turbulent transfer starting at the surface; there is no sublayer having only molecular transfer. The eddy transfer coefficient is (Garratt and Hicks, 1973)

$$K_h = \kappa + a_h u_{*k} z \qquad \text{(A-6)}$$

from which

$$z_H = \kappa/a_h k\nu \qquad \text{(A-7)}$$

The lower boundary condition is applied at z_0.

$$\theta_0 - \left(\frac{K_h}{a_h u_* k}\right) \ln(K_h/\kappa) \frac{\partial \theta}{\partial z} = \theta_B \qquad \text{(A-8)}$$

Condition 4. There is a molecular sublayer of thickness D, above which there is a blending of molecular and turbulent transfer. This condition is an improvement on Condition 1, providing the molecular sublayer with a continuous temperature gradient. The eddy transfer coefficient is

$$K_h = \kappa + a_h u_* k(z-D) \qquad \text{(A-9)}$$

from which

$$\tilde{z}_H = \left(\frac{\kappa}{a_h \nu k}\right) \exp(-a_h \tilde{D} k \nu/\kappa) \qquad \text{(A-10)}$$

The lower boundary condition applied at $z_0 \geq D$ is

$$\theta_0 - \frac{K_h D}{\kappa} \left[1 + \frac{\kappa}{D a_h u_* k} \ln (K_h/\kappa)\right] \frac{\partial \theta}{\partial z} = \theta_B \qquad \text{(A-11)}$$

Flat plate momentum data would indicate $\tilde{D}$ is about 7.1 for this formulation, that is

$$D = 7.1\ \nu/u_* \qquad \text{(A-12)}$$

The predicted heat fluxes, resulting from these boundary conditions in a simulation of the Badgley experiment, are found in Table A.1.

Table A. 1. Heat flux predictions.

Condition	Heat Flux at 7 Meters Fetch (mw/cm^2)
1	28.2
2	49.7
3	40.0
4	28.7

It appears that there is little difference in the flux predictions when using Condition 1 or 4. As discussed in Sections 3.4 and 3.6, there seem to be reasons for rejecting Conditions 2 and 3, and the analysis of wind tunnel data in Appendix B does not support their use. Conditions 2 and 3 have been included in this appendix because of mention by other authors (Taylor, 1970; Garratt and Hicks, 1973). Use of these conditions would obviously result in significantly higher flux predictions.

APPENDIX B

Bau On Young et al. (1973) give wind tunnel data which describe flows encountering abrupt increases in surface temperature, both over a flat plate and a free water surface. In this appendix, the data will be analyzed with the intent of determining the most reasonable lower boundary condition for the model (Appendix A). However, the data is not geophysical and not ideal for this purpose. The constant stress layer is very shallow in the wind tunnel; not all data points will lie in the layer, a situation which makes it difficult to apply conclusions to the model.

The data supplied by Bau On Young consists of profiles of temperature, vapor, velocity, heat flux, stress and vapor flux. The cases include flows over a flat plate (FP) and over water surfaces with free stream velocities of about 15 fps (V15) and 24 fps (V24). Measurement Stations 2 and 3 were located at fetches of 30 and 40 feet respectively.

Based on the lowest 7 to 10 profile points, the roughness parameters for velocity, temperature and vapor are estimated in two ways.

Eddy Diffusivity Method (ED). The temperature gradient is computed by

$$\frac{\partial \theta}{\partial z} = -\overline{\theta w}/a_h u_* kz \qquad \text{(B-1)}$$

where

$$a_h = \frac{\overline{\theta w}\frac{\partial U}{\partial z}}{\overline{uw}\frac{\partial \theta}{\partial z}} \qquad \text{(B-2)}$$

and the gradients in (B-2) are found by a least square fit. The logarithmic profile having the gradient given by (B-1) and passing through the mean of the lower data points is extrapolated downward to find the roughness parameter. Vapor and velocity data are treated in an analogous manner. This method seeks compatibility with the model formulation.

Least Square Method (LSQ). The lower profile points are subjected to a least square fit, and the resulting curve is extrapolated to find the roughness parameter. This method is direct and would probably suffice if the data points were all in a constant flux layer. ED serves as a useful comparison to LSQ.

Results of the computations are given in Table B. 1. The molecular layer thickness is computed assuming lower boundary Condition 1. Condition 2 is refuted by the free surface cases; there seems to be no basis for the general assumption that $z_0 = z_H$. Condition 3 seems to be refuted by all the ED calculations and most of the LSQ calculations, excepting perhaps V15-2 and V24-2 for temperature. Condition 4, as discussed in Appendix A, is merely a nicely formed Condition 1 and so will apply if Condition 1 applies.

Condition 1 is supported to some degree. For FP cases, the molecular sublayer is larger than is assumed in Chapter 3; $\tilde{D}$ is about 16. The vapor data also supports Condition 1 with $\tilde{D}$ averaging about 10. However, there is a problem with the free surface temperature cases. Using ED, $\tilde{D}$ seems to shrink to about 6, whereas, using LSQ, consistency with Condition 1 is marginal or nonexistent (indicated by *). Also surprising are the large values of a_h in the free surface cases. One might suspect that increased surface roughness results in an erosion of the molecular sublayer, but this does not explain why the sublayer for vapor remains substantial. Perhaps the temperature profiles are distorted by radiation divergence or latent heat release.

In conclusion, Condition 1 (and by refinement Condition 4) represents the lower boundary condition better than Conditions 2 or 3. Average values from ED and LSQ computations at FP-3, V15-3 and V24-3 were used to derive the points b, c and d in Figure 3.7.

Table B.1. Results of analysis of wind tunnel data.

Case	Velocity		Temperature					Vapor				
	ED	LSQ		ED		LSQ			ED		LSQ	
	$\tilde{z}_0$	$\tilde{z}_0$	a_h	$\tilde{z}_H$	$\tilde{D}$	$\tilde{z}_H$	$\tilde{D}$	a_e	$\tilde{z}_E$	$\tilde{D}$	$\tilde{z}_E$	$\tilde{D}$
FP-2	.166	.059	0.84	.332	16.	.130	21.					
FP-3	.182	.266	1.01	.155	16.	.183	15.					
V15-2	.385	1.87	2.00	.199	6.0	1.12	*	1.27	.137	15.	.630	8.4
V15-3	.585	1.84	2.01	.144	6.7	.578	2.7	1.06	.422	13.	1.34	5.4
V24-2	2.73	6.35	1.81	.454	4.4	1.50	*	1.63	.067	13.	.236	9.2
V24-3	3.32	4.58	1.69	.519	4.5	.795	1.5	1.34	.448	9.3	.687	7.2